

AD279186

# HANDBOOK OF SUPERSONIC AERODYNAMICS

## SECTION 16

### MECHANICS OF RAREFIED GASES

BY

Samuel A. Schaaf

Lawrence Talbot

University of California, Berkeley, California



Accession For	
NTIS CRA&I	<input checked="" type="checkbox"/>
DTIC TAB	<input type="checkbox"/>
Unannounced	<input type="checkbox"/>
Justification	
By	
Distribution /	
Availability Codes	
Dist	Avail and/or Special
A-1	

Produced and edited by the Aerodynamic Handbook Staff of the Johns Hopkins University Applied Physics Laboratory, Silver Spring, Maryland, under Contract NOrd 7386 with the Bureau of Ordnance, Department of the Navy. The selection and technical review of this material were functions of a Reviewing Committee of the Laboratory consisting of Ione D. V. Faro, Lester L. Cronvich, and Robert N. Schwartz (Chairman).

~~For sale by the Superintendent of Documents, U.S. Government Printing Office, Washington 25, D.C. : Price \$1.25~~

FEBRUARY 1959

## Series Contents

## VOLUME 1

Section 1	Symbols and Nomenclature	Published 1950
Section 2	Fundamental Equations and Formulae	Published 1950
Section 3	General Atmospheric Data	Published 1950
Section 4	Mechanics and Thermodynamics of Steady One-Dimensional Gas Flow	Published 1950

## VOLUME 2

Section 5	Compressible Flow Tables and Graphs	Published 1953
-----------	-------------------------------------	----------------

## VOLUME 3

Section 6	Two-Dimensional Airfoils	Published 1957
Section 7	Three-Dimensional Airfoils	Published 1958
Section 8	Bodies of Revolution	Author: David Adamson (In process)

## VOLUME 4

Section 9	Mutual Interference Phenomena	Cornell Aeronautical Laboratory (In process)
Section 10	Stability and Control Analysis Techniques	Author: Robert S. Swanson (In process)
Section 11	Stability and Control Parameters	Author: Robert S. Swanson (In process)
Section 12	Aeroelastic Phenomena	Published 1952

## VOLUME 5

Section 13	Viscosity Effects	Author: Robert E. Wilson (In process)
Section 14	Heat Transfer Effects	Author: Robert E. Wilson (In process)
Section 15	Properties of Gases	Published 1953
Section 16	Mechanics of Rarefied Gases	Authors: Samuel A. Schaaf and Lawrence Talbot (Herewith)

## VOLUME 6

Section 17	Ducts, Nozzles, and Diffusers	Author: Charles L. Dailey (In process)
Section 18	Shock Tubes	Author: Gordon N. Patterson (To be published 1959)
Section 19	Wind Tunnel Design	Author: Alan Pope (To be published 1959)
Section 20	Wind Tunnel Instrumentation	Author: R. J. Volluz (In process)
Section 21	Ballistic Ranges	No Statement

## HANDBOOK OF SUPERSONIC AERODYNAMICS

## Volume 5 Section 16

Preface

A preface to the entire Handbook of Supersonic Aerodynamics appears in Volume 1 and includes a brief history of the project. As stated in Volume 1, "The primary criterion used in selecting material for the Handbook is its expected usefulness to designers of supersonic vehicles. Thus a collection of data directly useful in the design of supersonic vehicles, results of the more significant experiments, and outlines of basic theory are included ...."

The present edition of the Handbook, printed and distributed by the Bureau of Ordnance, is being published in separate sections as material becomes available. The contents of the entire work is given on the back of the title page. The majority of sections of the Handbook are now being prepared by individual authors for the Applied Physics Laboratory. Those sections are noted for which an early publication date is expected. The selection of material, editing, and technical review of the Handbook of Supersonic Aerodynamics continue to be carried out by an editor and a technical reviewing committee at the Applied Physics Laboratory.

The numbering system of Section 16 is essentially the same as that used in the last preceding sections.

Agencies and individuals interested in the aeronautical sciences are invited to submit and to recommend material for inclusion in the Handbook; full credit will be given for all such material used. Regarding the selection of material and the preparation of the volumes in the Handbook Series, the Applied Physics Laboratory earnestly solicits constructive criticisms and suggestions. Correspondence relating to the editing of the Handbook should be directed to

Editor and Supervisor, Aerodynamics Handbook Project  
Applied Physics Laboratory  
The Johns Hopkins University  
8621 Georgia Avenue  
Silver Spring, Maryland

Communications concerning distribution of the Handbook should be directed to

Chief, Bureau of Ordnance  
Department of the Navy  
Washington 25, D. C.

## SECTION 16 MECHANICS OF RAREFIED GASES

## Contents

	<u>Subsection</u>	<u>Number</u>
Symbols. . . . .	Symbols Page	1
Introduction . . . . .		1600
General Scope of Contents . . . . .		1600.1
The Flow Regimes . . . . .		1601
Qualitative Description of the Flow Regimes . . . . .		1601.1
Real Gas Effects. . . . .		1601.11
Significant Parameters for Characterizing the Flow Regimes . . . . .		1601.2
Surface Interaction Parameters . . . . .		1601.3
Free Molecular Flow. . . . .		1602
Basic Energy Flux Relations . . . . .		1602.1
Basic Momentum Flux Relations . . . . .		1602.2
Heat Transfer to Typical Bodies (Calculated). . . . .		1602.3
The Flat Plate at Angle of Attack, $\alpha$ . . . . .		1602.31
The Infinite Right Circular Cylinder at Angle of Attack, $\alpha$ . . . . .		1602.32
The Sphere . . . . .		1602.33
The Cone at Angle of Attack, $\alpha$ (Conical Surface Only) . . . . .		1602.34
Practical Application of the Heat Transfer Equations . . . . .		1602.35
Aerodynamic Forces for Typical Bodies (Calculated) . . . . .		1602.4
The Flat Plate at Angle of Attack, $\alpha$ , with Both Sides Exposed to the Flow . . . . .		1602.41
The Sphere . . . . .		1602.42
The Right Circular Cylinder at Angle of Attack, $\alpha$ . . . . .		1602.43
The Cone at Angle of Attack, $\alpha$ . . . . .		1602.44
Example of a Composite Body . . . . .		1602.45
Slip Flow . . . . .		1603
The Velocity Slip and Temperature Jump at Body Surfaces . . . . .		1603.1
The Appropriate Differential Equations for Slip Flow. . . . .		1603.2
Viscous Interaction Effects--Hypersonic Flow Results . . . . .		1603.3
Heat Transfer for Typical Bodies (Experimental) . . . . .		1603.4
The Sphere . . . . .		1603.41
The Right Circular Cylinder . . . . .		1603.42
The Cone . . . . .		1603.43
Aerodynamic Forces for Typical Bodies (Experimental) . . . . .		1603.5
The Sphere . . . . .		1603.51
The Flat Plate . . . . .		1603.52
The Cone . . . . .		1603.53
Base Pressures . . . . .		1603.54
Impact Probe Measurements. . . . .		1603.55

Notes . . . . .	Notes Page	1
References. . . . .	Reference Page	1
Index . . . . .	Index Page	1

## Tables

<u>Table</u>	<u>Table Number</u> *
Thermal Accommodation Coefficient, $\bar{\alpha}$ , for Air . . . .	1601.3-I
Values of Reflection Coefficient, $\sigma$ . . . . .	1601.3-II

## Figures

<u>Figure</u>	<u>Figure Number</u>
The Regimes of Gas Dynamics . . . . .	1601.2-1
<u>Heat Transfer to Typical Bodies in Free Molecular Flow</u> <u>(Theoretical)</u>	
Modified Recovery Factor for the Front Side of an In- sulated Flat Plate . . . . .	1602.31-1
Modified Recovery Factor for the Back Side of an In- sulated Flat Plate . . . . .	1602.31-2
Modified Recovery Factor for a Flat Plate with the Front and Back Surfaces in Thermal Contact . . .	1602.31-3
Modified Stanton Number for the Front Side of an In- sulated Flat Plate . . . . .	1602.31-4
Modified Stanton Number for the Back Side of an In- sulated Flat Plate . . . . .	1602.31-5
Modified Stanton Number for a Flat Plate with the Front and Back Surfaces in Thermal Contact . . .	1602.31-6
Modified Recovery Factor for a Sphere and a Cylinder Transverse to the Flow Direction. . . . .	1602.32-1
Modified Stanton Number for a Sphere and a Cylinder Transverse to the Flow Direction. . . . .	1602.32-2
Functions for the Determination of the Recovery Factor and the Stanton Number for the Cylinder as a Function of Angle of Attack, $\alpha$ . . . . .	1602.32-3
<u>Aerodynamic Forces on Typical Bodies in Free Molecular</u> <u>Flow (Theoretical)</u>	
Lift Coefficient for a Flat Plate: $\sigma = \sigma' = 0$ . . .	1602.4-1

\* Tables and figures are numbered so as to correspond to the subsection in which they are discussed.

<u>Figure</u>	<u>Figure Number</u>
Lift Coefficient for a Flat Plate: $\sigma = \sigma' = 1$ and $T_w = T_\infty$ . . . . .	1602.4-2
Lift Coefficient for a Flat Plate: $\sigma = \sigma' = 1$ and $T_w = T_{w(eq.)}$ . . . . .	1602.4-3
Drag Coefficient for a Flat Plate: $\sigma = \sigma' = 0$ . . . . .	1602.4-4
Drag Coefficient for a Flat Plate: $\sigma = \sigma' = 1$ and $T_w = T_\infty$ . . . . .	1602.4-5
Drag Coefficient for a Flat Plate: $\sigma = \sigma' = 1$ and $T_w = T_{w(eq.)}$ . . . . .	1602.4-6
Drag Coefficients for a Sphere and a Cylinder Trans- verse to the Flow Direction . . . . .	1602.4-7
Lift Coefficient for a Cone: $\sigma = \sigma' = 0$ . . . . .	1602.4-8
Lift Coefficient for a Cone: $\sigma = \sigma' = 1$ and $T_w = T_\infty$ . . . . .	1602.4-9
Drag Coefficient for a Cone: $\sigma = \sigma' = 0$ . . . . .	1602.4-10
Drag Coefficient for a Cone: $\sigma = \sigma' = 1$ and $T_w = T_\infty$ . . . . .	1602.4-11
<u>Heat Transfer to Typical Bodies in Slip and Transition</u> <u>Flow (Experimental)</u>	
Convective Heat Transfer to Spheres in Supersonic Flow . . . . .	1603.41-1
Average Recovery Factors for Spheres in Supersonic Flow . . . . .	1603.41-2
Heat Transfer Coefficients for Spheres in Subsonic Flow . . . . .	1603.41-3
Heat Transfer to a Circular Cylinder Transverse to the Flow Direction in Supersonic Flow. . . . .	1603.42-1
Variation of Equilibrium Temperature for Right Cir- cular Cylinders Transverse to the Flow . . . . .	1603.42-2
Recovery Factors for Right Circular Cylinders Trans- verse to the Flow. . . . .	1603.42-3
Heat Transfer for Cones in Supersonic Flow . . . . .	1603.43-1
Thermal Recovery Factors for Cones in Supersonic Flow . . . . .	1603.43-2
<u>Aerodynamic Forces on Typical Bodies in Slip and Transi-</u> <u>tion Flow (Experimental)</u>	
Drag Coefficient for a Sphere . . . . .	1603.51-1
Skin Friction Drag Coefficient for a Flat Plate . . . . .	1603.52-1

FigureFigure Number

Normal Force Coefficient-Curve-Slope for Flat Plates at $M \sim 4$ . . . . .	1603.52-2
Surface Pressures on a Cone at $M \sim 4$ . . . . .	1603.53-1
Drag Coefficients for Cones with $15^\circ$ Semi-Vertex Angle . . . . .	1603.53-2
Base Pressure Coefficient for a Cone-Cylinder Con- figuration . . . . .	1603.54-1

Impact Pressure Measurements

Increment of Measured Pressure Coefficient over Ideal Value in Subsonic Flow ( $0.10 < M < 0.67$ ) . . . . .	1603.55-1
Correction Factors for Impact Pressure Measurements for Source-Shaped Tubes in Supersonic Flow . . . . .	1603.55-2
Correction Factors for Impact Pressure Measurements for Open-Ended Tubes in Supersonic Flow. . . . .	1603.55-3

## SECTION 16 MECHANICS OF RAREFIED GASES

## Primary Symbols

$a$	velocity of sound
$A$	aspect ratio
$C_D$	drag coefficient: $\frac{\text{Drag Force}}{\frac{1}{2} \rho v^2 S}$
$C_L$	lift coefficient: $\frac{\text{Lift Force}}{\frac{1}{2} \rho v^2 S}$
$C_N, C_A$	force coefficients normal to and parallel to body axis
$C_{N_\alpha}$	normal force curve-slope: $\frac{\partial C_N}{\partial \alpha}$
$c_p$	specific heat at constant pressure
$d$	characteristic body dimension
$E$	internal energy flux: $\frac{\text{energy}}{\text{unit time} \times \text{unit area}}$
$E_i, E_r, E_w$	flux of internal energy on surface due respectively to molecules incident to, and reemitted from surface, and that flux obtainable if molecules were reemitted in Maxwellian equilibrium with surface
$E_{\text{int.}}, E_{\text{trans.}}$	portions of internal energy flux due respectively to rotational-vibrational energies of the molecules, and that due to translational energy
$\text{erf}(s \sin \theta)$	error function: $\frac{2}{\sqrt{\pi}} \int_0^{s \sin \theta} e^{-x^2} dx$
(Values for this function are tabulated in Refs. 47 and 48.)	
$\text{erfc}(s \sin \theta)$	complementary error function: $\left[ 1 - \text{erf}(s \sin \theta) \right]$
$f$	molecular distribution function
$h$	heat transfer coefficient



$I_0(\frac{\xi^2}{2}), I_1(\frac{\xi^2}{2})$	modified Bessel functions of the first kind
j	number of molecular degrees of freedom
K	Knudsen number: $\lambda/d$
k	thermal conductivity
L	length along axis of body
M	Mach number: $\frac{V}{a}$
m	molecular mass
$N_i, N_w$	number flux of molecules incident to and leaving wall
Nu	Nusselt number: $\frac{hd}{k}$
p	normal stress per unit surface area; pressure
$p_i, p_r, p_w$	see $E_i, E_r, E_w$ for usage of subscripts
Pr	Prandtl number: $\frac{\mu c_p}{k}$
Q	total heat transfer
R	gas constant
r	recovery factor: $\frac{T_{w(eq.)} - T_\infty}{T_t - T_\infty}$
Re	Reynolds number: $\frac{V\rho d}{\mu}$
S	surface area
s	speed ratio: $V/\sqrt{2RT}$
St	Stanton number: $\frac{Q}{S \rho V c_p (T_{w(eq.)} - T_w)}$
T	temperature, absolute
$T_w, T_{w(eq.)}$	wall temperature; adiabatic wall temperature in the absence of heat transfer
U	x-component of flow velocity
u, v, w	components of molecular velocity in $x_1, x_2, x_3$ directions
V	velocity of undisturbed flow
$x_1, x_2, x_3$	local coordinates referred to a point on the surface of a body

$x, y, z$	rectangular Cartesian coordinates
$\alpha$	angle of attack of body
$\bar{\alpha}$	thermal accommodation coefficient: $\frac{dE_i - dE_r}{dE_i - dE_w}$
$\gamma$	ratio of specific heats, the isentropic exponent
$\delta$	boundary layer thickness; semi-vertex angle of the cone
$\theta$	local angle of attack
$\lambda$	molecular mean free path
$\mu$	gas viscosity
$\rho$	density (of ambient fluid)
$\sigma$	surface reflection coefficient for tangential momentum: $\frac{\tau_i - \tau_r}{\tau_i}$
$\sigma'$	surface reflection coefficient for normal momentum: $\frac{p_i - p_r}{p_i - p_w}$
$\tau$	tangential stress on element of surface area
$\tau_i, \tau_r, \tau_w$	see $E_i, E_r, E_w$ for usage of subscripts
$\theta$	angle in cylindrical coordinate system
$\xi$	$s \sin \alpha$

#### Auxiliary Symbols

##### General Subscripts

$b$	base
$t$	stagnation condition
(eq.)	under equilibrium conditions
(ideal)	theoretical result for inviscid flow
$\infty$	undisturbed free stream (This subscript is dropped in the subsection on Free Molecular Flow.)
$2$	condition behind normal shock wave or ideal flow condition at cone surface behind conical shock wave

## SECTION 16 MECHANICS OF RAREFIED GASES

1600 Introduction

This section of the Handbook of Supersonic Aerodynamics presents quantitative information of interest to the designer working with the problems of flight at very high altitudes. Together with Sections 13 and 14 (Viscosity and Heat Transfer Effects) and Section 15 (Properties of Gases), the present section comprises a single volume. The topics proper to the Mechanics of Rarefied Gases are gathered together here into a single section of the Handbook because the dominant phenomena and theoretical approaches are different from those found in continuum aerodynamics. This study is also restricted in the range of Mach numbers; therefore the effects of changing specific heat, dissociation, and so forth (the thermodynamics of which is treated in Section 15) are not considered. Furthermore, the present treatment has been limited to those aspects of the developing subject of the mechanics of rarefied gases which are capable of yielding reliable quantitative information. A more theoretical consideration of this subject has been presented by Schaaf and Chambre in an article entitled "Flow of Rarefied Gases" in Volume III of the Princeton Series on High Speed Aerodynamics and Jet Propulsion (Ref. 54).

1600.1 General Scope of Contents

It is possible to present reliable information for the case of a gas in which rarefaction effects are just becoming evident (slip flow) and for the case of a completely rarefied gas (free molecular flow). For these two cases, lift, drag, and heat transfer data for typical bodies are presented in the form of calculations and experimental results. Also, the various flow regimes of rarefied gas dynamics are discussed and defined.

In the presentation of this material theoretical analyses are reduced to a minimum consistent with intelligent use of the data, and reference is made to the original sources which contain the more detailed analyses.

1601      The Flow Regimes

At very high altitudes, the atmosphere becomes so rarefied that it no longer behaves like a continuous fluid. The basic molecular character of air then gives rise to important modifications in aerodynamic and heat transfer phenomena. Continuum gas dynamics first must be modified, then abandoned. The basic phenomena and theoretical approaches for highly rarefied flows are significantly different from those for flows that are only moderately rarefied. It is desirable therefore to divide rarefied gas dynamics into various flow regimes (Ref. 2).

1601.1      Qualitative Description of the Flow Regimes

The characteristic flow in a highly rarefied gas is called "free molecular flow." In this regime the mean free path is large compared to the characteristic dimension of an aerodynamic body in the flow; and molecules that impinge on the body, and are then reemitted from it will, in general, be far away from the body before they strike another molecule. It follows that the gas flow incident on the body is essentially undisturbed by the presence of the body. Aerodynamic and heat transfer characteristics depend only on the incident flow and the average momentum and energy interaction between incident molecules and the surface. Lift, drag, and heat transfer coefficients may be calculated in a straightforward way in terms of a few empirical surface interaction parameters. Experimental results, for the relatively small number of cases which have been investigated, are generally in good agreement with these theoretical predictions. However, these theoretical and experimental results have been confined to speeds and temperatures which are low enough to ensure that no internal molecular or atomic energy transformations of the gas molecules occur upon striking the surface. For very high velocity, high altitude applications it is to be expected that molecular dissociation, excitation, and even ionization will occur to some unknown extent on or perhaps near the surface. (A preliminary investigation of free molecular flow with surface interaction has been made by Sanger (Ref. 3), assuming thermodynamic equilibrium at the surface.)

Theoretical methods have been developed for correcting free molecular flow formulae to account for the effects of a few collisions (Refs. 4, 5, and 6). (See Notes, Item 1.)

The characteristic flow in a moderately rarefied gas is called "slip flow." This designation is taken from the phenomenon of "slip," which is one of the important effects known to occur in a moderately rarefied gas flow and which is directly ascribable to its non-continuum, molecular structure. The gas layer immediately adjacent to a surface does not stick to it, but instead slips along it with a definite velocity proportional to the product of the wall shear stress and the molecular mean free path. A corresponding jump or discontinuity in the temperature is also known to exist (see Eq. 1603.1-6).

The flow regime intermediate between slip and free molecular flow is known as the "transition flow regime." It corresponds to densities for which the mean free path has the same general order of magnitude as the characteristic dimension of the flow field. Theoretical treatments are presently unavailable and even experimental results (see Subsection 1603) are rather limited in this flow regime.

1601.11 Real Gas Effects

Flight at very high altitudes often involves extremely high velocities and resulting high gas temperatures. At velocities much in excess of  $M = 6$  the so-called "real gas" effects associated with these temperatures and due to the vibration, dissociation, and ionization of the gas molecules begin to be of importance. The present section of the Handbook is confined to low density effects only and will not consider real gas effects. Therefore application of the results presented here to velocities in excess of  $M = 6$  should be done with care.

1601.2 Significant Parameters for Characterizing the Flow Regimes

Modifications in aerodynamic and heat transfer phenomena due to the molecular character of air become significant when the molecular mean free path,  $\lambda$ , is comparable to a relevant characteristic dimension,  $d$ , of the flow field. The dimensionless parameter called the Knudsen number,  $K$ , where

$$K = \frac{\lambda}{d} , \quad (1601.2-1)$$

has been introduced to serve as a criterion for determining the relative importance of these rarefaction effects. The Knudsen number is expressible in terms of the more familiar moduli of aerodynamics, the Mach and Reynolds numbers

$$M = \frac{V}{a} \quad \text{and} \quad Re = \frac{V \rho d}{\mu} , \quad (1601.2-2)$$

where  $V$ ,  $\rho$ ,  $\mu$ , and  $a$  are the gas velocity, density, viscosity, and sound speed. Combining the kinetic theory relation (Ref. 1),

$$\mu = \frac{1}{2} \rho \lambda a \sqrt{\frac{8}{\pi \gamma}} , \quad (1601.2-3)$$

where  $\gamma$  is the isentropic exponent, one obtains a basic relation,

$$K = \frac{1.25 \sqrt{\gamma} M}{Re} . \quad (1601.2-4)$$

The mechanics of rarefied gas dynamics is concerned with flows in which  $K$  is not negligibly small.

The division of flow regimes can be formulated in terms of ranges of values of the Knudsen number or, by using Eq. 1601.2-4, in ranges of values of  $M$  and  $Re$ .

Free molecular flow is defined as that flow for which  $K > 10$ . The intermediate (transition) regime corresponds to densities for which the mean free path is of the same order of magnitude as the characteristic dimension of the flow field.

Slip Flow is characterized by a Knudsen number of a few per cent. Here the relevant characteristic dimension of the flow field is the boundary layer thickness,  $\delta$ , for large Reynolds numbers or the body dimension,  $d$ , itself for small Reynolds numbers (where there is no boundary layer). Since one has

$$\frac{\delta}{d} \sim \frac{1}{\sqrt{Re}}, \quad (1601.2-5)$$

at least two different Knudsen numbers,  $\lambda/\delta$ , or  $\lambda/d$ , are appropriate for characterizing the slip flow regime. Somewhat arbitrarily, but in general agreement with experiment, the slip flow regime is defined by the following limitations:

$$0.01 < \frac{M}{\sqrt{Re}} < 0.1, \quad Re > 1; \quad (1601.2-6)$$

$$0.01 < \frac{M}{Re} < 0.1, \quad Re < 1.$$

At very high Mach numbers and large Reynolds numbers the boundary layer thickness on a flat plate with an adiabatic wall behaves more like

$$\delta/d \sim \frac{M^2}{\sqrt{Re}},$$

so it may possibly be more appropriate at high Mach numbers to define the slip flow regime in terms of the parameter,

$$\frac{1}{M \sqrt{Re}},$$

with perhaps the same numerical values for limits as given above in Eq. 1601.2-6. For the heat transfer case or for blunt bodies, still other criteria for the flow regimes are more pertinent (see Notes, Item 2). The experimental data in this regime are not yet sufficient to settle this question.

These flow regimes, together with the equivalent altitudes corresponding to a characteristic dimension of one foot are indicated in Fig. 1601.2-1. A detailed presentation of the variation of the density, temperature, and composition of the upper atmosphere with altitude is contained in Section 3 (General Atmospheric Data) of the Handbook (see Notes, Item 3).

### 1601.3 Surface Interaction Parameters

Molecules incident on the surface are reemitted from it with a distribution of velocities which is characteristic of the surface and

its temperature, and the temperature, composition, and velocity of the incident gas flow. For air incident on most surfaces of engineering interest, the reemitted velocity distribution is almost Maxwellian at the actual surface temperature. This makes it convenient to describe empirically the over-all exchange of momentum and energy in terms of departures from complete Maxwellian equilibrium. The "thermal accommodation coefficient,"  $\bar{\alpha}$ , is defined by

$$\bar{\alpha} = \frac{dE_i - dE_r}{dE_i - dE_w}, \quad (1601.3-1)$$

where  $dE_i$  is the energy flux (per unit time and area) incident on the surface,  $dE_r$  the energy flux reemitted from the surface, and  $dE_w$  is the energy flux which would be reemitted if all incident molecules were reemitted in Maxwellian equilibrium with the surface. The corresponding coefficient,  $\sigma$ , sometimes called "Maxwell's reflection coefficient" for the exchange of tangential momentum, is defined by

$$\sigma = \frac{\tau_i - \tau_r}{\tau_i}, \quad (1601.3-2)$$

where  $\tau_i$  is the tangential momentum flux (shear stress) incident on the surface, and  $\tau_r$  that for the reemitted molecules. A third coefficient,  $\sigma'$ , to describe the over-all exchange of normal momentum is defined by

$$\sigma' = \frac{p_i - p_r}{p_i - p_w}, \quad (1601.3-3)$$

where  $p_i$  is the flux of normal momentum (pressure) incident on the surface,  $p_r$  that reemitted, and  $p_w$  is the flux which would be reemitted if all molecules were reemitted in Maxwellian equilibrium with the surface.

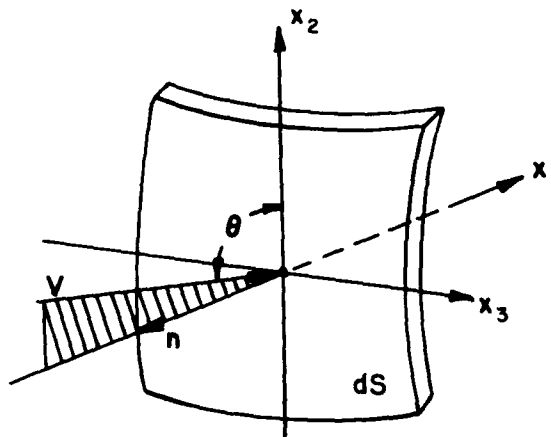
The case in which  $\bar{\alpha} = \sigma = \sigma' = 1$  is called "diffuse reflection," although it clearly implies more than mere spatial randomness in the reflection. It corresponds to an interaction in which the incident molecules achieve complete thermodynamic equilibrium with the surface. The case in which  $\bar{\alpha} = \sigma = \sigma' = 0$  is called "specular reflection" and corresponds to the case of no energy or tangential momentum exchange between molecules and surface. This type of interaction would be observed if all the incident molecules were reflected specularly, i.e., with no change in tangential velocity and simple reversal of normal velocity. Empirical values (Refs. 7 and 8) of  $\bar{\alpha}$  and  $\sigma$  are given in Tables I and II. No empirical values for  $\sigma'$  have been obtained at present. It will be noted, however, that for air incident on most surfaces,  $\bar{\alpha} \cong \sigma \cong 1$ . It is therefore to be expected that  $\sigma' \cong 1$  also. (See Notes, Item 4.)

1602 Free Molecular Flow

The free molecular flow regime is the flow regime of great rarefaction. The air density must be so low that the mean free path is many times the characteristic dimension of the body under consideration. This density is found only at great altitudes, generally of the order of 100 miles or more (see Fig. 1601.2-1). The basic assumption for theoretical free molecular flow calculations is that the flow of molecules incident on a body is undisturbed by the presence of the body, even when it is in supersonic flight. Aerodynamic heat and force characteristics may be calculated by considering separately the incident and reflected flows of molecules. Experimental agreement with the predictions of theory are satisfactory (Refs. 9 and 10). For a brief discussion of nonuniform, unsteady, and surface interacting free molecular flows, see Schaaf and Chambre (Ref. 54, pp. 705-708).

1602.1 Basic Energy Flux Relations

It is necessary to obtain the basic energy and momentum flux relations for a differential element of area,  $dS$ , which is inclined at an angle,  $\theta$ , to the incident flow. The coordinate system used is indicated in the figure below.



It is assumed that the incident flow is in Maxwellian equilibrium so that its molecular distribution function,  $f$ , is given by

$$f = \frac{\rho}{m} (2\pi RT)^{-3/2} \exp \left\{ - \frac{(u - V \sin \theta)^2 + (v + V \cos \theta)^2 + w^2}{2RT} \right\}, \quad (1602.1-1)$$

where  $\exp \{x\} = e^{\{x\}}$ . Here  $m$  is the molecular mass;  $\rho$ ,  $T$ ,  $R$ , and  $V$  are respectively density, absolute temperature, gas constant (length<sup>2</sup> per degree per time<sup>2</sup>), and velocity of the incident flow; and  $u$ ,  $v$ ,  $w$  are the  $x_1$ ,  $x_2$ ,  $x_3$  components of velocity of a molecule, where  $x_1$ ,  $x_2$ ,  $x_3$  are the local coordinates of the surface. Then  $f \cdot du \cdot dv \cdot dw$  is the number of molecules per unit volume with velocity components in the range  $u$ ,  $u + du$ ;  $v$ ,  $v + dv$ ;  $w$ ,  $w + dw$ . The flux of energy incident on the



surface is partly of translational energy,  $dE_{i(\text{trans.})}$ , and partly of internal energy,  $dE_{i(\text{int.})}$ . The former is given by

$$\begin{aligned} dE_{i(\text{trans.})} &= \int_{-\infty}^{\infty} dw \int_{-\infty}^{\infty} dv \int_0^{\infty} \frac{1}{2} m (u^2 + v^2 + w^2) f u du dS \\ &= \rho RT \sqrt{\frac{RT}{2\pi}} \left\{ (s^2 + 2) e^{-(s \sin \theta)^2} \right. \\ &\quad \left. + \sqrt{\pi} (s^2 + \frac{5}{2}) (s \sin \theta) [1 + \text{erf}(s \sin \theta)] \right\} dS, \end{aligned} \quad (1602.1-2)$$

where  $s = \frac{v}{\sqrt{2RT}}$  is the molecular speed ratio. The number flux,  $dN_i$ , of molecules incident on the surface is given by

$$\begin{aligned} dN_i &= \int_{-\infty}^{\infty} dw \int_{-\infty}^{\infty} dv \int_0^{\infty} f u du dS \\ &= \frac{\rho}{m} \sqrt{\frac{RT}{2\pi}} \left\{ e^{-(s \sin \theta)^2} + \sqrt{\pi} (s \sin \theta) (1 + \text{erf}[s \sin \theta]) \right\} dS. \end{aligned} \quad (1602.1-3)$$

By the principle of equipartition of energy, these molecules carry, on the average,  $\frac{j}{2} m RT$  units of internal energy per molecule, where  $j$  is the number of degrees of freedom for the internal modes which partake in the energy exchange.\* For air at normal temperatures,  $j \approx 2$ . In general  $j$  is related to the isentropic exponent,  $\gamma$ , by

$$j = \frac{5 - 3\gamma}{\gamma - 1}. \quad (1602.1-4)$$

The flux of internal energy is

$$\begin{aligned} dE_{i(\text{int.})} &= \frac{5 - 3\gamma}{\gamma - 1} \frac{m RT}{2} dN_i \\ &= \frac{\rho(5 - 3\gamma)}{(\gamma - 1) \sqrt{\pi}} \left( \frac{RT}{2} \right)^{3/2} \left\{ e^{-(s \sin \theta)^2} \right. \\ &\quad \left. + \sqrt{\pi} (s \sin \theta) [1 + \text{erf}(s \sin \theta)] \right\} dS. \end{aligned} \quad (1602.1-5)$$

---

\*It should be noted that here each vibrational degree of freedom must be counted as two "degrees of freedom" because potential as well as motional energy can be stored in the vibrating system.

By a similar line of reasoning, the total energy flux,  $dE_w$ , is given by

$$dE_w = (4 + j) \frac{mRT_w}{2} dN_w = \frac{\gamma + 1}{2(\gamma - 1)} mRT_w dN_w, \quad (1602.1-6)$$

where  $dN_w$  is the number flux leaving the surface. For steady state,

$$dN_i = dN_w. \quad (1602.1-7)$$

The net convective heat transfer,  $dQ$ , to the surface,  $dS$ , is given by

$$dQ = dE_{i(\text{trans.})} + dE_{i(\text{int.})} - dE_r. \quad (1602.1-8)$$

The unknown quantity,  $dE_r$ , may be expressed in terms of  $\bar{\alpha}$  and  $dE_w$  by use of the relation defining the thermal accommodation coefficient, Eq. 1601.3-1, to give

$$dQ = \bar{\alpha} (dE_{i(\text{trans.})} + dE_{i(\text{int.})}) - \bar{\alpha} dE_w. \quad (1602.1-9)$$

It will be noted that it is implicitly assumed that  $\bar{\alpha}$  is the total accommodation coefficient for all modes of energy which partake in the transfer. There is some experimental evidence which suggests that separate coefficients exist for translational, rotational, and vibrational degrees of freedom. The present treatment will not consider such refinements, although it is to be expected that they will become important at elevated temperatures. Expressing the foregoing relation in terms of the appropriate integrals,

$$dQ = \bar{\alpha} \rho RT \sqrt{\frac{RT}{2\pi}} \left\{ \left( s^2 + \frac{\gamma}{\gamma-1} - \frac{\gamma+1}{2(\gamma-1)} \frac{T_w}{T} \right) \left( e^{-(s \sin \theta)^2} + \sqrt{\pi} (s \sin \theta) \left[ 1 + \operatorname{erf} (s \sin \theta) \right] \right) - \frac{1}{2} e^{-(s \sin \theta)^2} \right\} dS. \quad (1602.1-10)$$

This basic relation may be integrated over the surface of any convex aerodynamic body to yield over-all heat transfer characteristics. In general, the quantities  $\bar{\alpha}$  and  $T_w$  will vary over the surface in a manner dependent on the surface material and the internal heat flow characteristics of the body. However, for the special case where  $\bar{\alpha}$  and  $T_w$  are constant over the entire surface area, the indicated integrations have been carried out for a number of basic geometries (Refs. 11 and 12).

The results which are of major interest are the equilibrium body temperature,  $T_{w(eq.)}$ , for which the total heat transfer,  $Q$ , is zero, and the heat transfer rate for body temperatures different from this. These results are presented most conveniently in terms of a thermal recovery factor,  $r$ , and a Stanton number,  $St$ , defined by

$$r = \frac{T_{w(eq.)} - T_{\infty}}{T_t - T_{\infty}} \quad (1602.1-11)$$

$$St = \frac{Q}{S \rho V c_p (T_{w(eq.)} - T_{\infty})} \quad (1602.1-12)$$

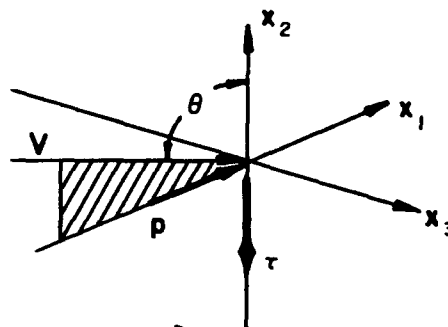
where  $T_t$  is the adiabatic stagnation temperature,  $\rho$  is the gas density,  $c_p$  is the specific heat at constant pressure,  $S$  is the total heat transfer surface area, and  $V$  is the stream velocity. These results are given for the case of convection only. It is to be noted that at high altitudes the relative importance of radiative heat transfer increases. The complete determination of thermal characteristics for high altitude flight conditions thus must include a consideration of radiative heat transfer.

## 1602.2 Basic Momentum Flux Relations

The momentum flux per unit area to the surface element,  $dS$ , is most conveniently broken up into a normal component  $p_i$  (pressure) and a tangential component  $\tau_i$  (shear stress). These are given in terms of the incident and reflected molecular flux by

$$p_i = \int_{-\infty}^{\infty} dw \int_{-\infty}^{\infty} dv \int_0^{\infty} \mu u^2 f du$$

$$= \frac{\rho V^2}{2 \sqrt{\pi} s^2} \left\{ (s \sin \theta) e^{-(s \sin \theta)^2} + \sqrt{\pi} \left[ \frac{1}{2} + (s \sin \theta)^2 \right] [1 + \operatorname{erf}(s \sin \theta)] \right\} \quad (1602.2-1)$$



$$\tau_i = - \int_{-\infty}^{\infty} dw \int_{-\infty}^{\infty} dv \int_0^{\infty} \mu u v f du$$

$$= \frac{\rho V^2 \cos \theta}{2 \sqrt{\pi} s} \left\{ e^{-(s \sin \theta)^2} + \sqrt{\pi} (s \sin \theta) [1 + \operatorname{erf}(s \sin \theta)] \right\} \quad (1602.2-2)$$

Using the reflection coefficients,  $\sigma$  and  $\sigma'$ , one obtains

$$\begin{aligned} p &= p_i + p_r \\ &= (2 - \sigma') p_i + \sigma' p_w \end{aligned} \quad (1602.2-3)$$

$$\begin{aligned} \tau &= \tau_i - \tau_r \\ &= \sigma \tau_i \end{aligned} \quad (1602.2-4)$$

The quantity,  $p_w$ , is calculated in the same manner as the corresponding energy flux component,  $dE_w$ :

$$\begin{aligned} p_w &= \frac{1}{2} m \sqrt{2\pi RT_w} \frac{dN_i}{ds} \\ &= \frac{\rho}{2} \sqrt{2\pi RT_w} \sqrt{\frac{RT}{2\pi}} \left\{ e^{-(s \sin \theta)^2} + \sqrt{\pi} (s \sin \theta) [1 + \operatorname{erf} (s \sin \theta)] \right\}. \end{aligned} \quad (1602.2-5)$$

The final expression for the normal and tangential stresses acting on  $dS$  are thus

$$\begin{aligned} p &= \frac{\rho V^2}{2 s^2} \left\{ \left( \frac{2 - \sigma'}{\sqrt{\pi}} s \sin \theta + \frac{\sigma'}{2} \sqrt{\frac{T_w}{T}} \right) e^{-(s \sin \theta)^2} \right. \\ &\quad \left. + \left[ (2 - \sigma') (s^2 \sin^2 \theta + \frac{1}{2}) + \frac{\sigma'}{2} \sqrt{\frac{\pi T_w}{T}} (s \sin \theta) \right] [1 + \operatorname{erf} (s \sin \theta)] \right\} \end{aligned} \quad (1602.2-6)$$

$$\tau = \frac{\sigma \rho V^2 \cos \theta}{2 s \sqrt{\pi}} \left\{ e^{-(s \sin \theta)^2} + \sqrt{\pi} (s \sin \theta) [1 + \operatorname{erf} (s \sin \theta)] \right\}. \quad (1602.2-7)$$

These relations can be used (see Refs. 13, 14, and 15) to calculate pressure and skin friction distributions over the surface of any convex body, i.e., one which does not permit molecular trajectories from one surface element to another. It will be observed that the skin friction depends only on the properties of the incident gas stream and the proper reflection coefficient. The pressure, on the other hand, depends also on the local body temperature. Thus a determination of the thermal state of a body is usually necessary to determine total lift and drag

characteristics in free molecular flow. Two limiting cases seem to be of most interest. The first is the case of a "cold" body, taken to be at the ambient gas temperature,  $T$ , and characteristic of a body that is cooled or is in the early part of its trajectory. The second is the case of a "hot" body which has attained convective thermal equilibrium with the air flow and is at the temperature  $T_w(\text{eq.})$ . Both of these cases are confined to constant body temperature. However, they seem to bracket the practical possibilities and give an indication of the magnitude of the effect of varying body temperature. For specific applications, it will probably be necessary to make a complete transient thermal calculation including both internal conduction and external radiation as well as convection before an accurate calculation of lift and drag forces can be made.

At very high velocities and for  $\theta > 0$ , the limiting forms for Eqs. 1602.2-6 and 1602.2-7 are given by

$$p \longrightarrow \rho v^2 \left[ (2 - \sigma') \sin^2 \theta \right]$$

(for a body at ambient temperature),

$$p \longrightarrow \rho v^2 \left[ (2 - \sigma') \sin^2 \theta + \sigma' \sin \theta \sqrt{\frac{\pi (\gamma - 1)}{2 (\gamma + 1)}} \right];$$

(for a body at equilibrium temperature), (1602.2-8)

and

$$\tau \longrightarrow \sigma \rho v^2 \sin \theta \cos \theta . \quad (1602.2-9)$$

These may be compared with "Newtonian Flow," an approximation sometimes used for a hypersonic continuum flow (Ref. 16) in which it is assumed that all incident normal momentum is absorbed on the surface, but that no tangential momentum is absorbed. The corresponding expressions are

$$P_{(\text{Newtonian})} = \rho v^2 \sin^2 \theta \quad (1602.2-10)$$

$$\tau_{(\text{Newtonian})} = 0 . \quad (1602.2-11)$$

It will be noted that the pressure terms agree for diffuse reflection for the "cold" case, otherwise the two theories are different and yield different results.

For lift and drag calculation it is necessary to resolve the pressure and skin friction forces into the components normal and parallel to the direction of  $V$ . When the differential lift and drag forces acting on  $dS$  are denoted by  $dF_L$  and  $dF_D$  respectively, the proper relations are

$$dF_L = (p \cos \theta - \tau \sin \theta) dS \quad (1602.2-12)$$

$$dF_D = (\tau \cos \theta + p \sin \theta) dS . \quad (1602.2-13)$$

The total lift and drag forces are then obtained by integration over the surface area. It is convenient to express these results in terms of lift and drag coefficients,  $C_L$  and  $C_D$ , defined by

$$C_L = \frac{\text{Lift Force}}{\frac{1}{2} \rho V^2 S} \quad (1602.2-14)$$

$$C_D = \frac{\text{Drag Force}}{\frac{1}{2} \rho V^2 S}, \quad (1602.2-15)$$

where  $S$  is the reference area. In keeping with usual aerodynamic terminology the area,  $S$ , has been taken as the maximum cross sectional area of the aerodynamic configuration normal to the body axis, except as otherwise noted.

### 1602.3 Heat Transfer for Typical Bodies (Calculated)

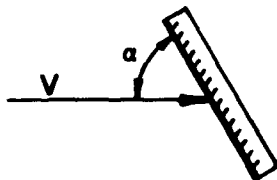
The results of integrating Eq. 1602.1-10 over the total surface for several different geometries are presented below.

#### 1602.31 The Flat Plate at Angle of Attack, $\alpha$

The results for the flat plate with front and back surfaces insulated from one another are, for the front surface only,

$$r = \frac{\gamma}{(\gamma + 1)s^2} \left\{ 2s^2 + 1 - \frac{1}{1 + \sqrt{\pi} (s \sin \alpha) [1 + \operatorname{erf} (s \sin \alpha)] e^{(s \sin \alpha)^2}} \right\} \quad (1602.31-1)$$

$$St = \frac{\bar{\alpha}(\gamma + 1)}{4 \sqrt{\pi} s \gamma} \left\{ e^{-(s \sin \alpha)^2} + \sqrt{\pi} (s \sin \alpha) [1 + \operatorname{erf} (s \sin \alpha)] \right\}. \quad (1602.31-2)$$

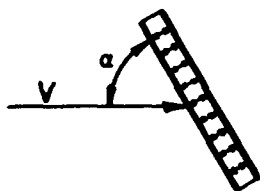


These results are plotted in Figs. 1602.31-1 and 1602.31-4. The formulas for the back side are obtained by replacing  $\alpha$  and  $-\alpha$  and are plotted in Figs. 1602.31-2 and 1602.31-5.

The results for the flat plate with front and back surfaces in thermal contact are:

$$r = \frac{\gamma}{(\gamma + 1)s^2} \left\{ 2s^2 + 1 - \frac{1}{1 + \sqrt{\pi} (s \sin \alpha) \operatorname{erf} (s \sin \alpha) e^{(s \sin \alpha)^2}} \right\} \quad (1602.31-3)$$

$$St = \frac{\bar{\alpha}(\gamma + 1)}{4\sqrt{\pi} s \gamma} \left\{ e^{-(s \sin \alpha)^2} + \sqrt{\pi} s \sin \alpha \operatorname{erf} (s \sin \alpha) \right\} . \quad (1602.31-4)$$

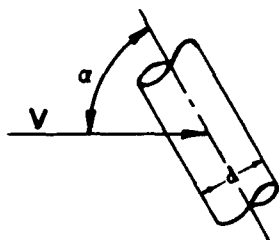


These results are plotted in Figs. 1602.31-3 and 1602.31-6.

#### 1602.32 The Infinite Right Circular Cylinder at Angle of Attack, $\alpha$

$$r = \frac{\gamma}{(\gamma + 1)s^2} \cdot \frac{\left[ \xi^2 + 2s^2(1 + \xi^2) \right] I_0\left(\frac{\xi^2}{2}\right) + \left[ \xi^2(1 + 2s^2) \right] I_1\left(\frac{\xi^2}{2}\right)}{(1 + \xi^2) I_0\left(\frac{\xi^2}{2}\right) + \xi^2 I_1\left(\frac{\xi^2}{2}\right)} \quad (1602.32-1)$$

$$St = \frac{\bar{\alpha}(\gamma + 1)}{4\gamma\sqrt{\pi} s} e^{-\frac{\xi^2}{2}} \left\{ (1 + \xi^2) I_0\left(\frac{\xi^2}{2}\right) + \xi^2 I_1\left(\frac{\xi^2}{2}\right) \right\}, \quad (1602.32-2)$$



where  $\xi = s \sin \alpha$  and  $I_0\left(\frac{\xi^2}{2}\right)$  and  $I_1\left(\frac{\xi^2}{2}\right)$  are modified Bessel Functions of the first kind, i.e.,  $I_n(x) = i^{-n} J_n(ix) = i^n J_n(-ix)$ . Values for these functions of order 0 and 1 are tabulated in Ref. 49. The total heat transfer area is taken as the curved surface area,  $\pi L d$ , where  $L$  is the length of the cylinder.

For  $\alpha = 0$ , these results reduce to:

$$r(\alpha = 0) = \frac{2\gamma}{\gamma + 1}$$

$$St(\alpha = 0) = \frac{(\gamma + 1)\bar{\alpha}}{4\gamma\sqrt{\pi} s} .$$

For purposes of graphical representation it is convenient to let

$$\frac{\gamma+1}{\gamma} r = 2 + \sin^2 \alpha \cdot h(\xi) \quad (1602.32-3)$$

and

$$\frac{\gamma}{\alpha(\gamma+1)} St = \frac{\sin \alpha}{4\sqrt{\pi}} \cdot g(\xi) \quad , \quad (1602.32-4)$$

where

$$h(\xi) = \frac{I_0\left(\frac{\xi^2}{2}\right) + I_1\left(\frac{\xi^2}{2}\right)}{(1+\xi^2) I_0\left(\frac{\xi^2}{2}\right) + \xi^2 I_1\left(\frac{\xi^2}{2}\right)} \quad (1602.32-5)$$

and

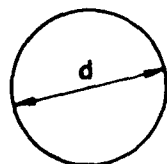
$$g(\xi) = \left[ \left( \frac{1}{\xi} + \xi \right) I_0\left(\frac{\xi^2}{2}\right) + \xi I_1\left(\frac{\xi^2}{2}\right) \right] e^{-\xi^2/2} \quad . \quad (1602.32-6)$$

See Figs. 1602.32-1, 1602.32-2, and 1602.32-3.

### 1602.33 The Sphere

$$r = \frac{\gamma}{\gamma+1} \left\{ \frac{(2s^2 + 1) \left( 1 + \frac{1}{s} \text{ierfc}(s) \right) + \frac{2s^2 - 1}{2s^2} \text{erf}(s)}{s^2 \left( 1 + \frac{1}{s} \text{ierfc}(s) \right) + \frac{1}{2s^2} \text{erf}(s)} \right\} \quad (1602.33-1)$$

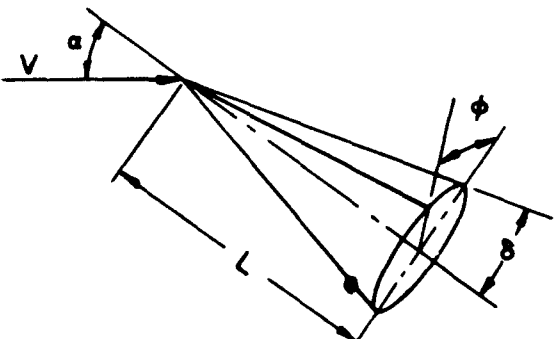
$$St = \frac{\alpha(\gamma+1)}{8\gamma s^2} \left\{ s^2 + s \text{ierfc}(s) + \frac{1}{2} \text{erf}(s) \right\} \quad , \quad (1602.33-2)$$



where  $\text{ierfc}(s)$  is the complementary error function integrated over the total heat transfer area,  $\pi d^2$ . See Figs. 1602.32-1 and 1602.32-2.



1602.34 The Cone at Angle of Attack,  $\alpha$  (Conical Surface Only)

$$Q = L^2 \bar{\alpha}_{pRT} \sqrt{\frac{RT}{2\pi}} \frac{\tan \delta}{\cos \delta} \int_0^\pi \left\{ \left( s^2 + \frac{\gamma}{\gamma-1} - \frac{\gamma+1}{2(\gamma-1)} \frac{T_w}{T} \right) \left( e^{-(s \sin \theta)^2} + \sqrt{\pi} (s \sin \theta) \left[ 1 + \operatorname{erf}(s \sin \theta) \right] - \frac{1}{2} e^{-(s \sin \theta)^2} \right) \right\} d\theta, \quad (1602.34-1)$$


where the height of the cone is  $L$  and the semi-vertex angle is  $\delta$ . The total heat transfer area is the curved surface area, and

$$\sin \theta = -\cos \delta \cos \phi \sin \alpha + \cos \alpha \sin \delta.$$

(1602.34-2)

The Stanton number,  $St$ , for the cone may be obtained by substituting Eq. 1602.34-1 into Eq. 1602.1-12. The value of  $r$  will be found as before by equating the integral in Eq. 1602.34-1 above to zero, i.e.,  $Q = 0$ , and by making the following substitution for  $\frac{T_w}{T}$ :

$$\frac{T_w(\text{eq.})}{T} = 1 + r \frac{(\gamma-1)}{\gamma} s^2.$$

(The cone at zero angle of attack may be treated by using the flat plate result with  $\alpha$  replaced by  $\delta$ , see Eqs. 1602.31-1 through 1602.31-4.)

1602.35 Practical Application of the Heat Transfer Equations

Composite bodies that are convex may be treated in relatively simple fashion. If the thermal characteristics,  $r_j$ , and  $St_j$ , and areas  $S_j$ , where  $j = 1, \dots, n$ , of a series of  $n$  basic shapes are known, the heat transfer characteristics for the combined configuration can be obtained from

$$r = \frac{1}{SSt} \sum_{j=1}^n r_j S_j St_j$$

$$St = \frac{1}{S} \sum_{j=1}^n St_j S_j,$$

provided the temperature of the composite body is constant. The areas,  $S_j$ , used here are the total surface areas for each portion of the composite shape exposed to the flow.

As indicated in Subsection 1602.1 Page 4, the values of  $r$  and  $St$  in the equations above are average or over-all values of these parameters. In order to calculate the heat transfer or temperature at specific points on the configuration, it will be necessary to integrate Eq. 1602.1-10 for specific values of  $\theta$ .

Also, it will be observed that the thermal recovery factors are in general greater than unity. Body equilibrium temperatures, with respect to convection, are greater than the adiabatic stagnation temperature of the gas flow. This striking phenomena is one of the more important and unusual features of the free molecular flow regime. It will also be observed that heat transfer to a "cold" body is proportional to  $\rho V^3 S$  for high velocity flight. This is in accord with meteor observations.

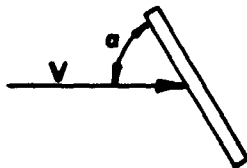
#### 1602.4 Aerodynamic Forces for Typical Bodies (Calculated)

The results of integrating Eqs. 1602.2-12 and 1602.2-13 over the total surface area of several different typical geometrical shapes are presented below. These calculations have been carried out under the assumption that  $T_w$ ,  $\sigma$ , and  $\sigma'$  are constant over the entire surface.

##### 1602.41 The Flat Plate at Angle of Attack, $\alpha$ , with Both Sides Exposed to the Flow

$$C_L = \frac{2(2 - \sigma - \sigma')}{\sqrt{\pi} s} \cos \alpha \sin \alpha e^{-(s \sin \alpha)^2} + \frac{\sigma'}{s} \sqrt{\frac{\pi T_w}{T}} \sin \alpha \cos \alpha + \cos \alpha \left[ 2(2 - \sigma - \sigma') \sin^2 \alpha + \frac{2 - \sigma'}{s^2} \right] \text{erf}(s \sin \alpha) \quad (1602.41-1)$$

$$C_D = \left[ \frac{2(2 - \sigma')}{\sqrt{\pi} s} \sin^2 \alpha + \frac{2\sigma}{\sqrt{\pi} s} \cos^2 \alpha \right] e^{-(s \sin \alpha)^2} + \frac{\sigma'}{s} \sqrt{\frac{\pi T_w}{T}} \sin^2 \alpha + 2 \sin \alpha \left[ (2 - \sigma') \left( \sin^2 \alpha + \frac{1}{2s^2} \right) + \sigma \cos^2 \alpha \right] \text{erf}(s \sin \alpha) \quad (1602.41-2)$$

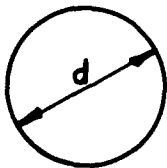


The reference area is taken as the area of one side of the plate. These results are plotted in Figs. 1602.4-1 through 1602.4-6.

1602.42 The Sphere

$$C_D = \frac{2 - \sigma' + \sigma}{2s^3} \left\{ \frac{4s^4 + 4s^2 - 1}{2s} \operatorname{erf}(s) + \frac{(2s^2 + 1)}{\sqrt{\pi}} e^{-s^2} \right\} + \frac{2}{3} \frac{\sigma'}{s} \sqrt{\frac{\pi T_w}{T}} .$$

(1602.42-1)



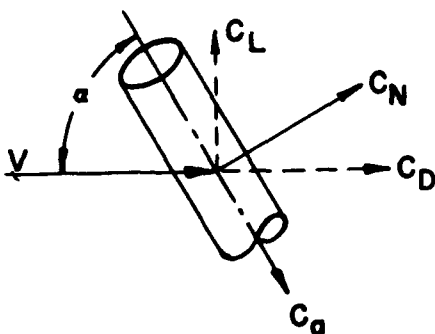
The reference area is the projected area,  $\frac{\pi d^2}{4}$ .  
This equation is plotted in Fig. 1602.4-7.

1602.43 The Cylinder at Angle of Attack,  $\alpha$ 

$$C_N = \frac{\sigma' \pi^{3/2} \sin \alpha}{4s \sqrt{\frac{T}{T_w}}} + \frac{\sin \alpha}{s} (\sigma + 4 - 2\sigma') \sqrt{\pi} e^{-\xi^2/2} \left\{ \left( \frac{1}{2} + \frac{1}{3} \xi^2 \right) I_0\left(\frac{\xi^2}{2}\right) + \left( \frac{1}{6} + \frac{1}{3} \xi^2 \right) I_1\left(\frac{\xi^2}{2}\right) \right\} .$$

(1602.43-1)

$$C_A = \frac{\sigma \sqrt{\pi} e^{-\xi^2/2} \cos \alpha}{s} \left\{ (1 + \xi^2) I_0\left(\frac{\xi^2}{2}\right) + \xi^2 I_1\left(\frac{\xi^2}{2}\right) \right\} , \quad (1602.43-2)$$



where the reference area is diameter,  $d$ , times unit length.

Here,

$$C_N = C_L \cos \alpha + C_D \sin \alpha , \quad C_A = C_D \cos \alpha - C_L \sin \alpha ,$$

(1602.43-3)

and the notation is otherwise the same as for the cylinder heat transfer case. For purposes of graphical representation, it is convenient to let

$$C_A = \sqrt{\pi} \sigma \cos \alpha \sin \alpha g(\xi) \quad (1602.43-4)$$

and

$$C_N = \frac{\sigma' \sin \alpha}{4s} \pi^{3/2} \sqrt{\frac{T_w}{T}} + (4 + \sigma - 2\sigma') \sin^2 \alpha f(\xi) , \quad (1602.43-5)$$

where

$$f(\xi) = \sqrt{\pi} \left[ \left( \frac{1}{2\xi} + \frac{1}{3} \xi \right) I_0\left(\frac{\xi^2}{2}\right) + \left( \frac{1}{6\xi} + \frac{\xi}{3} \right) I_1\left(\frac{\xi^2}{2}\right) \right] e^{-\xi^2/2} \quad (1602.43-6)$$

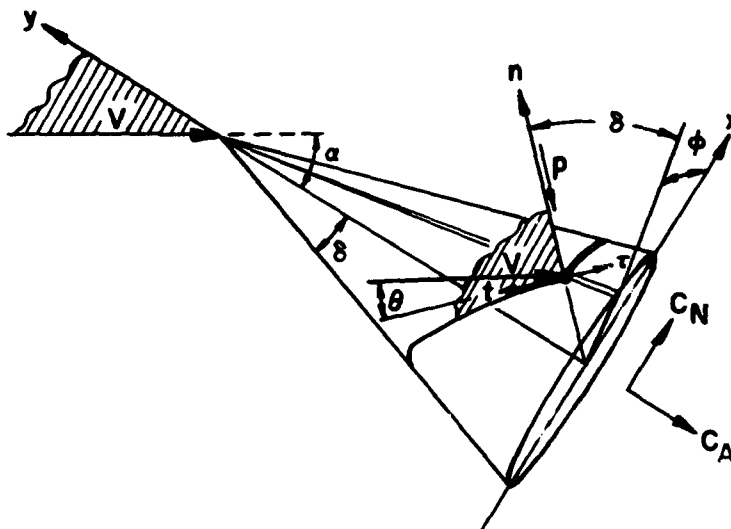
and  $g(\xi)$  is defined in Eq. 1602.32-6. See Figs. 1602.32-3 and 1602.4-7.

#### 1602.44 The Cone at Angle of Attack, $\alpha$

$$C_N = \frac{2}{\rho V^2 \pi \sin \delta} \int_0^\pi (p \cos(n, x) + \tau \cos(t, x)) d\theta \quad (1602.44-1)$$

$$C_A = \frac{2}{\rho V^2 \pi \sin \delta} \int_0^\pi (p \cos(n, y) + \tau \cos(t, y)) d\theta \quad (1602.44-2)$$

where  $\delta$  is semi-vertex angle,  $p$  and  $\tau$  are the expressions given in Eqs. 1602.2-6 and 1602.2-7, and  $\sin \theta$  in these expressions is the same as that given in Eq. 1602.34-2. The coefficients  $C_N$  and  $C_A$  are referred to the base area. The angles and coordinate systems used in the cone equations are indicated in the figure below.



The direction cosines are:

$$\cos(n, x) = \cos \delta \cos \theta \quad (1602.44-3)$$

$$\cos(n, y) = \sin \delta \quad (1602.44-4)$$

$$\cos(t, x) = \frac{\sin \delta (\sin \alpha \sin \delta + \cos \alpha \cos \delta \cos \theta) + \sin \alpha \cos^2 \delta \sin^2 \theta}{\pm \sqrt{\cos^2 \delta \sin^2 \theta + (\sin \delta \sin \alpha + \cos \delta \cos \theta \cos \alpha)^2}} \quad (1602.44-5)$$

$$\cos(t, y) = \frac{\cos \alpha \cos^2 \delta \sin^2 \theta + \cos \delta \cos \theta (\cos \alpha \cos \delta \cos \theta + \sin \alpha \sin \delta)}{\pm \sqrt{\cos^2 \delta \sin^2 \theta + (\sin \delta \sin \alpha + \cos \delta \cos \theta \cos \alpha)^2}} \quad (1602.44-6)$$

The values of  $\cos(n, y)$  and  $\cos(t, y)$  are always positive. The value of  $\cos(n, x)$  goes from positive to negative values as  $\theta$  goes from 0 to  $\pi$  while  $\cos(t, x)$  goes from negative to positive values as  $\theta$  goes from 0 to  $\pi$ . The  $\pm$  sign in Eqs. 1602.44-5 and 1602.44-6 is chosen so that this is the case. These results can be expressed in terms of  $C_L$  and  $C_D$  using Eq. 1602.43-3 and are so plotted in Figs. 1602.4-8 through 1602.4-11. (See Notes, Item 5.)

#### 1602.45 Example of a Composite Body

Composite bodies which are convex may be treated similarly to the heat transfer case. If a configuration consists of  $n$  different parts, each of which has a known lift and drag coefficient,  $(C_L)_j$ ,  $(C_D)_j$ ,  $j = 1, \dots, n$ , then the lift and drag coefficients,  $C_L$  and  $C_D$ , of the total are given by

$$C_L = \frac{1}{S} \sum_{j=1}^n (C_L)_j S_j \quad (1602.45-1)$$

$$C_D = \frac{1}{S} \sum_{j=1}^n (C_D)_j S_j, \quad (1602.45-2)$$

where  $S_j$  and  $S$  are all the appropriate reference areas.

1603 Slip Flow

The slip flow regime is the regime of moderate rarefaction, corresponding to densities at which the gas first begins to exhibit its non-continuum molecular structure. The mean free path is a few per cent of the characteristic dimension of the flow field. Typical altitudes of interest are in the range from 20-50 miles, depending on the Mach number and size under consideration.

1603.1 The Velocity Slip and Temperature Jump at Body Surfaces

The slip flow regime takes its name from the phenomenon of "slip" according to which a gas at low pressures does not stick to a surface but rather slips along it at a definite rate determined by the mean free path, the shear stress, and other quantities.

A very simple analysis will serve to indicate how this comes about. Consider a gas moving with velocity  $U(y)$  in the  $x$ -direction past a surface lying on the  $x$ -axis. The layer of gas immediately adjacent to the surface consists of molecules of which approximately half have just been emitted from the surface, while the remainder have, on the average, come from a layer a mean free path distant from the surface. The average tangential velocity of these incident molecules will be given by

$$U(\lambda) = U(0) + \lambda \frac{dU}{dy} . \quad (1603.1-1)$$

If  $\sigma$  is the reflection coefficient for tangential momentum, the average tangential velocity component of the reemitted molecules is given by

$$(1 - \sigma)U(\lambda) = (1 - \sigma) \left[ U(0) + \lambda \frac{dU}{dy} \right] . \quad (1603.1-2)$$

The velocity of the gas layer itself is thus given by

$$U(0) = \frac{1}{2} \left\{ U(0) + \lambda \frac{dU}{dy} + (1 - \sigma) \left[ U(0) + \lambda \frac{dU}{dy} \right] \right\} . \quad (1603.1-3)$$

From this it follows that

$$U(0) = \frac{2 - \sigma}{\sigma} \lambda \frac{dU}{dy} . \quad (1603.1-4)$$

At normal pressures,  $\lambda$  is so small that  $U(0) = 0$  to a very good approximation. At very low pressures, however,  $\lambda$  becomes large enough to make possible an appreciable slipping velocity. It will be noted that the phenomenon occurs even for completely diffuse reflection, i.e.,  $\sigma = 1$ .

By similar analyses, the velocity slip due to a tangential temperature gradient and the discontinuity between gas and surface

temperature for the case of heat flow may be obtained. The complete expressions (Ref. 24) are

$$U(\text{gas}) = \frac{2 - \sigma}{\sigma} \lambda \left( \frac{\partial U}{\partial y} \right)_w + \frac{3}{\sqrt{8\pi\gamma}} \left[ a\lambda \frac{\partial}{\partial x} (\ln T) \right]_w$$

(1603.1-5)

$$T(\text{gas}) - T(\text{wall}) = \frac{2 - \bar{\alpha}}{\bar{\alpha}} \cdot \frac{2\gamma}{\gamma + 1} \frac{\lambda}{\text{Pr}} \left( \frac{\partial T}{\partial y} \right)_w$$

(1603.1-6)

where  $\bar{\alpha}$  is the thermal accommodation coefficient, Pr is the Prandtl number,  $\text{Pr} = \mu c_p/k$ , and  $\gamma$  is the isentropic exponent. Special attention should be called to the second term on the right hand side of Eq. 1603.1-5, according to which a flow is induced along a surface in the direction of increasing temperature. This is called "thermal creep" and can be of considerable importance in very low pressure instrumentation. These relations are approximate in the sense that they apply only for moderate departures from equilibrium. If either the velocity or temperature gradients are very large, more complicated relations apparently exist. In the slip flow range, as defined in Subsection 1601.2, however, they are quite satisfactory and have been well verified by numerous experiments. It will be observed that slip and temperature jump phenomena--by themselves--have the effect of reducing skin friction and heat transfer, acting in many ways as if an extra film of air of the order of a mean free path thick rested on the solid surface.

### 1603.2 The Appropriate Differential Equations for Slip Flow

There is still some question as to the appropriate set of differential equations to describe a gas flow in the slip flow regime. The most recent experimental and theoretical evidence seems to indicate that the Navier-Stokes equations, together with a bulk viscosity modulus of the order of two-thirds of the shear modulus, are satisfactory for air in the slip flow regime. Other, more complicated sets of equations, known as the Burnett equations (Refs. 17 and 18), the Thirteen Moment equations (Ref. 19), and others (Ref. 20) have been formulated for monatomic gases by means of the kinetic theory of gases. However, these sets of equations do not appear to be as yet adequately substantiated by either experimental evidence (Refs. 21 and 22) or by theoretical evidence (Ref. 23) for monatomic gases, let alone air. They are in general not superior to the simpler Navier-Stokes relations. (See Notes, Item 6. For a more detailed discussion of the Thirteen Moment and the Burnett equations and some of the difficulties associated with these equations, see Schaaf and Chambre, Ref. 54, pp. 710-718.) In the transition regime no set of macroscopic differential equations yet proposed seems to be valid.

### 1603.3 Viscous Interaction Effects--Hypersonic Flow Results

From the basic relationships indicated in Eq. 1601.2-6, i.e., the limitation on  $K = \frac{\lambda}{\delta} \sim \frac{M}{\sqrt{\text{Re}}}$ , it follows that non-continuum phenomena

will occur in general at high Mach numbers or at low Reynolds numbers, or perhaps both. But, to some extent, this is also the same range of parameters for which "interaction effects" between the viscous and inviscid parts of a flow field are known to occur. Generally speaking, boundary layers are thick; they force the inviscid flow past the body outwards a distance the order of the displacement thickness, thus presenting an effectively thicker body to the flow; and this perturbs the surface pressure distribution which in turn feeds back into the boundary layer flow to increase the skin friction. These are really continuum flow effects. The effects of slip and temperature jump at the surface are non-continuum phenomena but are of importance for aerodynamic applications usually only in the presence of strong interaction effects. Slip and temperature jump have the effect of reducing skin friction and heat transfer, while interaction phenomena have the effect of increasing skin friction and heat transfer. Thus, there is a competition of two tendencies of opposite sign. No complete theoretical solution for a flow situation of aerodynamic interest is presently available. However, a growing body of empirical data relating to heat transfer and aerodynamic characteristics for basic geometrical shapes in slip and transition flow does exist and seems to indicate that, with decreasing density, interaction effects are initially dominant but, at lower densities, the trend is reversed and slip and temperature jump effects dominate. This body of data will be summarized below.

#### 1603.4 Heat Transfer for Typical Bodies (Experimental)

Heat transfer characteristics are most conveniently presented in terms of a thermal recovery factor,  $r$ , and a Nusselt number,  $Nu$ :

$$r = \frac{T_{w(eq.)} - T_{\infty}}{T_t - T_{\infty}} \quad (1603.4-1)$$

$$Nu = \frac{hd}{k}, \quad (1603.4-2)$$

where  $h$  is given from

$$Q = hS (T_{w(eq.)} - T_w) ; \quad (1603.4-3)$$

and where  $k$  is the thermal conductivity of the gas,  $T_{\infty}$  is the free stream gas temperature,  $T_t$  is the stagnation temperature,  $T_w$  is the wall temperature,  $T_{w(eq.)}$  is the wall temperature under equilibrium conditions,  $h$  is the heat transfer coefficient, and  $d$  is a characteristic dimension. The body geometries for which values of these parameters have been determined are denoted in the following subsections.

#### 1603.41 The Sphere

Heat transfer measurements have been obtained for spheres (Refs. 25 and 26) over the ranges  $2.7 < M < 6$ ,  $15 < Re < 7000$  and  $0 < M < 0.7$ ,  $2 < Re < 100$ . These results are presented in Figs. 1603.41-1, 1603.41-2, and 1603.41-3.



In the reduction of these data, free stream properties are used for the evaluation of the Nusselt and Reynolds numbers for the subsonic data and for the Reynolds number for the supersonic recovery factor data; properties and flow conditions behind a normal shock wave are used for the evaluation of the Nusselt and Reynolds numbers for the supersonic heat transfer data; and the total surface area of the sphere,  $\pi d^2$ , is taken as the reference area.

#### 1603.42 The Right Circular Cylinder

Heat transfer results have been obtained for right circular cylinders cross stream to the flow (Refs. 27, 28, and 29) over the range  $1.1 < M < 4.5$ ,  $0.1 < Re_2 < 200$ . These results are presented in Figs. 1603.42-1, 1603.42-2, and 1603.42-3.

The Reynolds number,  $Re_2$ , is based on the velocity, density, and viscosity behind a normal shock wave, and the characteristic dimension is the cylinder diameter. The reference area (per unit length of the cylinder) is taken as  $\pi d$ . (See Notes, Item 7.)

#### 1603.43 The Cone

Heat transfer results have been obtained for cones at zero angle of attack (Ref. 30) over range  $10^\circ \leq \delta \leq 60^\circ$ ,  $2.16 < M < 3.54$ ,  $80 < Re < 1800$  (where  $\delta$  is the semi-vertex angle). These results are presented in Figs. 1603.43-1 and 1603.43-2.

The Reynolds number is based on the free stream velocity, density, and viscosity, and the characteristic dimension is the cone slant length. The reference area is the total conical surface area.

The results for cones were obtained from experiments using an insulated base area shielded from the flow; therefore, they apply to the conical surface portion only.

#### 1603.5 Aerodynamic Forces for Typical Bodies (Experimental)

The lift and drag characteristics, as well as some surface pressure distributions, which have been determined for a number of basic geometrical shapes in the slip flow and transition flow regimes are denoted and briefly discussed in the following subsections.

##### 1603.51 The Sphere

Drag characteristics have been determined for spheres (Refs. 31 and 32) over the ranges  $M \sim 0$ ,  $20 < Re < 300$  and  $M \sim 2.5$ ,  $8 < Re_2 < 400$ . These results are presented in Fig. 1603.51-1 in terms of a drag coefficient,  $C_D$ , where the reference area is the projected area,  $\frac{\pi d^2}{4}$ . The Reynolds number,  $Re$ , is based on the velocity, density, and viscosity behind a normal shock wave and the diameter,  $d$ , of the sphere.

1603.52 The Flat Plate

Drag forces on flat plates at zero angle of attack (Refs. 33 and 34) have been determined over the range  $0 < M < 3.80$ ,  $3 < Re < 2000$ . These results are presented in Fig. 1603.52-1 in terms of a drag coefficient based on total drag force, free stream flow conditions, and a reference area taken to be one side of the flat plate. The Reynolds number is based on the free stream flow and the length of the plate. These results apply to flat plates of finite length, and thus contain the induced drag due to the wake at the trailing edge (Ref. 35). Span and thickness effects, however, have been essentially eliminated, so that the results correspond to infinitely thin plates with infinite aspect ratio.

Lift forces for flat plates (Ref. 36) at an angle of attack,  $\alpha$ , have been obtained over the range  $3.70 < M < 4.13$ ,  $630 < Re < 2400$ . These results are given in terms of a normal force coefficient,  $C_N$ , given by

$$C_N = \frac{\text{Normal Force}}{\frac{1}{2} \rho V^2 S}, \quad (1603.52-1)$$

where  $S$  is the plate area, and  $\rho$  and  $V$  are the free stream density and velocity respectively. The Mach number and Reynolds number are based on free stream flow conditions, and the characteristic dimension is the length of the flat plate. It was observed experimentally that  $C_N$  varied linearly with  $\alpha$  in the range  $0 \leq \alpha < 8^\circ$ , so that the quantity

$$C_{N_\alpha} \equiv \frac{dC_N}{d\alpha} \quad (1603.52-2)$$

could be determined. For the inviscid supersonic case and for flat plates of finite aspect ratio,  $A$ , this quantity can be calculated on the basis of linearized theory, i.e.,

$$C_{N_\alpha} (\text{Lin.Th.}) = \left( \frac{4}{\sqrt{M^2 - 1}} \right) \left( 1 - \frac{0.5}{A \sqrt{M^2 - 1}} \right).$$

The experimental results are hence presented in Fig. 1603.52-2 in terms of the ratio  $C_{N_\alpha} / C_{N_\alpha} (\text{Lin.Th.})$ . (See Notes, Item 8.)

1603.53 The Cone

Cone surface pressure variation, due to the thick laminar boundary layer, has been determined (Refs. 37 and 38) over the range  $3.7 < M < 5.8$ ,  $185 < Re < 30,000$ . The cones had  $3^\circ$  and  $5^\circ$  semi-vertex angles and were at zero angle of attack. The local Reynolds number was based on the flow behind an ideal conical shock and the cone slant length from vertex to pressure orifice. These results are presented

in Fig. 1603.53-1 in terms of the variation of a local fractional pressure increase with the local Reynolds number. The fractional pressure increase is expressed as

$$\frac{p - p_{(\text{ideal})}}{p_{(\text{ideal})}}, \quad (1603.53-1)$$

where  $p$  is the cone surface pressure and  $p_{(\text{ideal})}$  is the theoretical inviscid pressure on the cone surface.

Cone drag forces for cones at zero angle of attack and  $15^\circ$  semi-vertex angle have been determined (Ref. 39) over the range  $M \sim 2$ ,  $75 < Re < 1800$ ;  $M \sim 4$ ,  $500 < Re < 7000$ . Only the tip region was investigated; hence the shoulder effect was not present and the cones were essentially infinite in length. The results are presented in Fig. 1603.53-2 in terms of the increase in the drag coefficient,  $C_D - C_{D(\text{ideal})}$ , over and above the inviscid supersonic drag coefficient,  $C_{D(\text{ideal})}$ , at the test Mach number. The drag coefficient,  $C_D$ , is based on free stream flow conditions, the projected cone surface area, and the total measured drag. It thus consists partly in skin friction drag and partly in wave drag. The curves indicated in Fig. 1603.53-2 are taken from theory (Ref. 40). (See Notes, Item 9.)

#### 1603.54 Base Pressures

The variation of base pressure on a cone-cylinder configuration at zero angle of attack has been determined (Refs. 41, 42, and 43) over a very large range of Reynolds numbers. The Reynolds numbers were based on free stream flow conditions and the model length. The configuration consisted of a cone of  $30^\circ$  semi-vertex angle followed by a cylindrical afterbody so that the over-all length diameter ratio was 10:3. The results are presented in Fig. 1603.54-1 in terms of the ratio of base pressure,  $p_b$ , to ambient pressure,  $p_\infty$ , versus the Reynolds number. In the lower Reynolds number range the pressure varied considerably with radius over the base region. The base pressures in the figure are area averages.

#### 1603.55 Impact Probe Measurements

At low Reynolds numbers the pressure at the forward stagnation point of a two- or three-dimensional body increases above the value of the local stagnation pressure. The effect depends upon the Mach number and Reynolds number, as well as the geometry of the body. This effect is particularly important in connection with the interpretation of impact or total head probes. Early experiments in incompressible flow were carried out by Homann (Ref. 44). More recent experiments have been carried out by Kane and Maslach (Ref. 45) and Sherman (Ref. 46). The results (Ref. 46) for subsonic flow are presented in Fig. 1603.55-1 in terms of the pressure coefficient versus Reynolds number, based on free stream flow conditions and the probe diameter. The results for the supersonic case (Ref. 46) are presented in Figs. 1603.55-2 and 1603.55-3 in terms of the ratio of the measured impact pressure to the ideal value, i.e., the stagnation pressure behind a normal shock wave at the free stream Mach number. (See Notes, Item 10.)

## SECTION 16 MECHANICS OF RAREFIED GASES

## Notes

Some of the more important theoretical and experimental results which have appeared since the preparation of this manuscript and which could not be included in the body of the text are listed below.

1. Calculations of the drag and heat transfer for a sphere in the near-free molecular flow range are given in

Baker, R. M. L. and Charwat, A. F. "Transitional Correction to the Drag of a Sphere in Free Molecule Flow," Phys. of Fluids, Vol. 1 (March-April 1958), pp. 73-81.

Hammerling, P. and Kivel, B. "Heat Transfer to a Sphere at the Transition from Free Molecule Flow," Phys. of Fluids, Vol. 1 (July-August 1958), p. 357.

2. A discussion of the regimes of flow for highly cooled blunt bodies is given in

Adams, Mac C. and Probst, R. F. "On the Validity of Continuum Theory for Satellite and Hypersonic Flight Problems at High Altitudes," Jet Propulsion, Vol. 28 (February 1958), pp. 86-90.

3. The estimated properties of the upper atmosphere are undergoing considerable revision as a result of satellite measurements. For a discussion of some of these measurements and references, see

La Gow, H. E. and Horowitz, R. "Comparison of High Altitude Rocket and Satellite Density Measurements," Phys. of Fluids, Vol. 1 (November-December 1958), pp. 478-479.

4. A few measurements of the variation with speed of the accommodation coefficients of several gases on engineering surfaces are given in

Devienne, F. M. "An Experimental Study of the Stagnation Temperature in a Free Molecular Flow," J. Aeronaut. Sci., Vol. 24 (June 1957), pp. 403-406.

Rotating cylinder measurements of the slip coefficient  $\sigma$  indicate that its value may depend on the pressure "history" of the surface. See

Merlic, E. An Experimental Determination of Reflection Coefficients for Air on Aluminum. Report HE-150-141. University of California Engineering Project, August 1956.

5. The aerodynamic stability characteristics of a wedge at angle of attack in free molecular flow have been computed. Results are given in

King, H. H. Static Stability Analysis for a Wedge in Free Molecule Flow. Report HE-150-165. University of California Engineering Project, December 1958.

6. The most recent experiments and theory indicate that the Navier-Stokes and Burnett equations give about the same results in the regime of slight rarefaction. See

Talbot, L. and Sherman, F. S. Structure of Weak Shock Waves in a Monatomic Gas. NASA Memo. 12-14-58W, January 1959.

Greenspan, M. "Propagation of Sound in Five Monatomic Gases," J. Acoust. Soc. Am., Vol. 28 (July 1956), pp. 644-648.

7. Local heat transfer measurements on the surface of a circular cylinder perpendicular to a low density flow are reported in

Tewfik, O. and Giedt, W. H. Heat Transfer, Recovery Factor and Pressure Distributions Around a Cylinder Normal to a Supersonic Rarefied Gas Stream. Report HE-150-162. University of California Engineering Project, January 1959.

8. Considerable data are available for the induced pressures on flat plates. See, for example,

Aroesty, J. Induced Pressures on Flat Plates at  $M = 4$  in Low Density Flow. Report HE-150-156. University of California Engineering Project, July 1958.

9. Pressure distributions on spherically-blunted cones in low density flow are reported in

Talbot, L., Schaaf, S. A., and Hurlbut, F. C. "Pressure Distributions on Blunt-Nosed Cones in Low Density Hypersonic Flow," Jet Propulsion, Vol. 28 (December 1958), pp. 832-833.

Aerodynamic characteristics of a cone-cylinder configuration are given in

Nark, T. Lift and Drag on Cone Cylinders. Report HE-150-154. University of California Engineering Project, December 1957.

Lift, drag, and pitching moment characteristics of a pointed cone at angle of attack in a low density flow are reported in

Langelo, V. and Lengyel, A. Aerodynamic Coefficients of a  $9^\circ$  Half-Angle Pointed Cone in Rarefied Gas Flow. Report No. 538-270. General Electric Company, May 1958.

10. Additional data on impact probe corrections can be found in

Matthews, M. L. An Experimental Investigation of Viscous Effects on Static and Impact Pressure Probes in Hypersonic Flow. GALCIT Hypersonic Research Project Memorandum No. 44. Guggenheim Aeronautical Laboratory, California Institute of Technology, June 1958.

1601.3 Table I

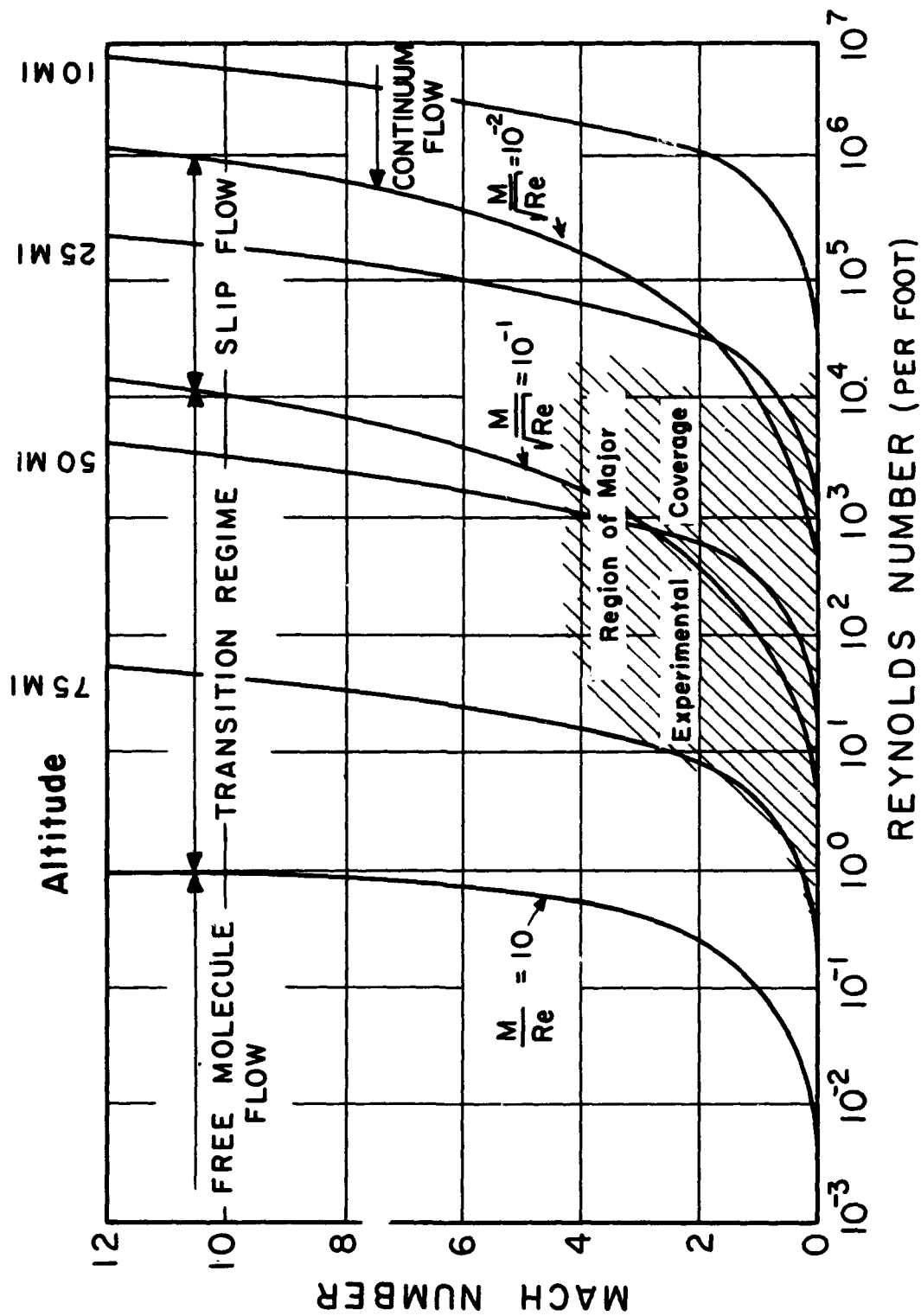
Thermal accommodation coefficient,  $\bar{\alpha}$ , for air (Ref. 7)

<u>Surface</u>	<u><math>\bar{\alpha}</math></u>
Flat lacquer on bronze	0.88-0.89
Polished bronze	0.91-0.94
Machined bronze	0.89-0.93
Etched bronze	0.93-0.95
Polished cast iron	0.87-0.93
Machined cast iron	0.87-0.88
Etched cast iron	0.89-0.96
Polished aluminum	0.87-0.95
Machined aluminum	0.95-0.97
Etched aluminum	0.89-0.97

1601.3 Table II

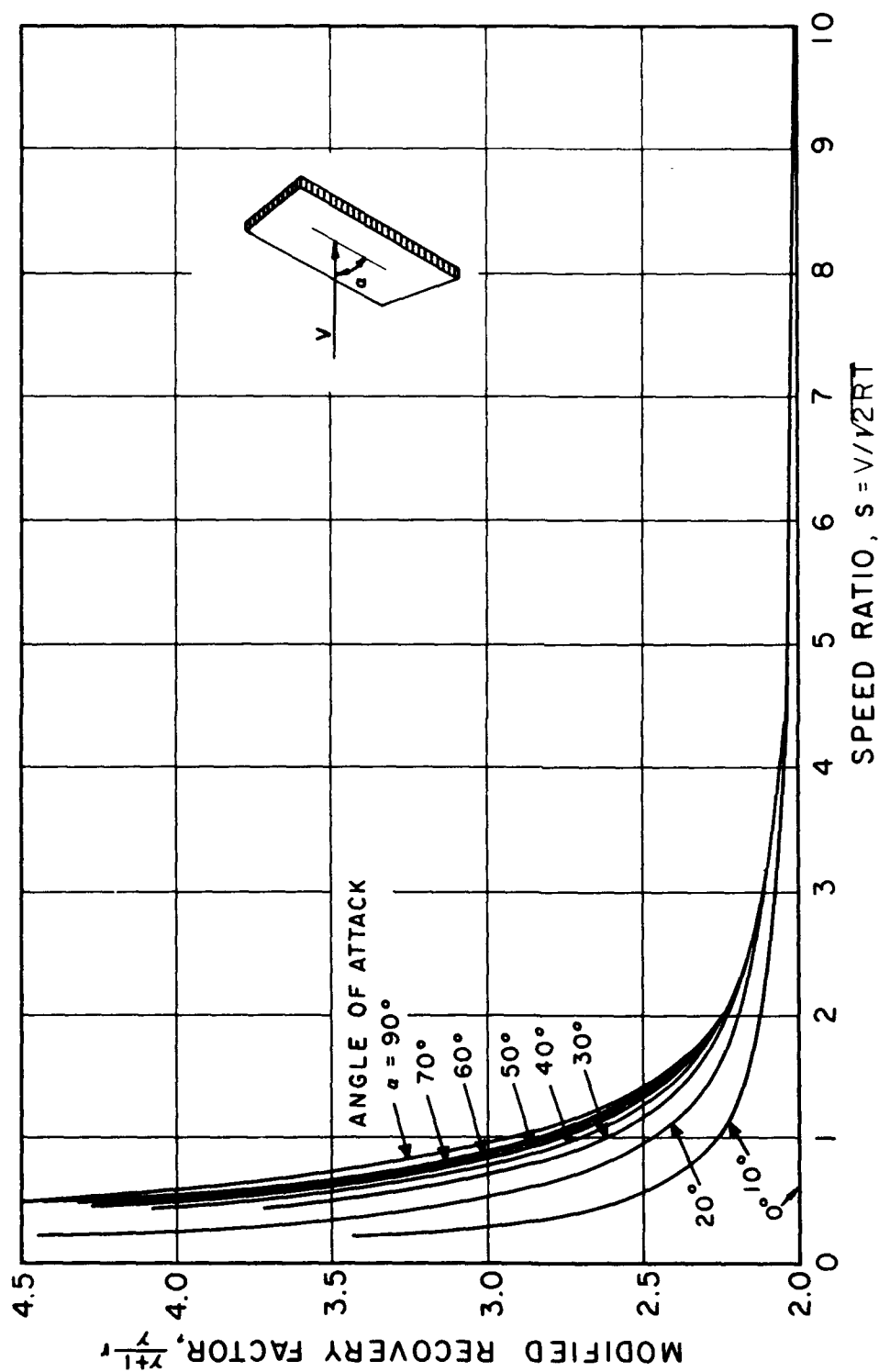
Values of reflection coefficient,  $\sigma$ , (Ref. 8)

<u>Gas and Surface Condition</u>	<u><math>\sigma</math></u>
Air or CO <sub>2</sub> on machined brass or old shellac	1.00
Air on oil	0.895
CO <sub>2</sub> on oil	0.92
H <sub>2</sub> on oil	0.93
Air on glass	0.89
He on oil	0.87
Air on fresh shellac	0.79

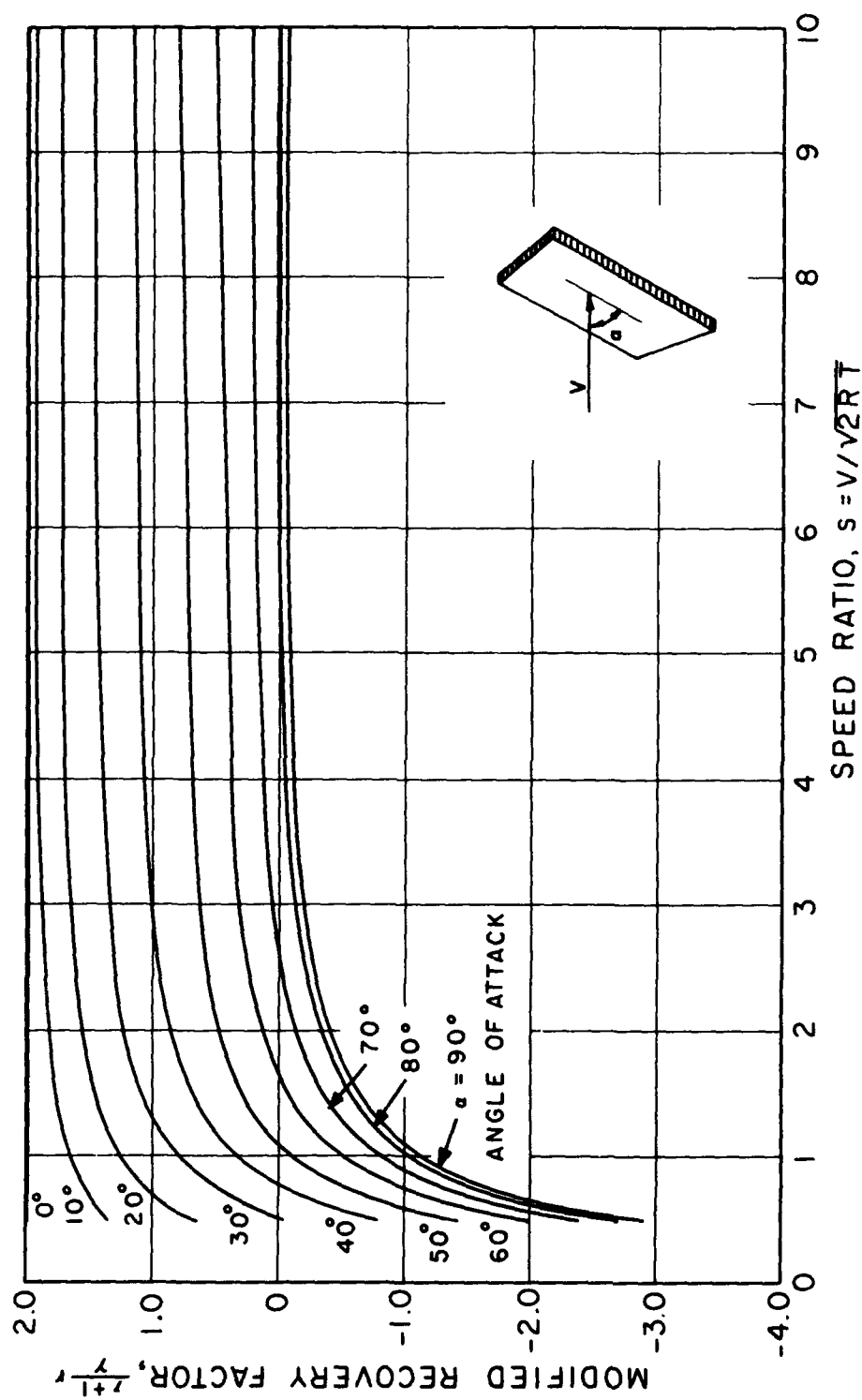


1601.2 Figure 1. The regimes of gas dynamics.

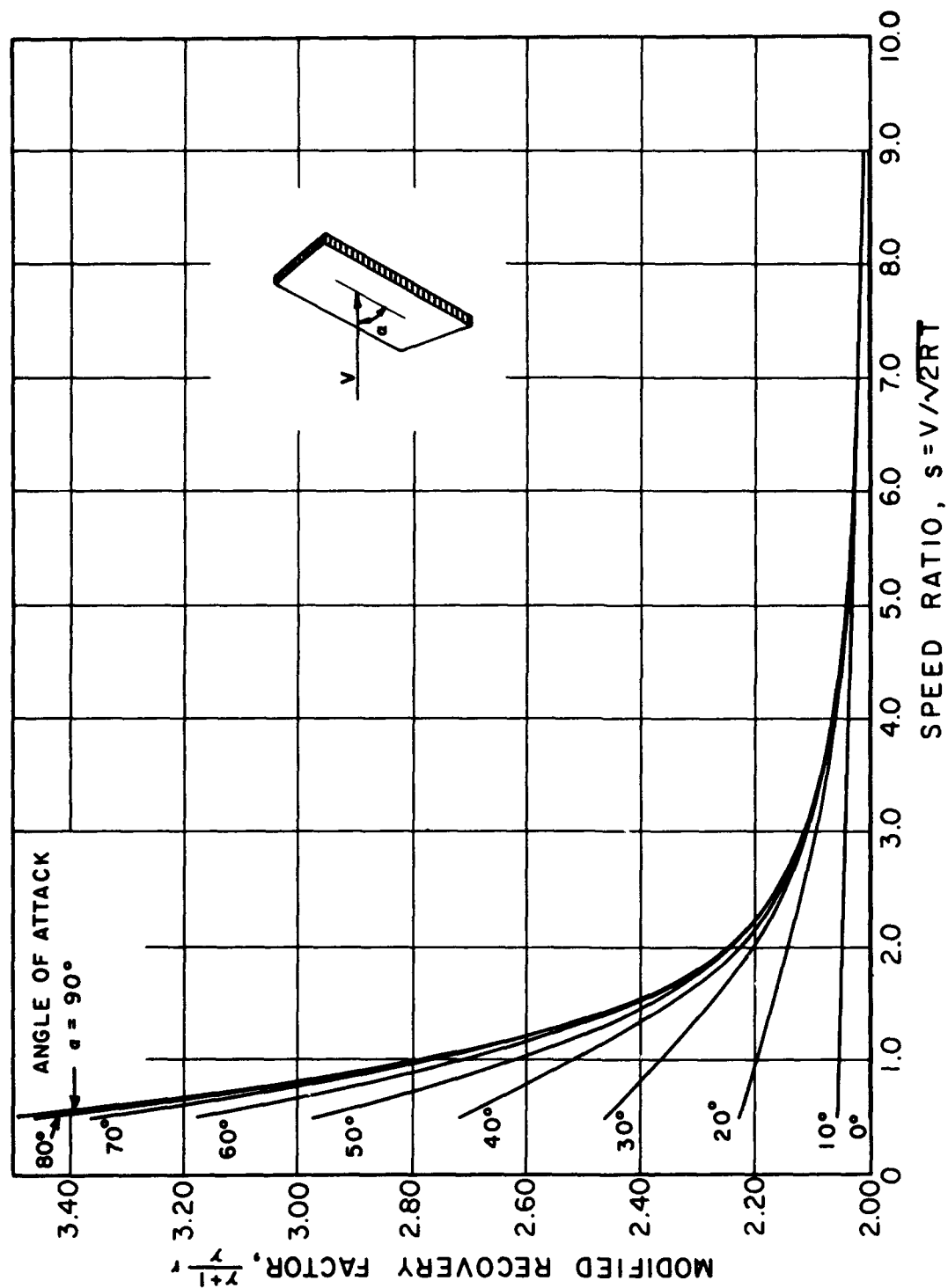




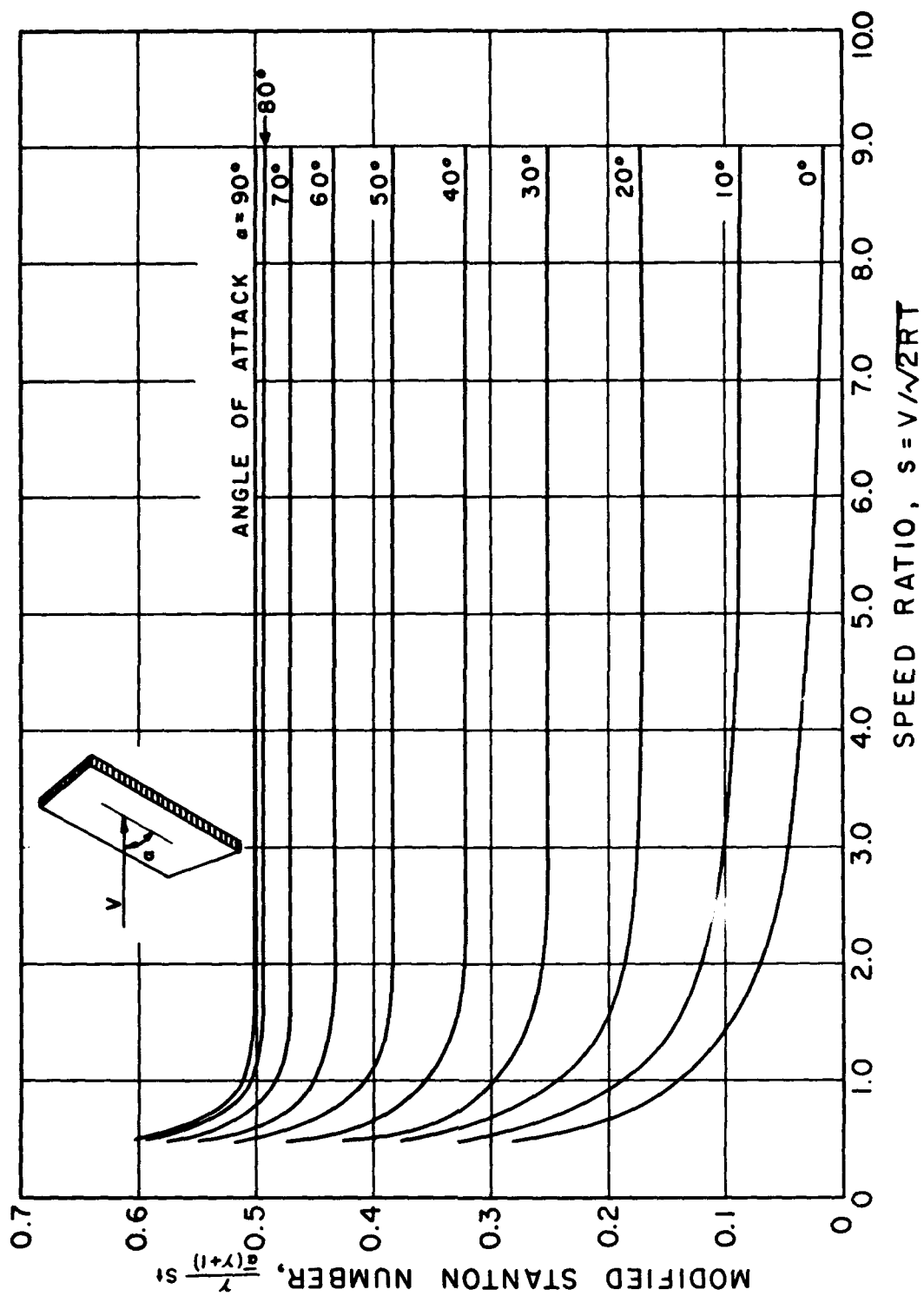
1602.31 Figure 1. Modified recovery factor for the front side of an insulated flat plate in free molecular flow.



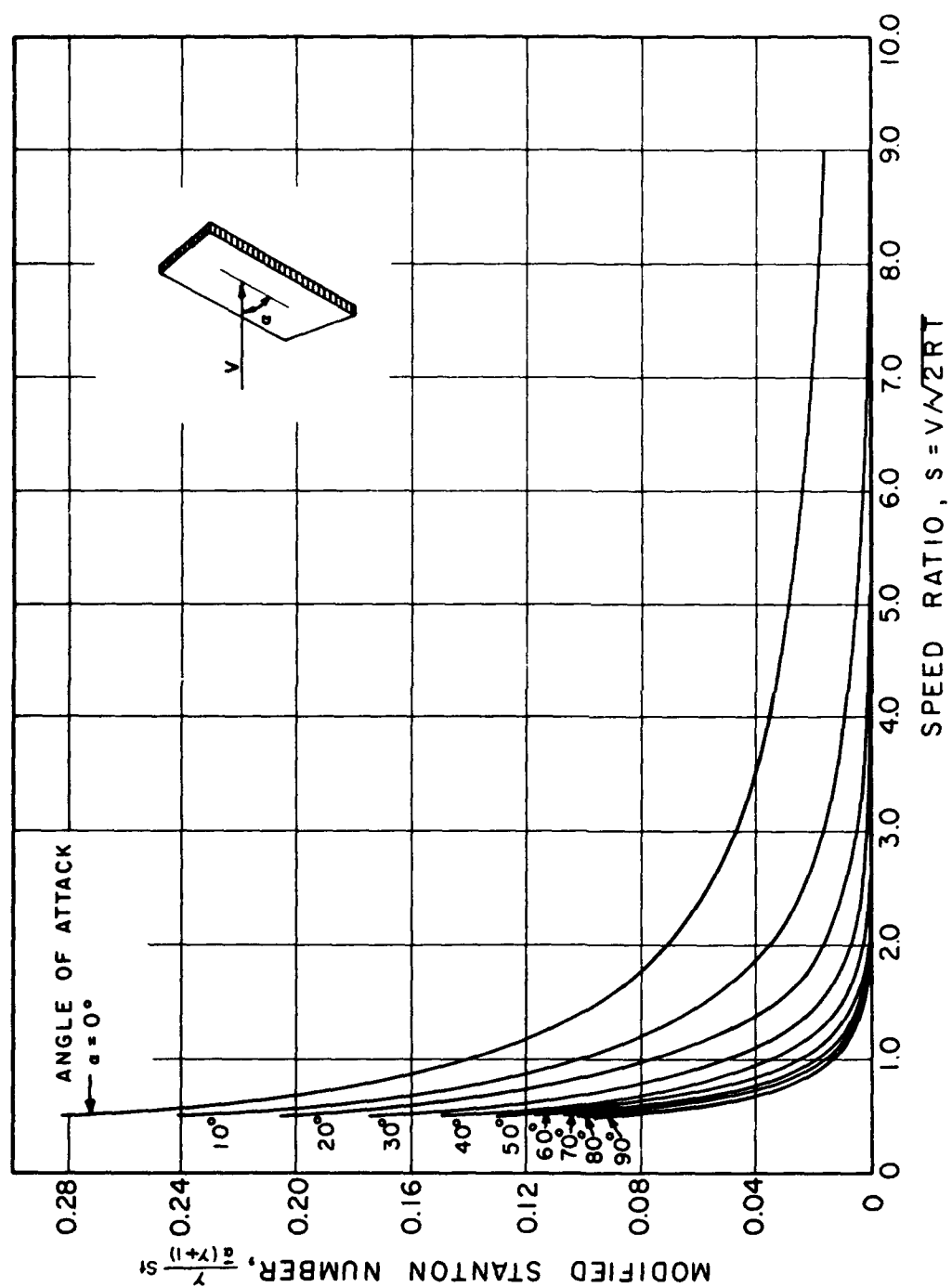
1602.31 Figure 2. Modified recovery factor for the back side of an insulated flat plate in free molecular flow.



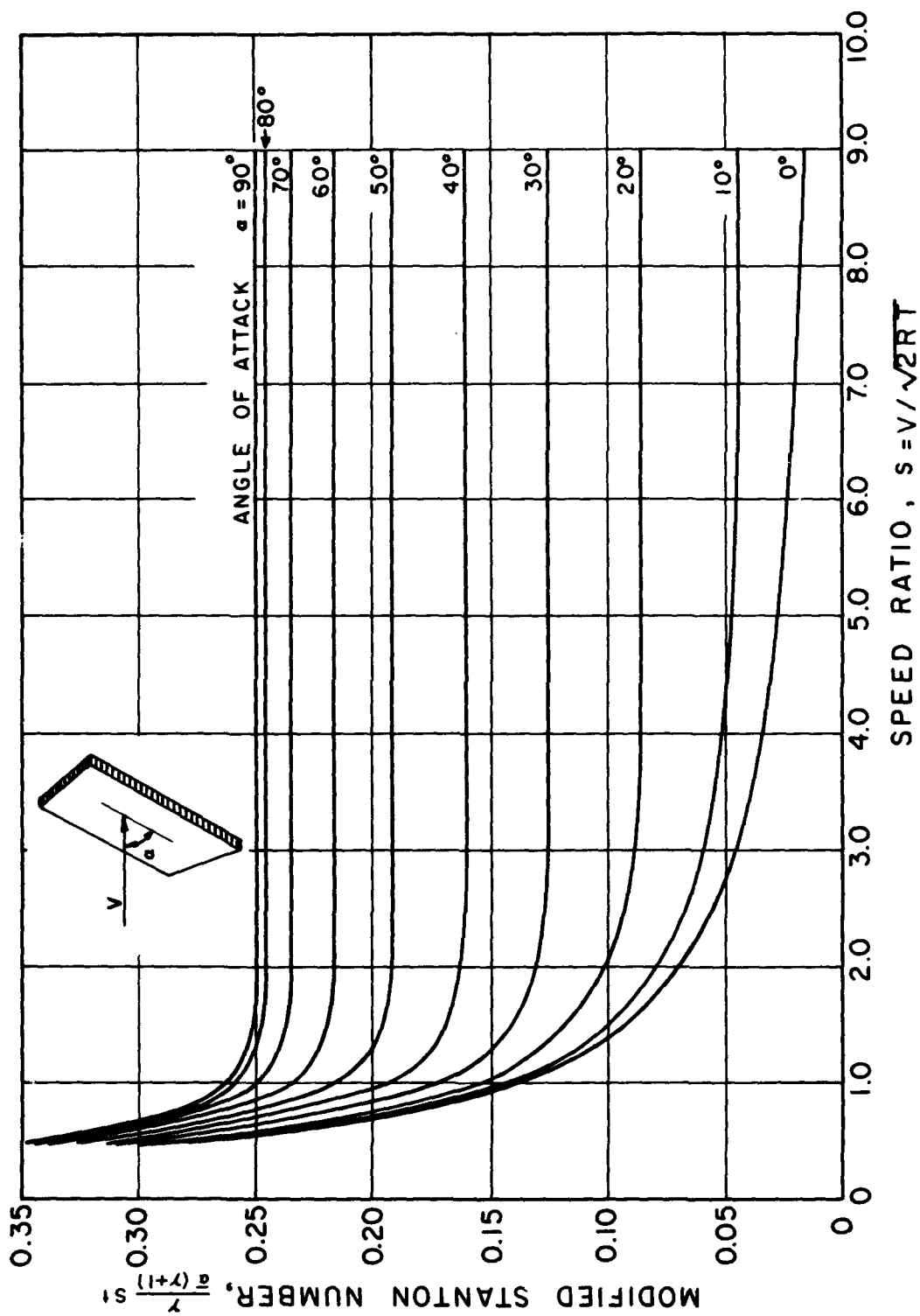
1602,31 Figure 3. Modified recovery factor for a flat plate in free molecular flow with the front and back surfaces in thermal contact.



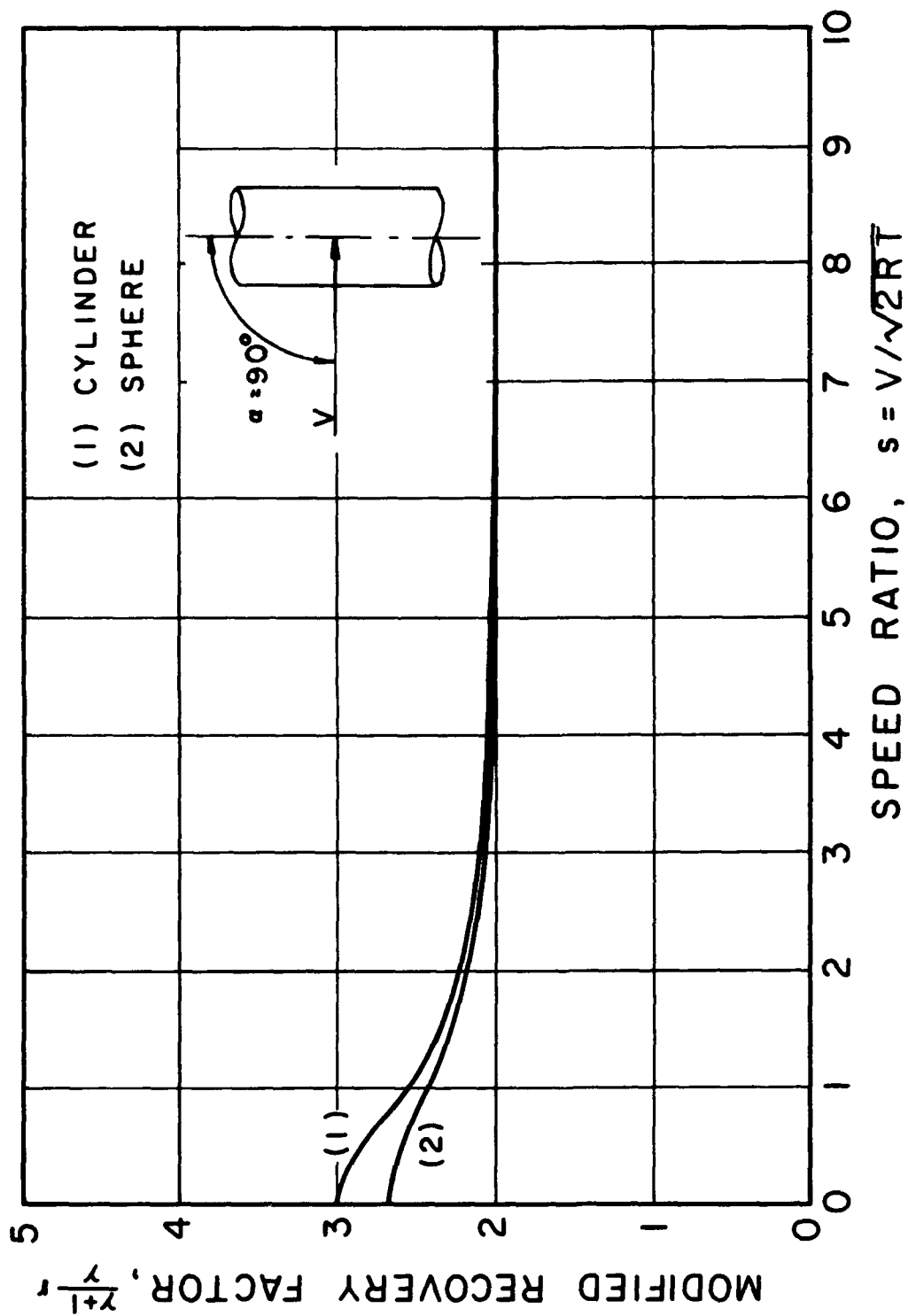
1602.31 Figure 4. Modified Stanton number for the front side of an insulated flat plate in free molecular flow.



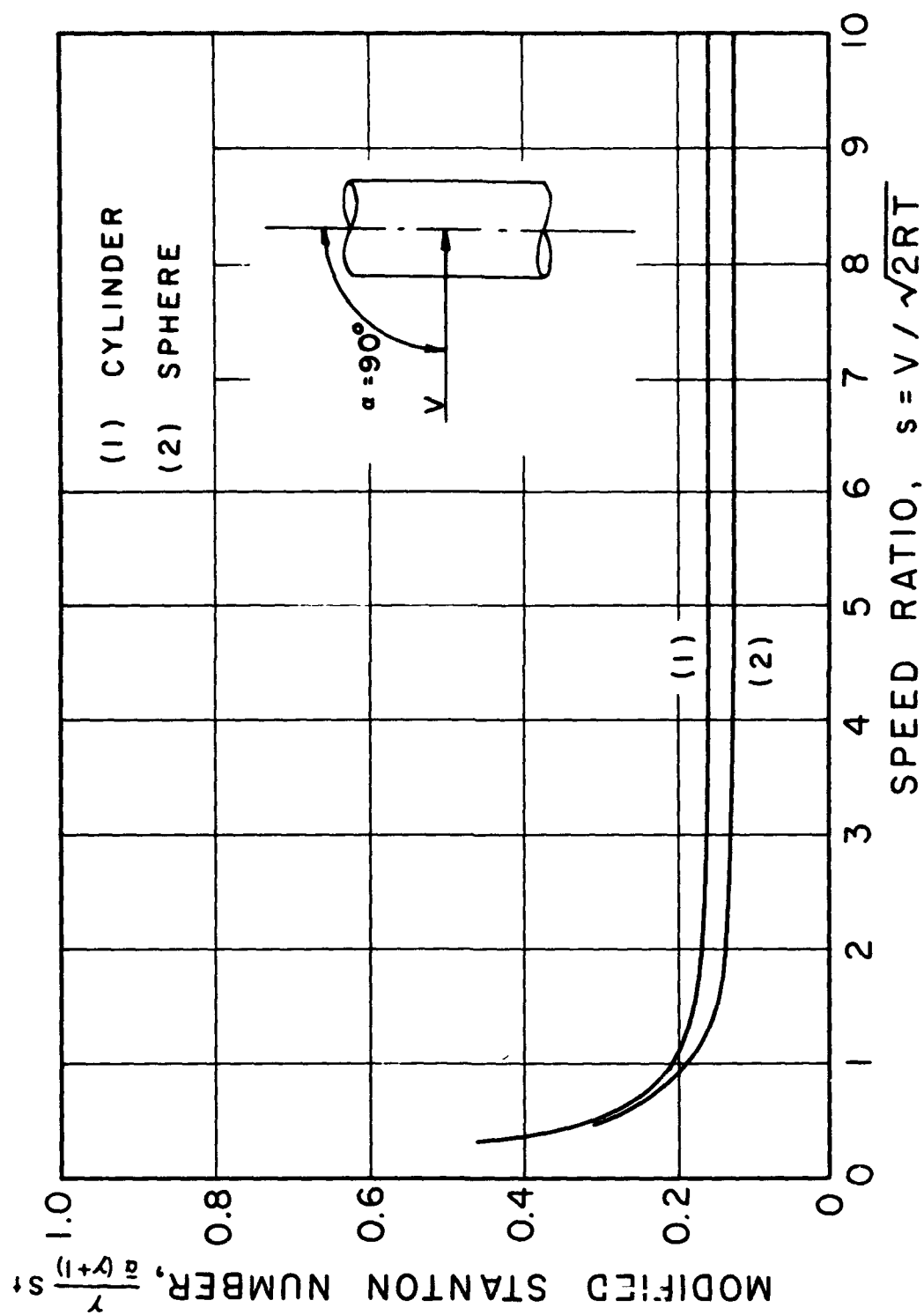
1602.31 Figure 5. Modified Stanton number for the back side of an insulated flat plate in free molecular flow.



1602.31 Figure 6. Modified Stanton number for a flat plate in free molecular flow with the front and back surfaces in thermal contact.

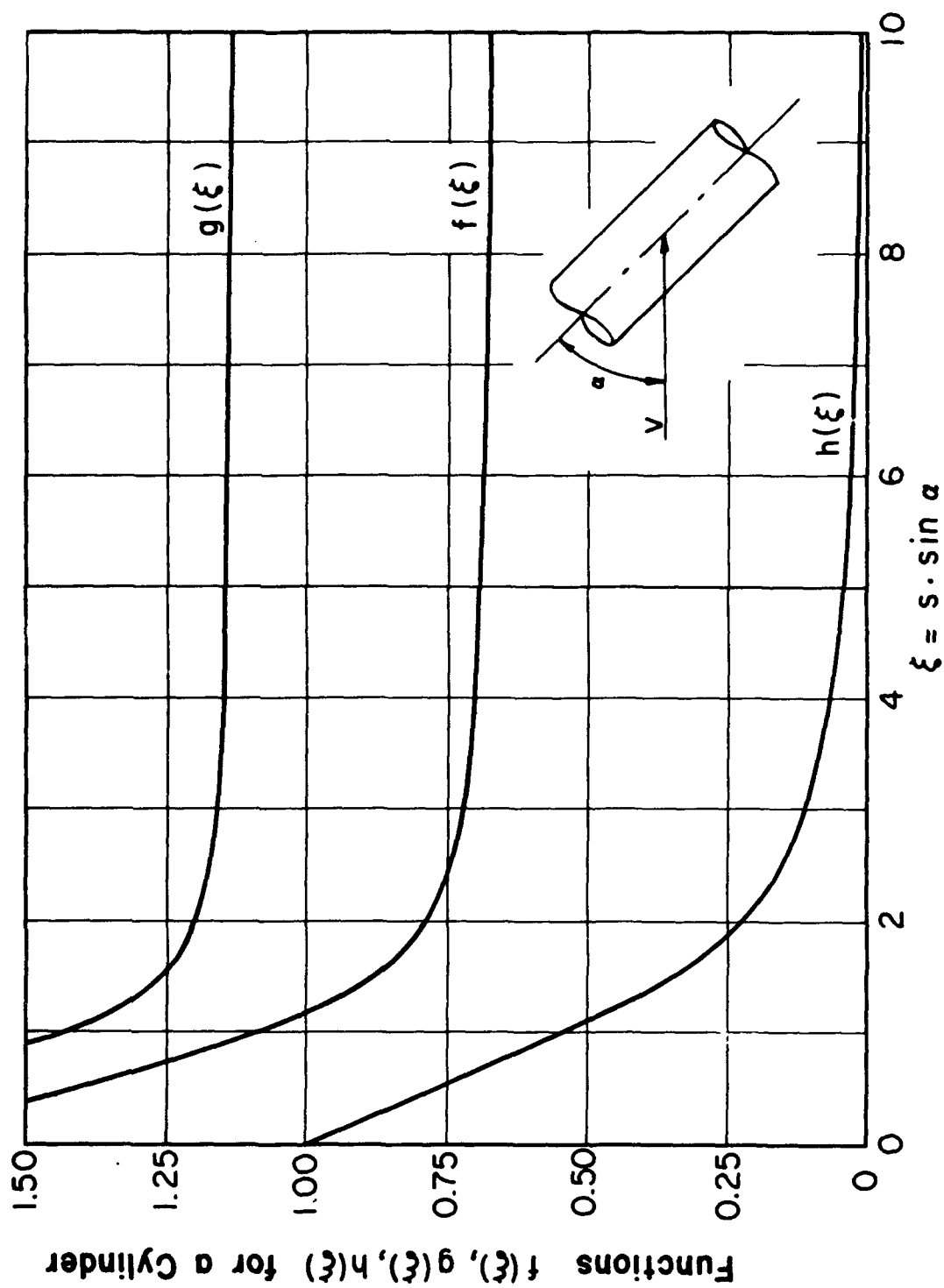


1602.32 Figure 1. Modified recovery factor for a sphere and a cylinder transverse to the flow direction in free molecular flow.

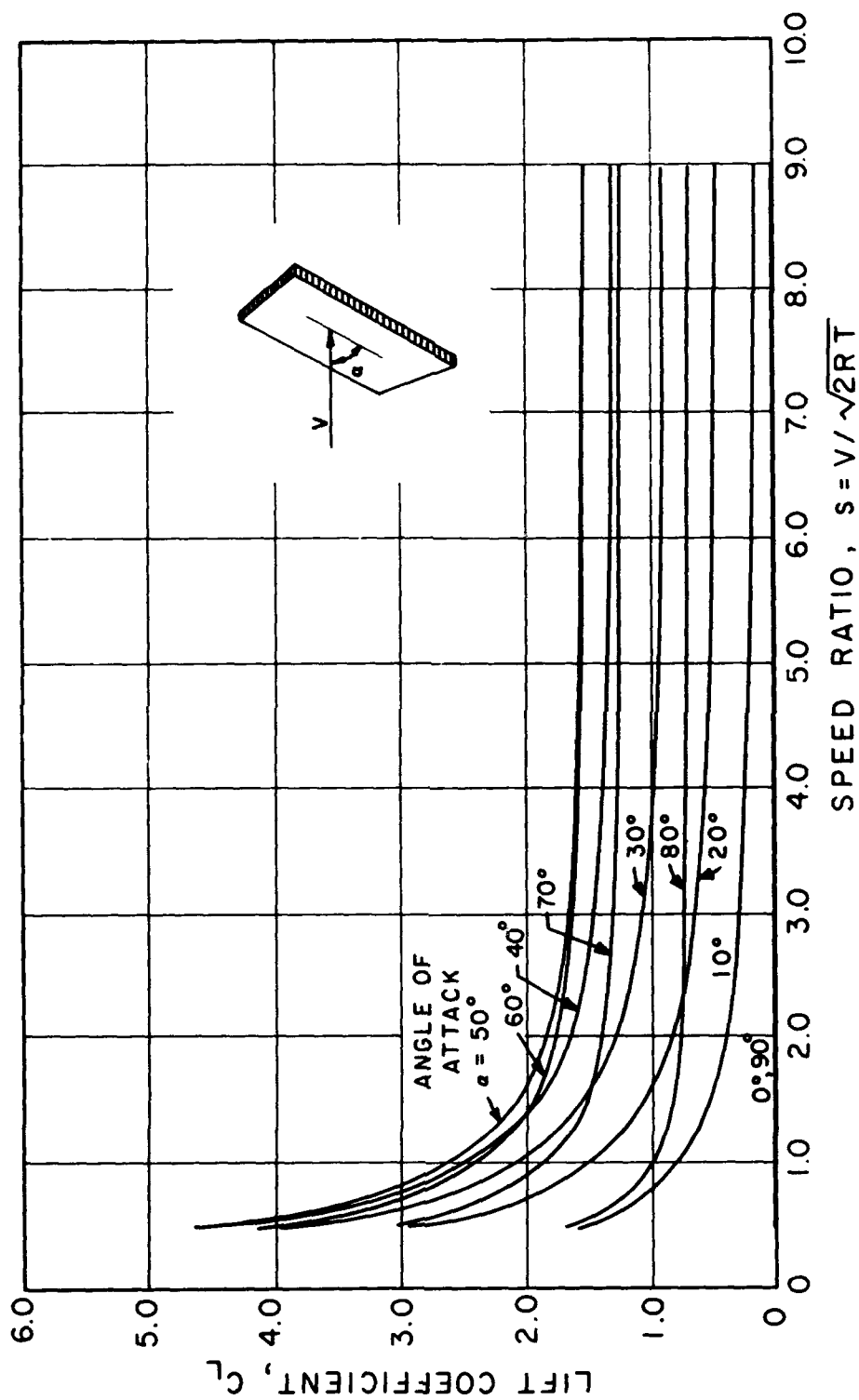


1602.32 Figure 2. Modified Stanton number for a sphere and a cylinder transverse to the flow direction in free molecular flow.

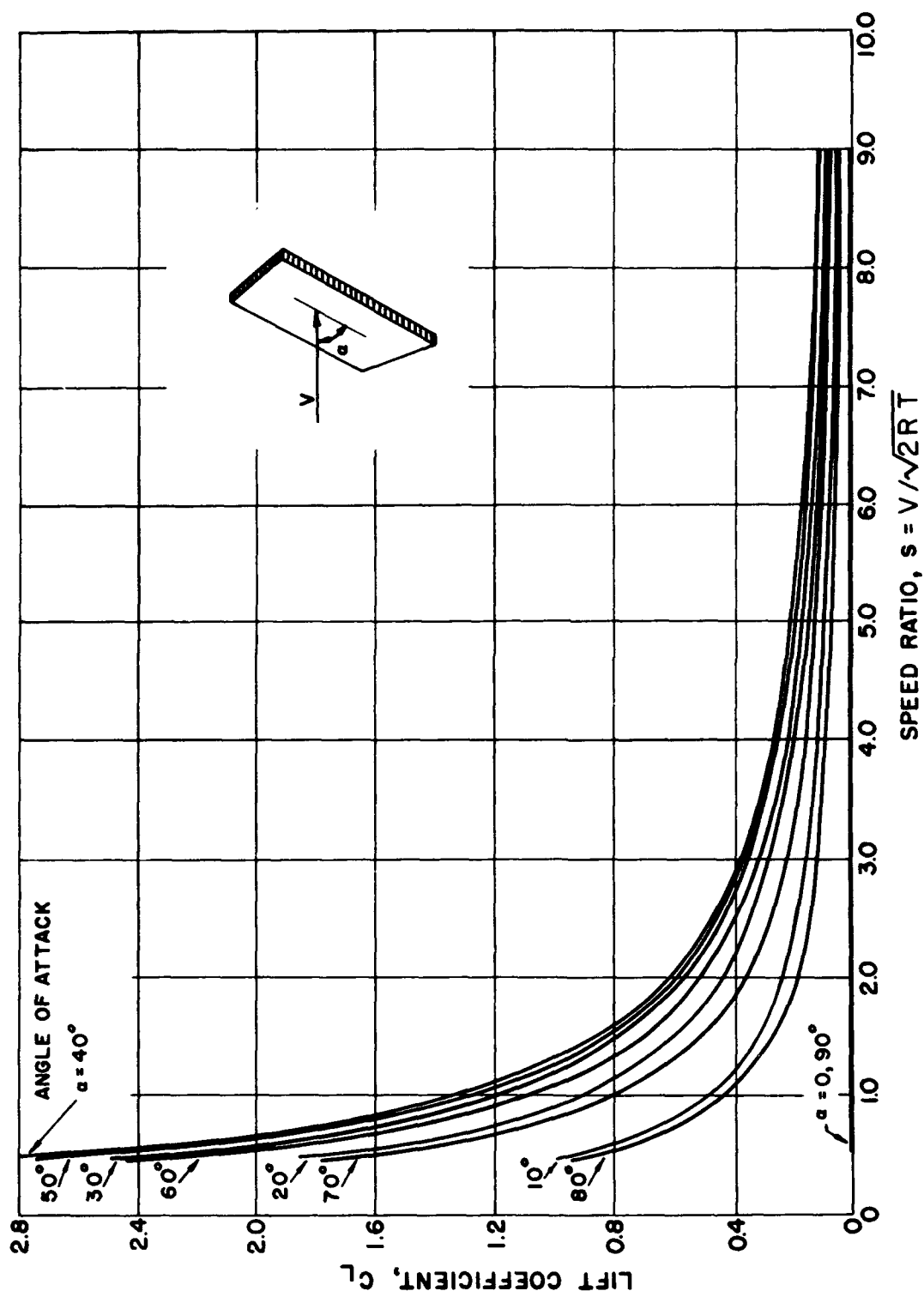




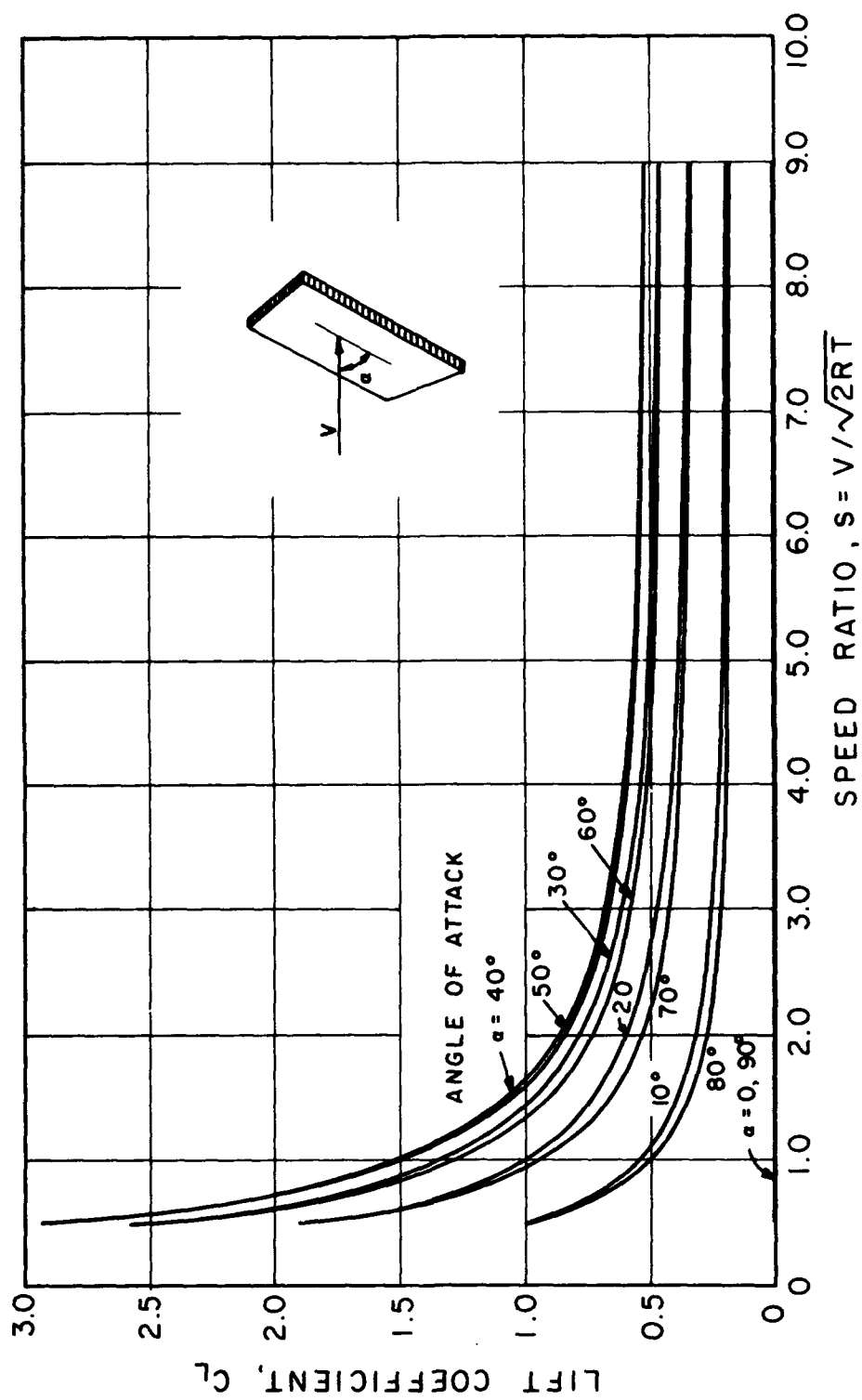
1602.32 Figure 3. Functions for the determination of the recovery factor and the Stanton number for the cylinder as a function of the angle of attack,  $\alpha$ .



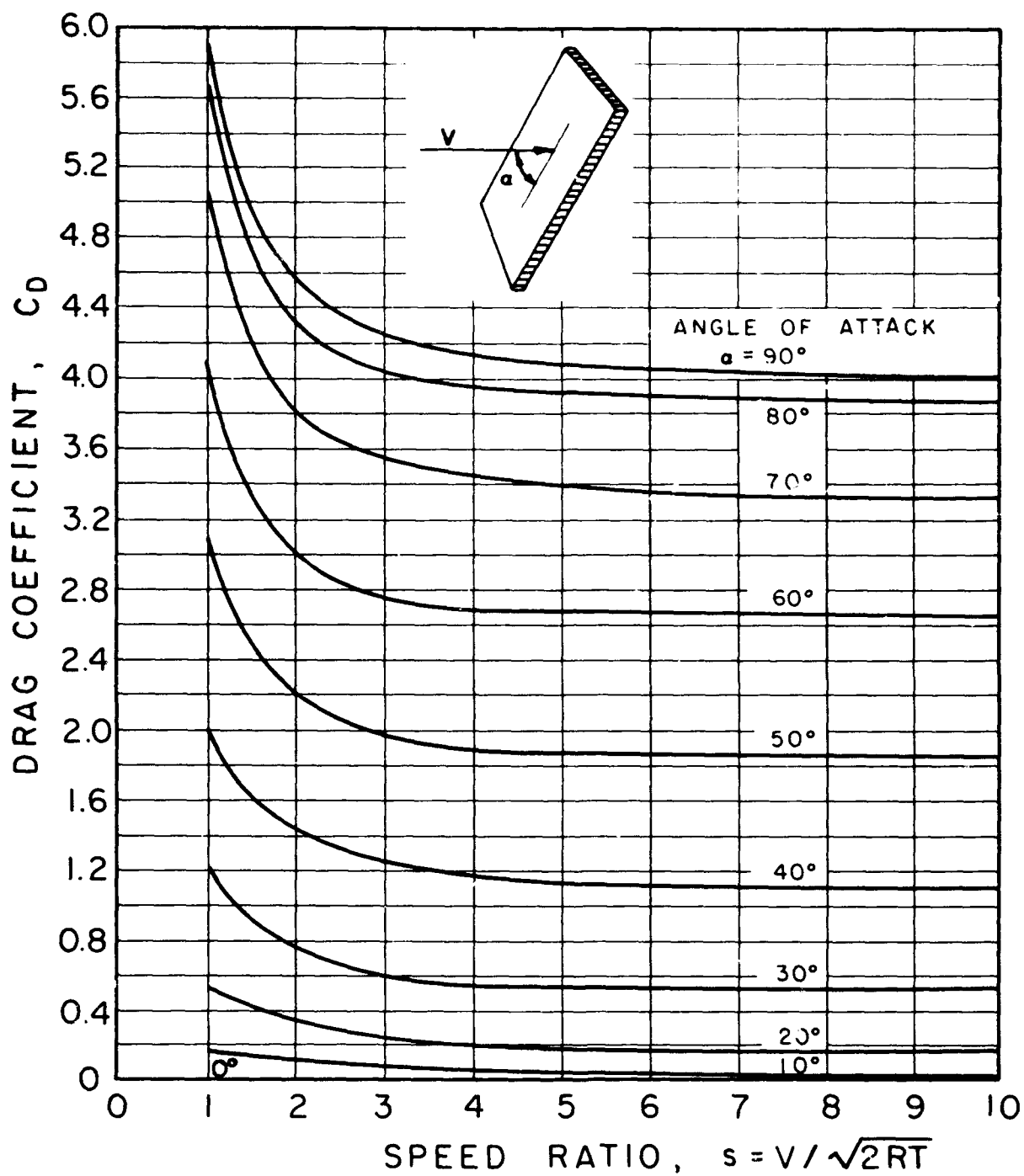
1602.4 Figure 1. Lift coefficients for a flat plate in free molecular flow:  $\sigma = \sigma' = 0$ .



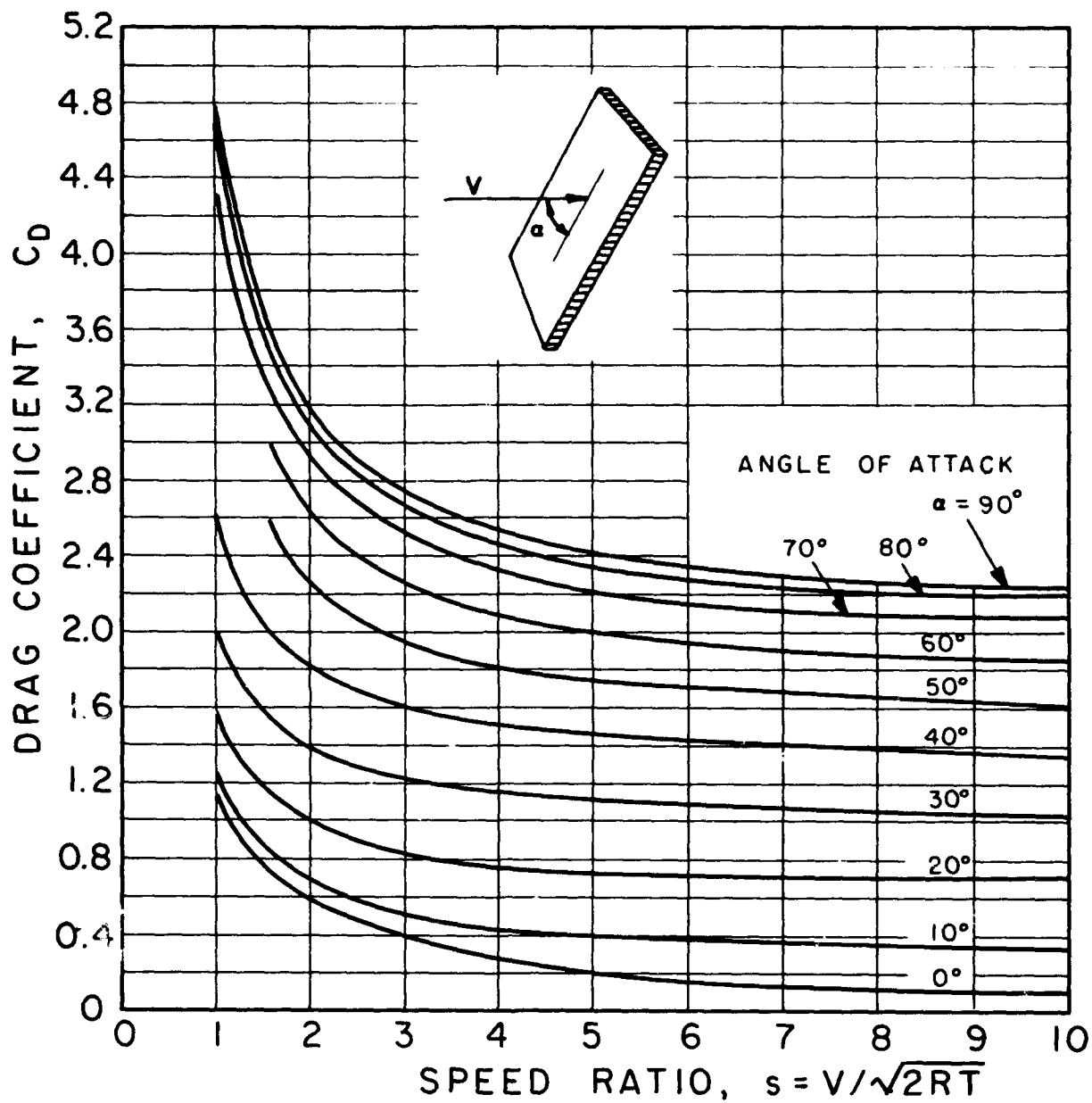
1602.4 Figure 2. Lift coefficients for a flat plate in free molecular flow:  $\sigma = \sigma' = 1$  and  $T_w = T_\infty$ .



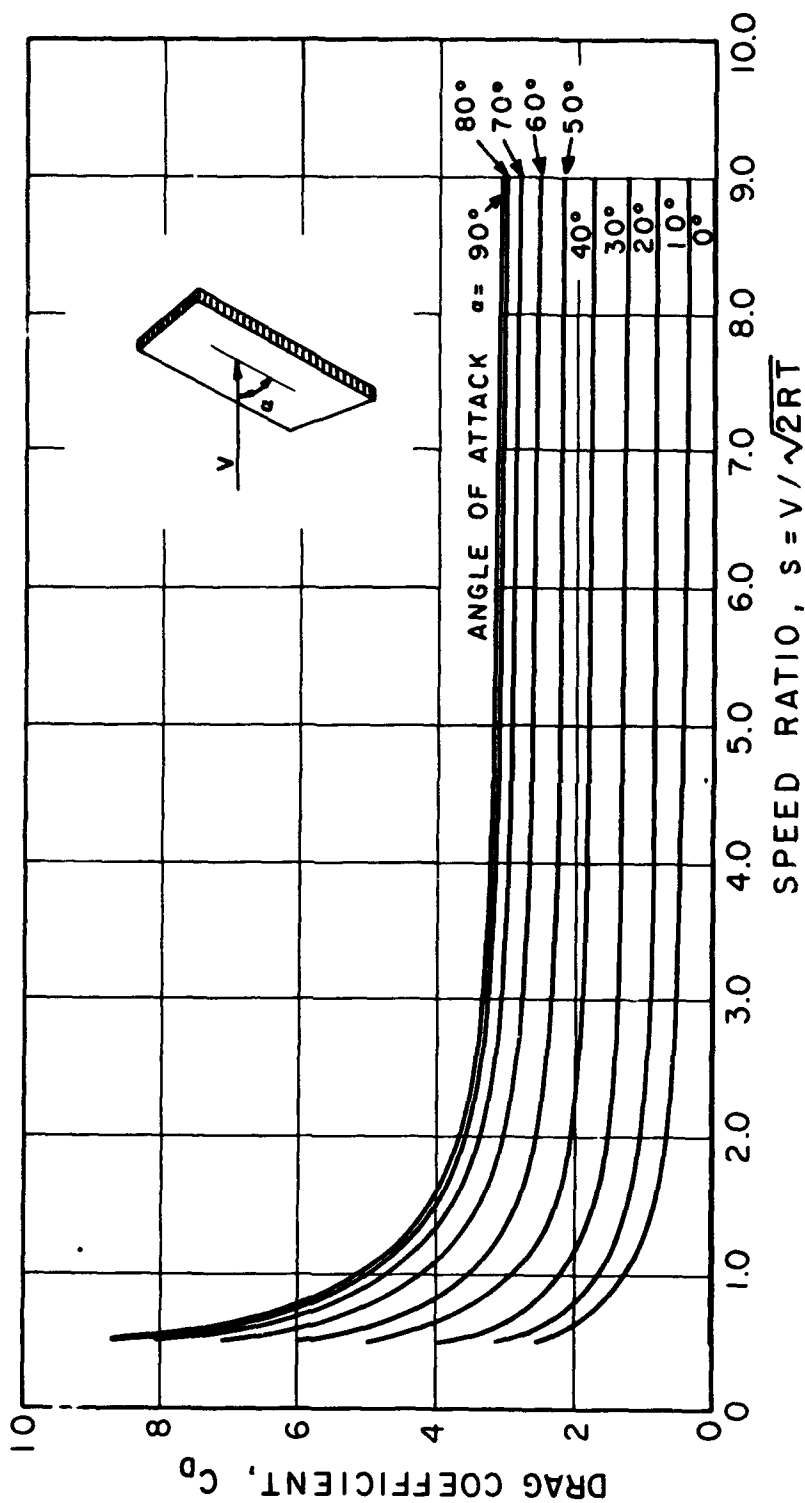
1602.4 Figure 3. Lift coefficients for a flat plate in free molecular flow:  $\sigma = \sigma' \approx 1$  and  $T_w = T_w(\text{eq.})$ .



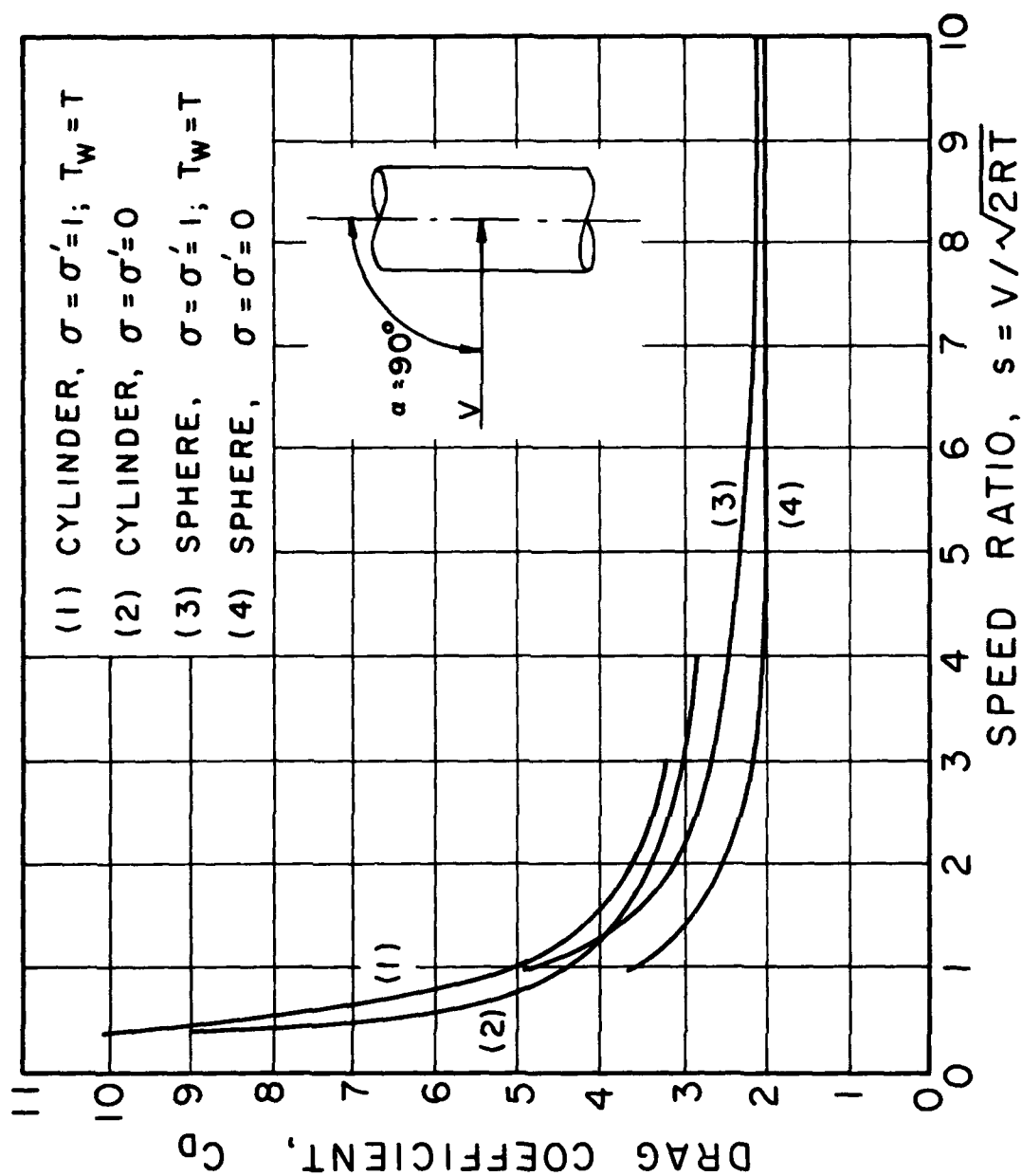
1602.4 Figure 4. Drag coefficients for a flat plate in free molecular flow:  $\sigma = \sigma' = 0$ .



1602.4 Figure 5. Drag coefficients for a flat plate in free molecular flow:  $\sigma = \sigma' = 1$  and  $T_w = T_\infty$ .

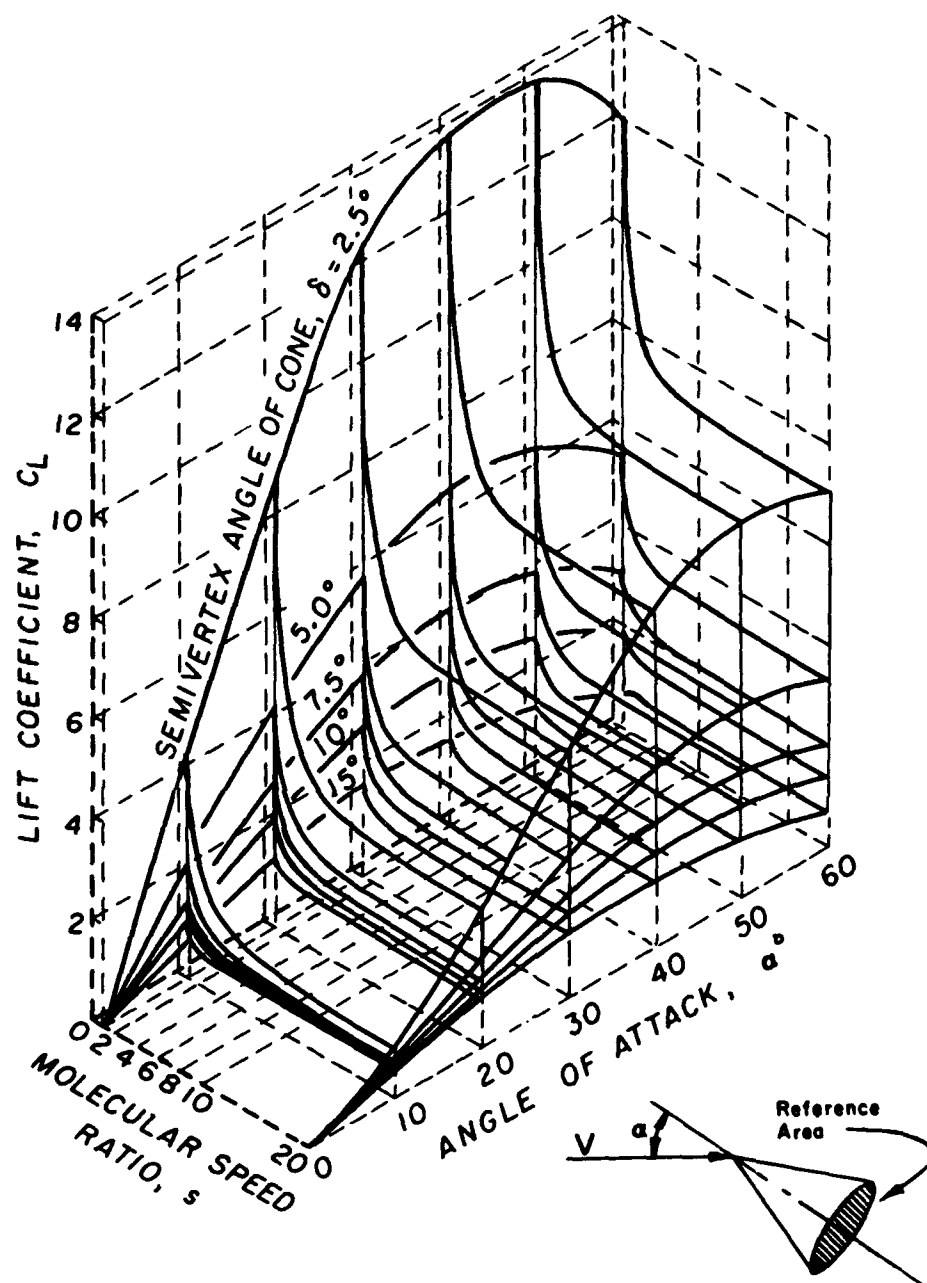


1602.4 Figure 6. Drag coefficients for a flat plate in free molecular flow:  
 $\sigma = \sigma' = 1$  and  $T_w = T_w(\text{eq.})$ .

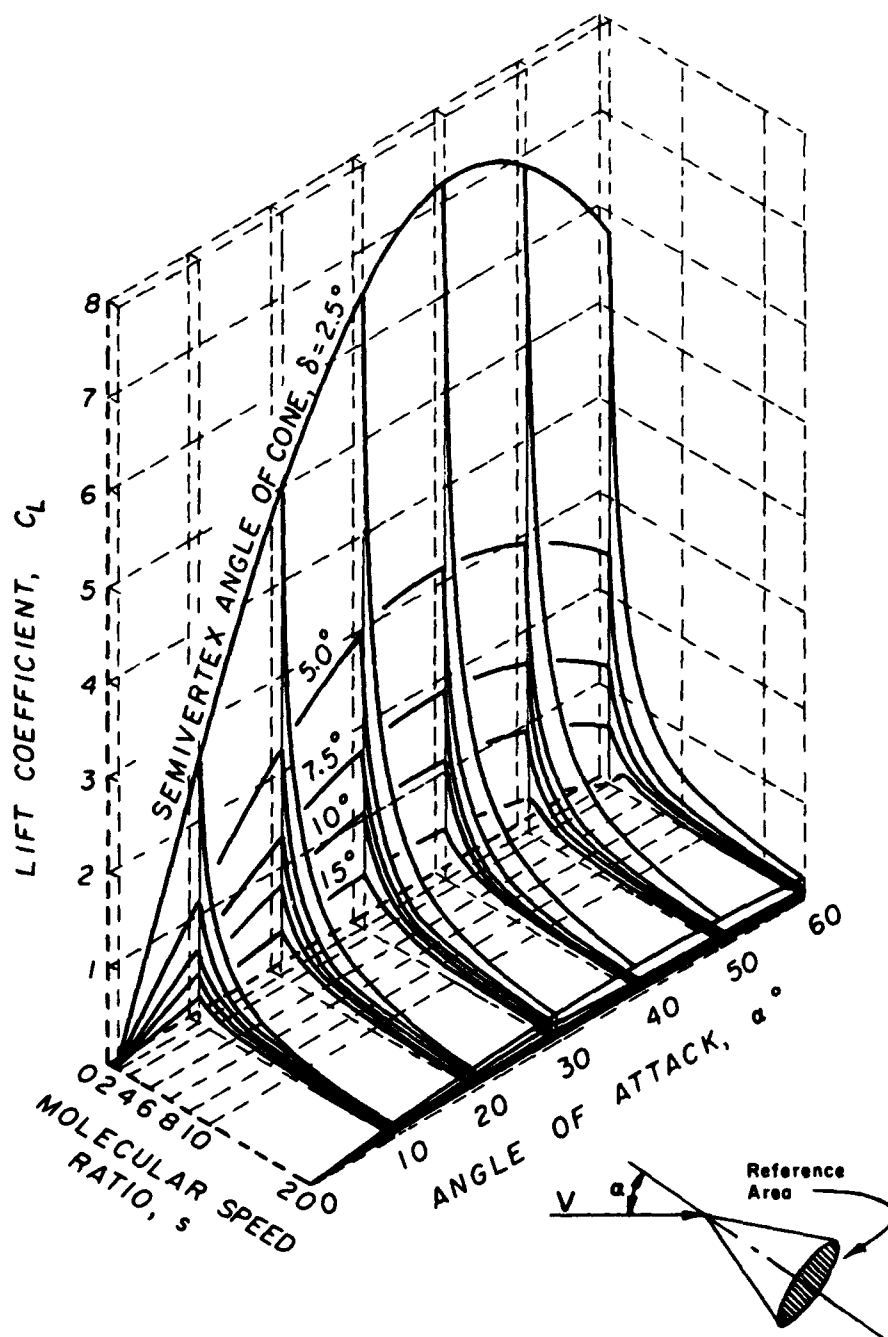


1602.4 Figure 7. Drag coefficients for a sphere and a cylinder transverse to the flow direction in free molecular flow.

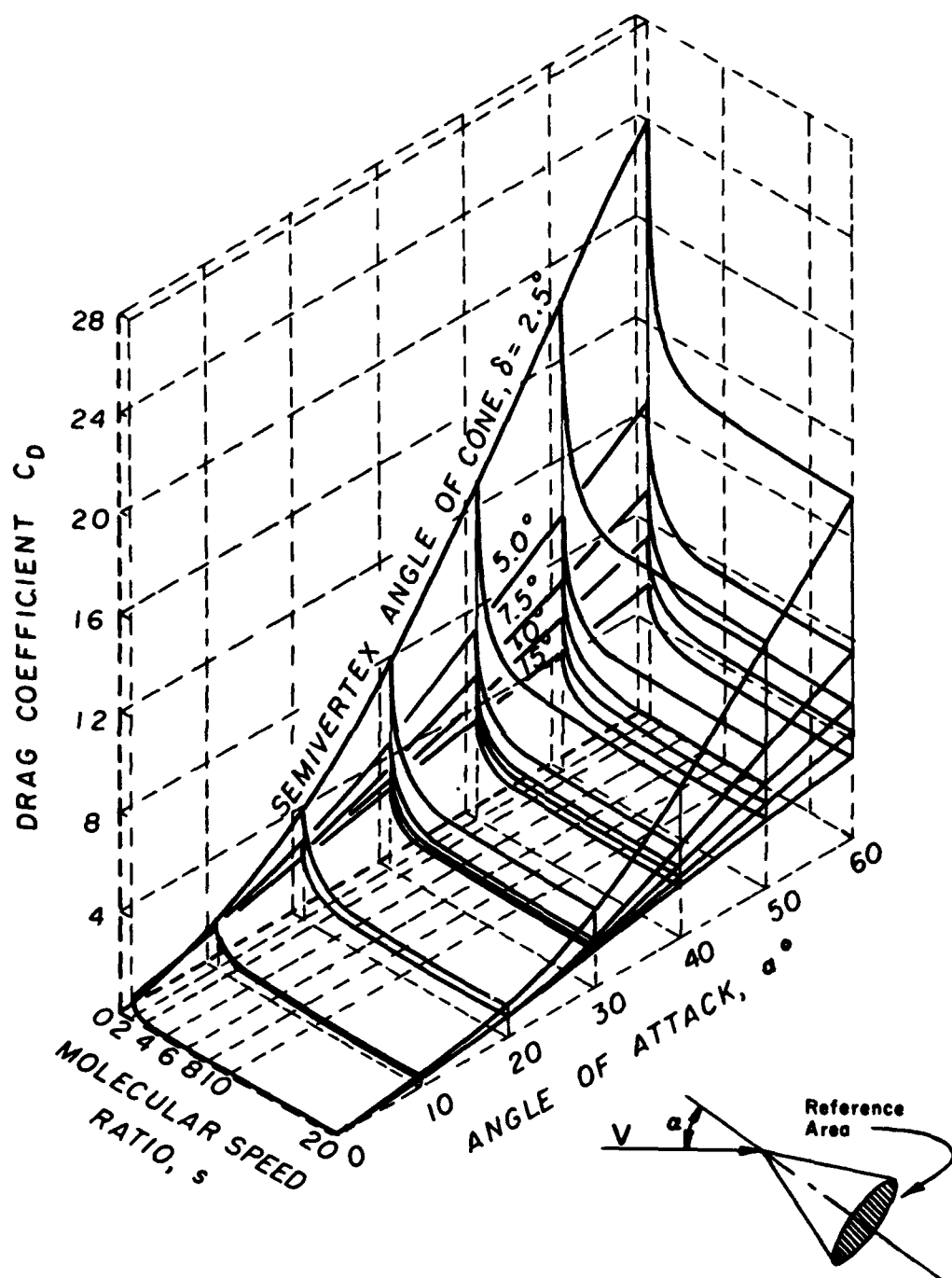




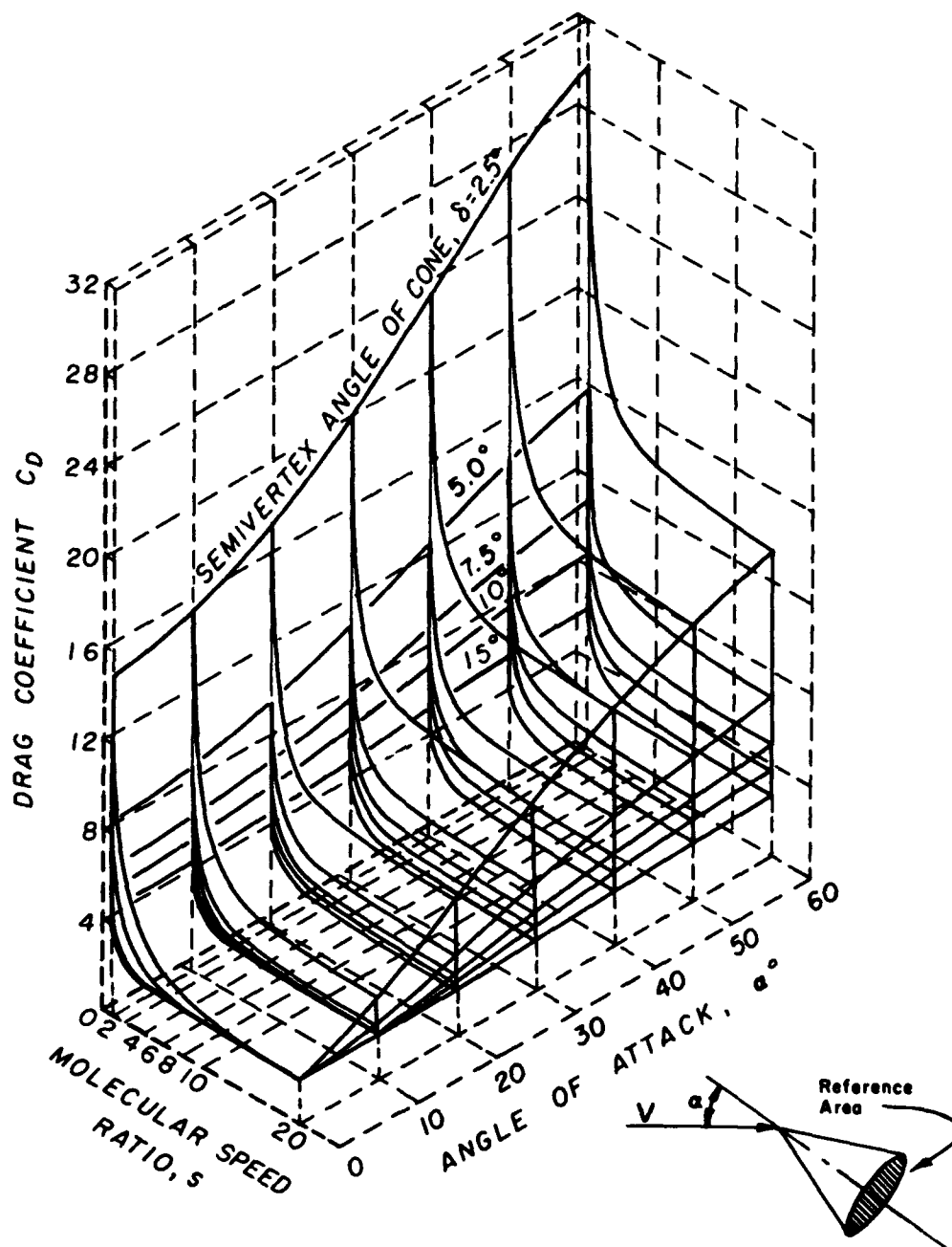
1602.4 Figure 8. Lift coefficient for a cone in free molecular flow:  $\sigma = \sigma' = 0$  (Ref. 15).



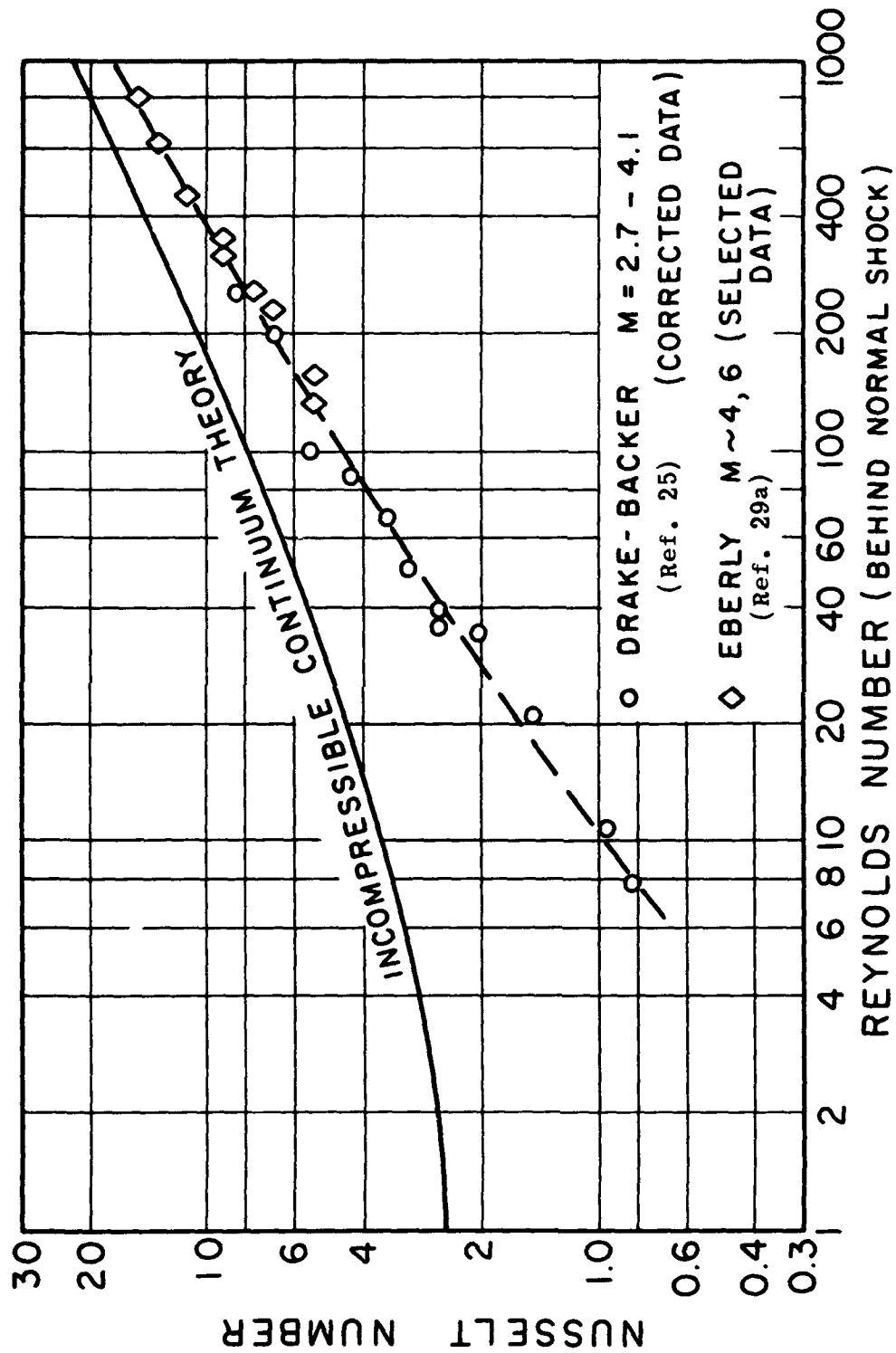
1602.4 Figure 9. Lift coefficient for a cone in free molecular flow:  $\sigma = \sigma' = 1$  and  $T_w = T_\infty$  (Ref. 15).



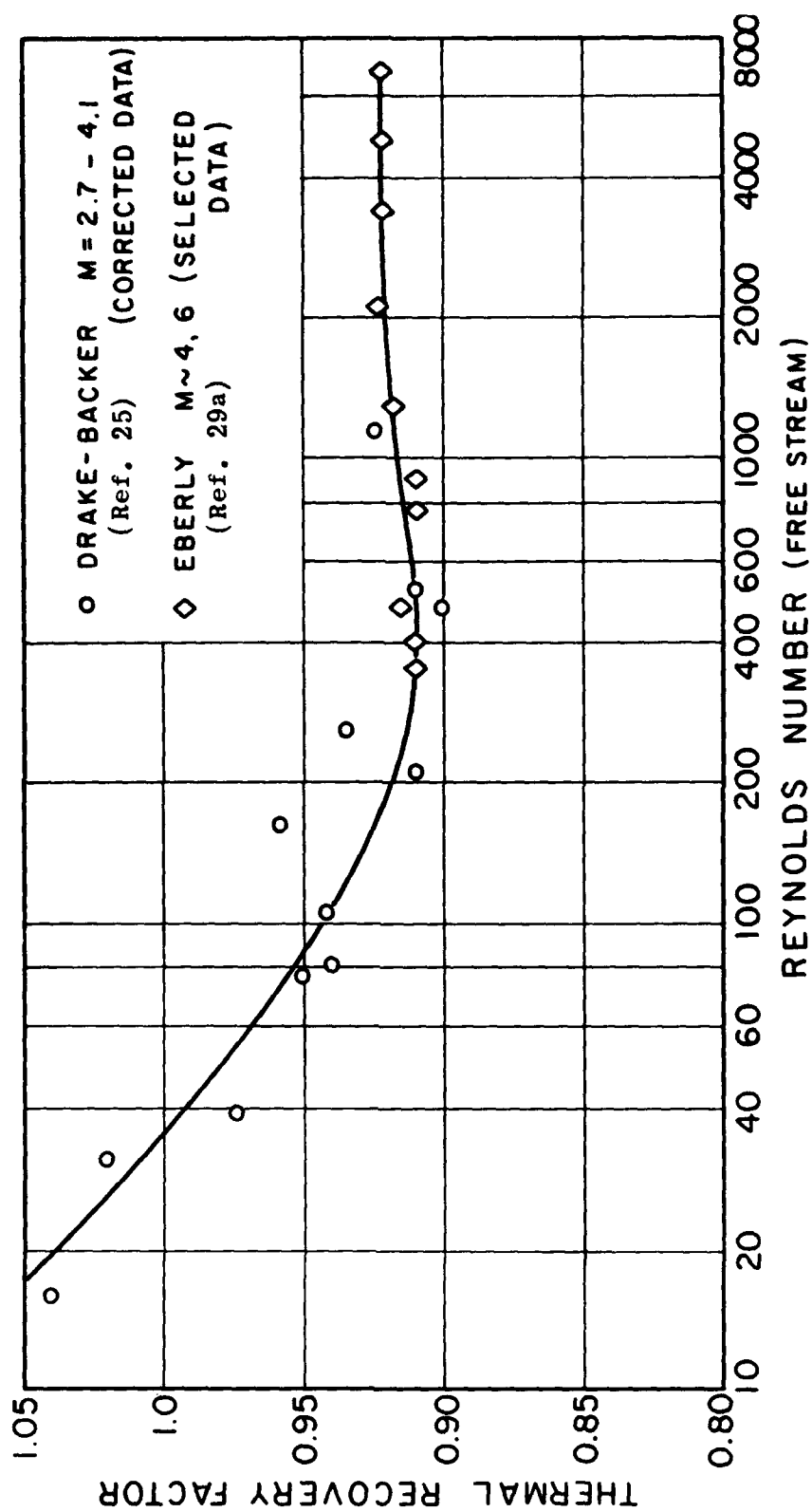
1602.4 Figure 10. Drag coefficient for a cone in free molecular flow:  $\sigma = \sigma' = 0$  (Ref. 15).



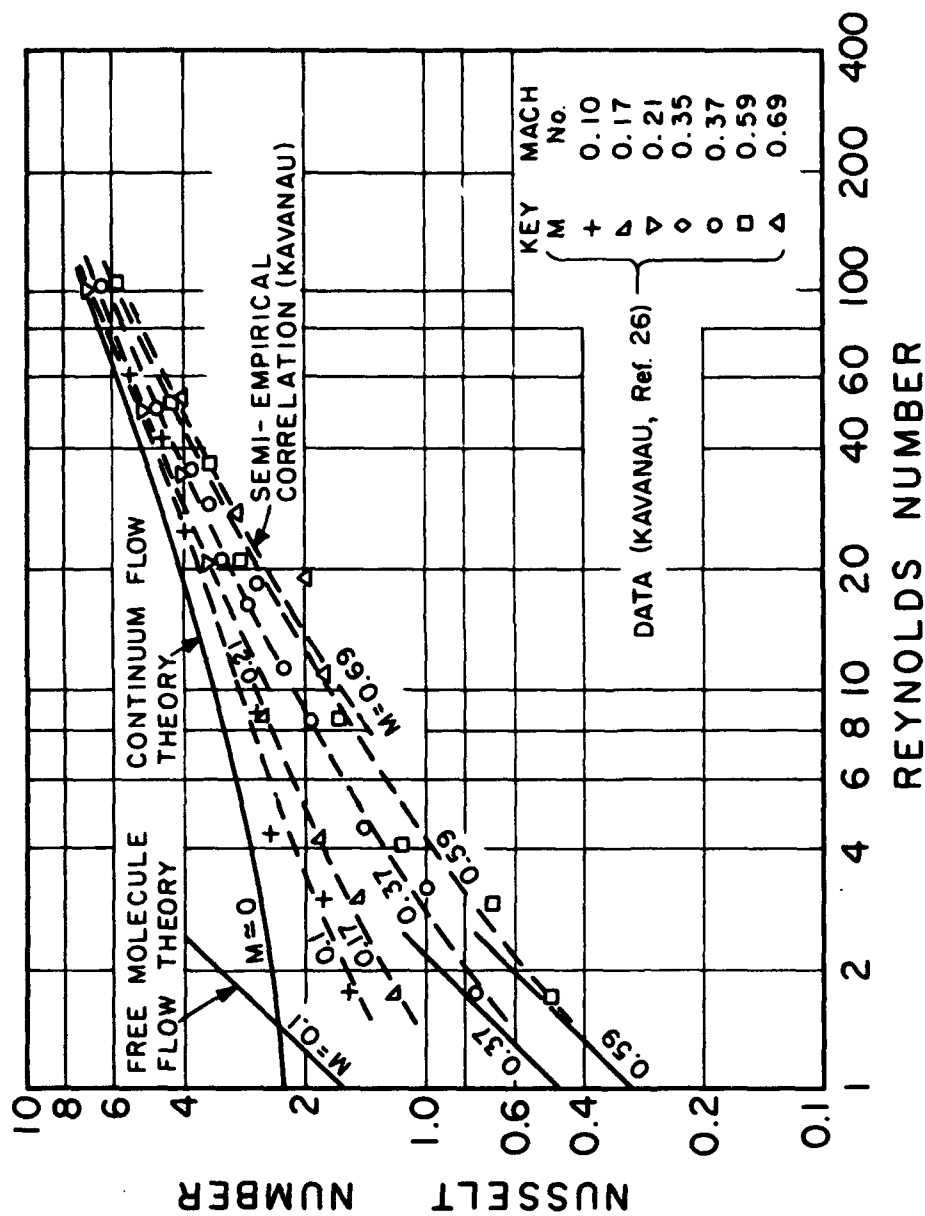
1602.4 Figure 11. Drag coefficient for a cone in free molecular flow:  $\sigma = \sigma' = 1$  and  $T_w = T_\infty$  (Ref. 15).



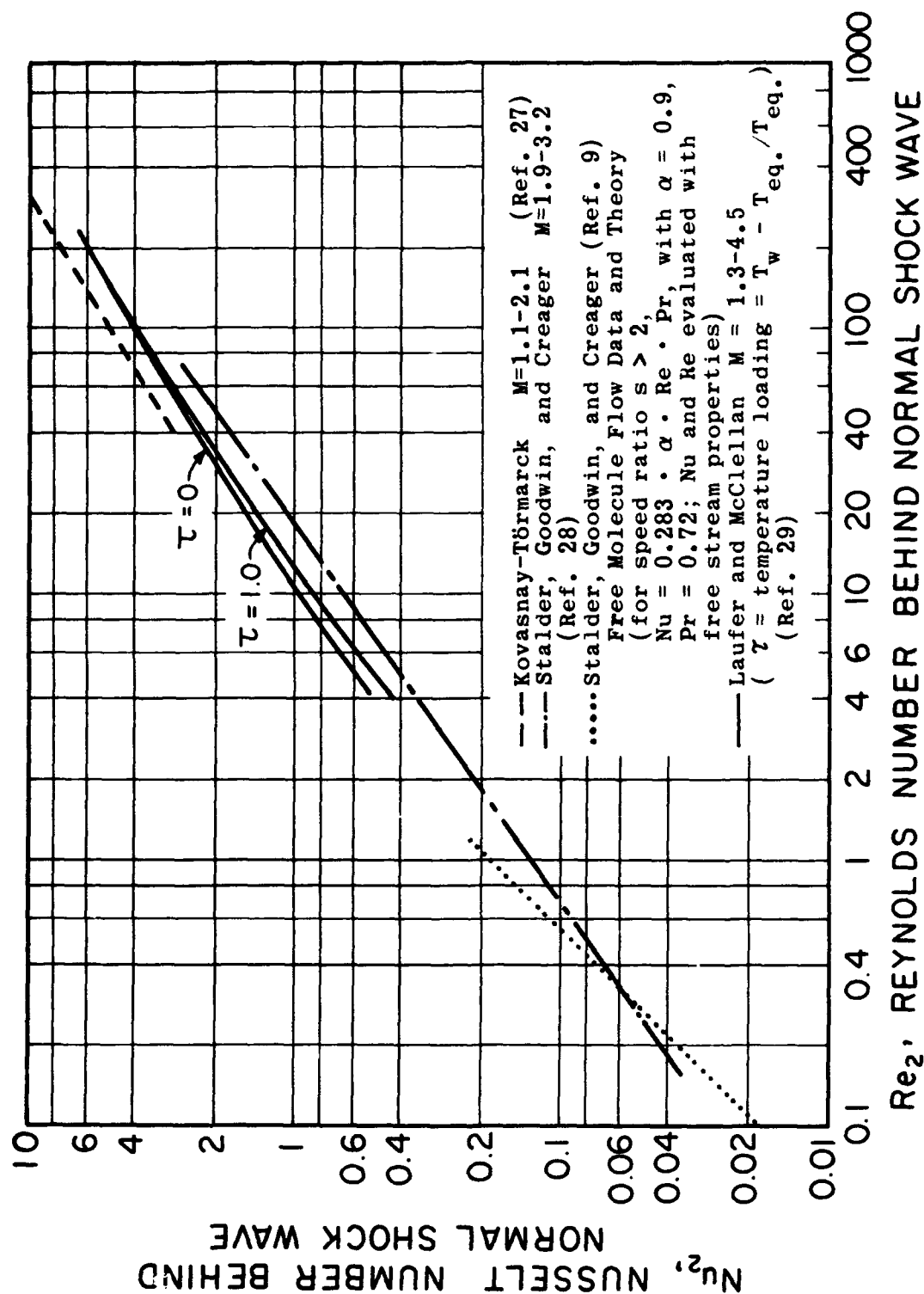
1603.41 Figure 1. Convective heat transfer to spheres in supersonic flow.



1603.41 Figure 2. Average recovery factors for spheres in supersonic flow.

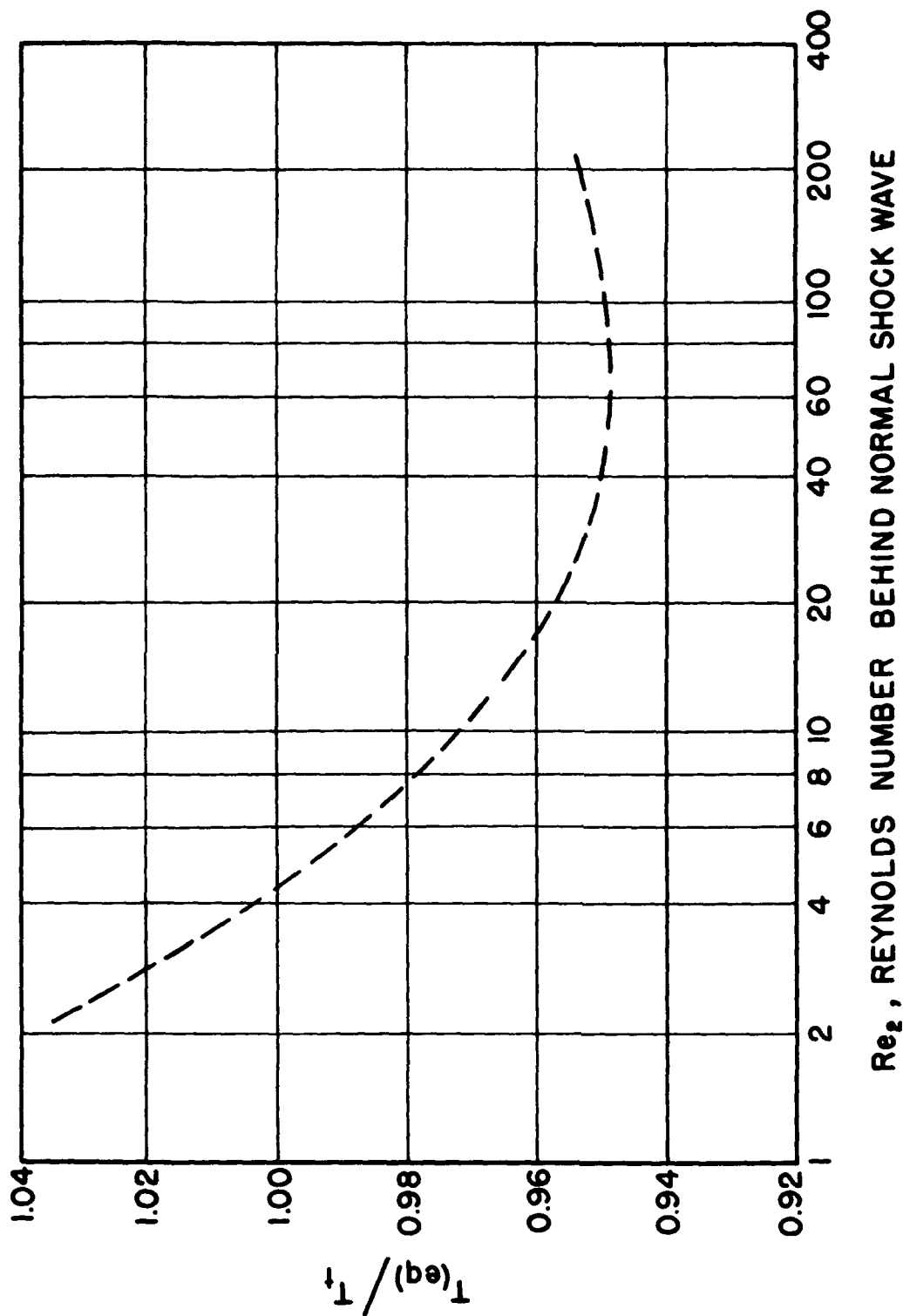


1603.41 Figure 3. Heat transfer coefficients for spheres in subsonic flow.

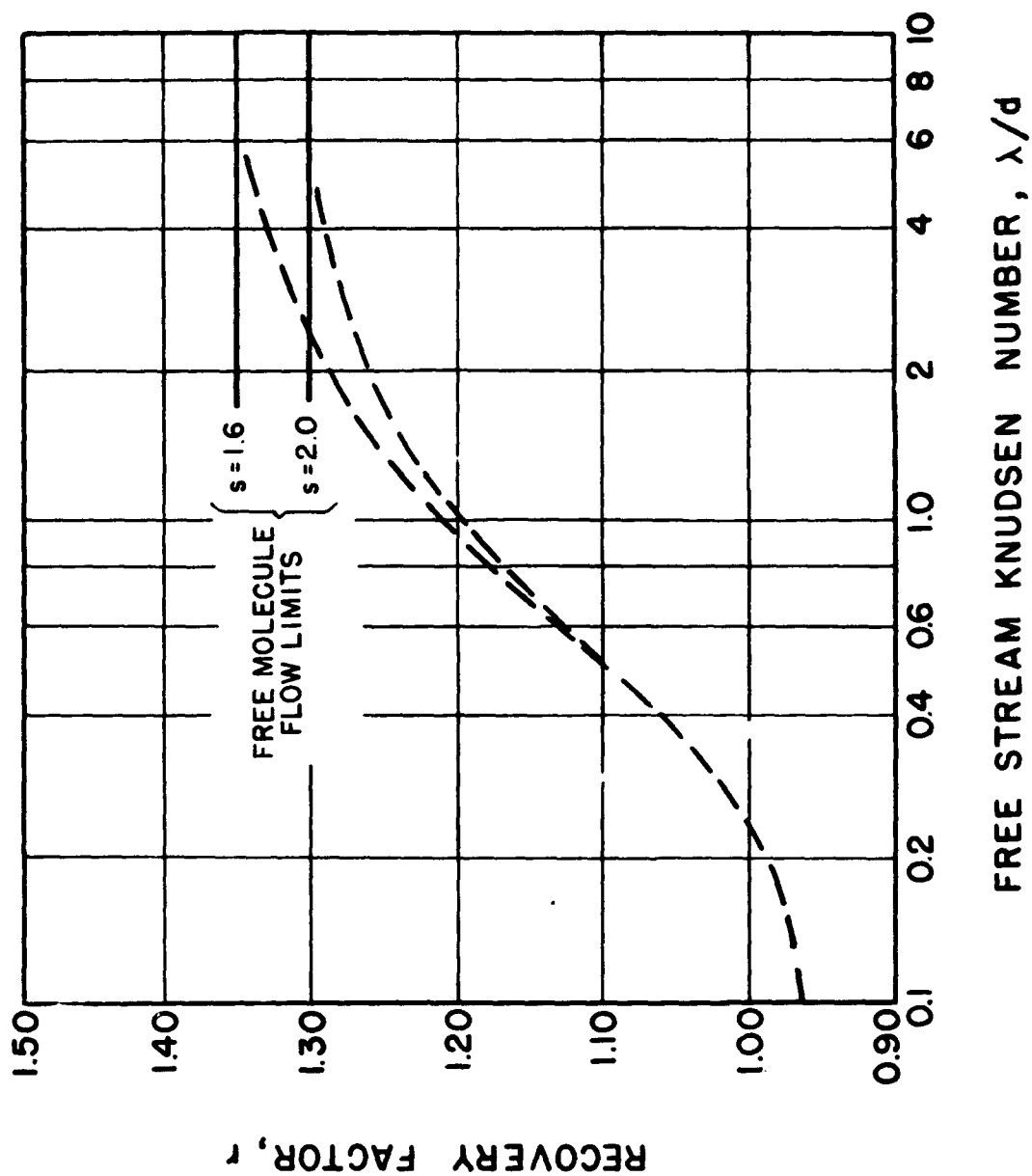


1603.42 Figure 1. Heat transfer to a circular cylinder transverse to the flow direction in supersonic flow.

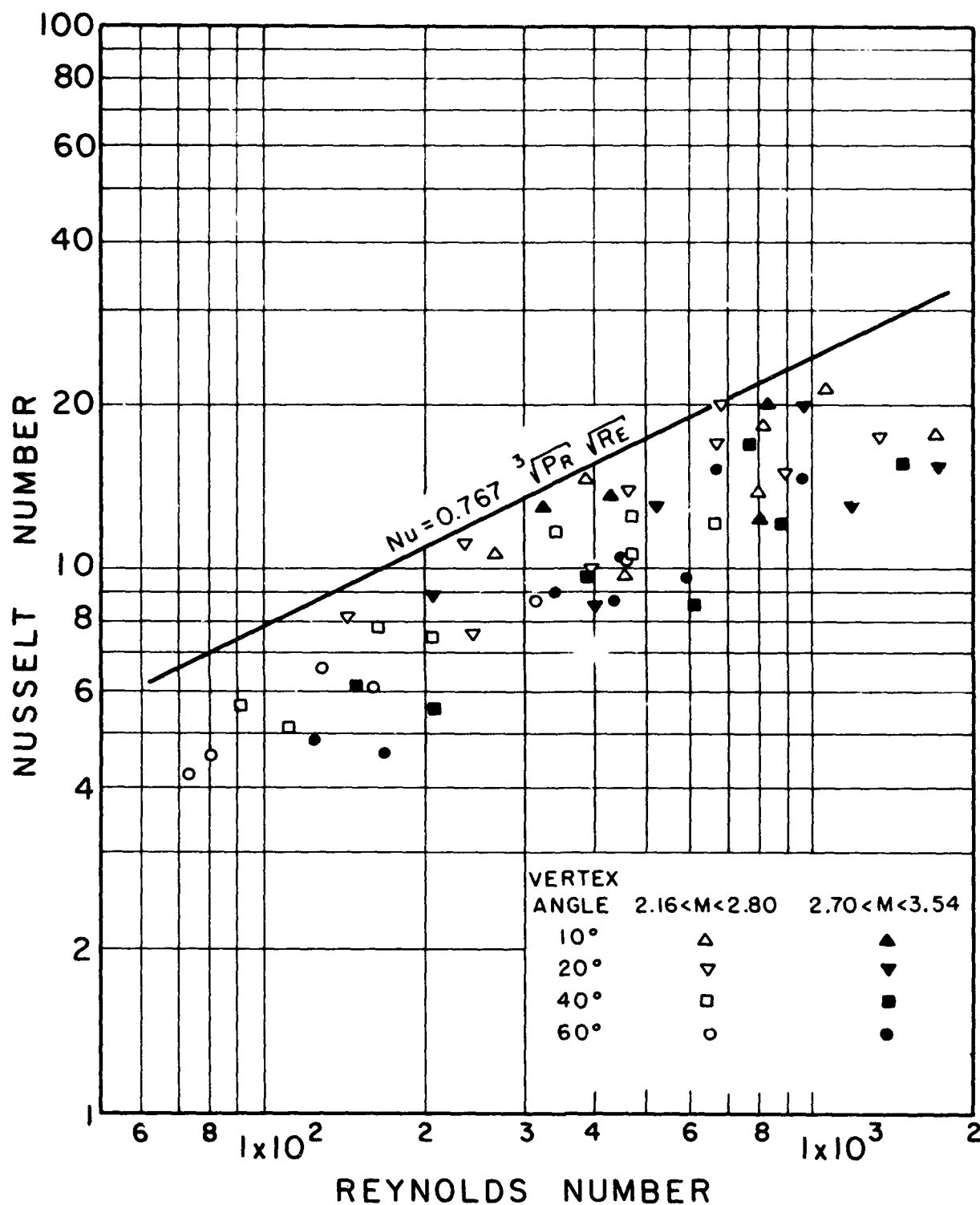




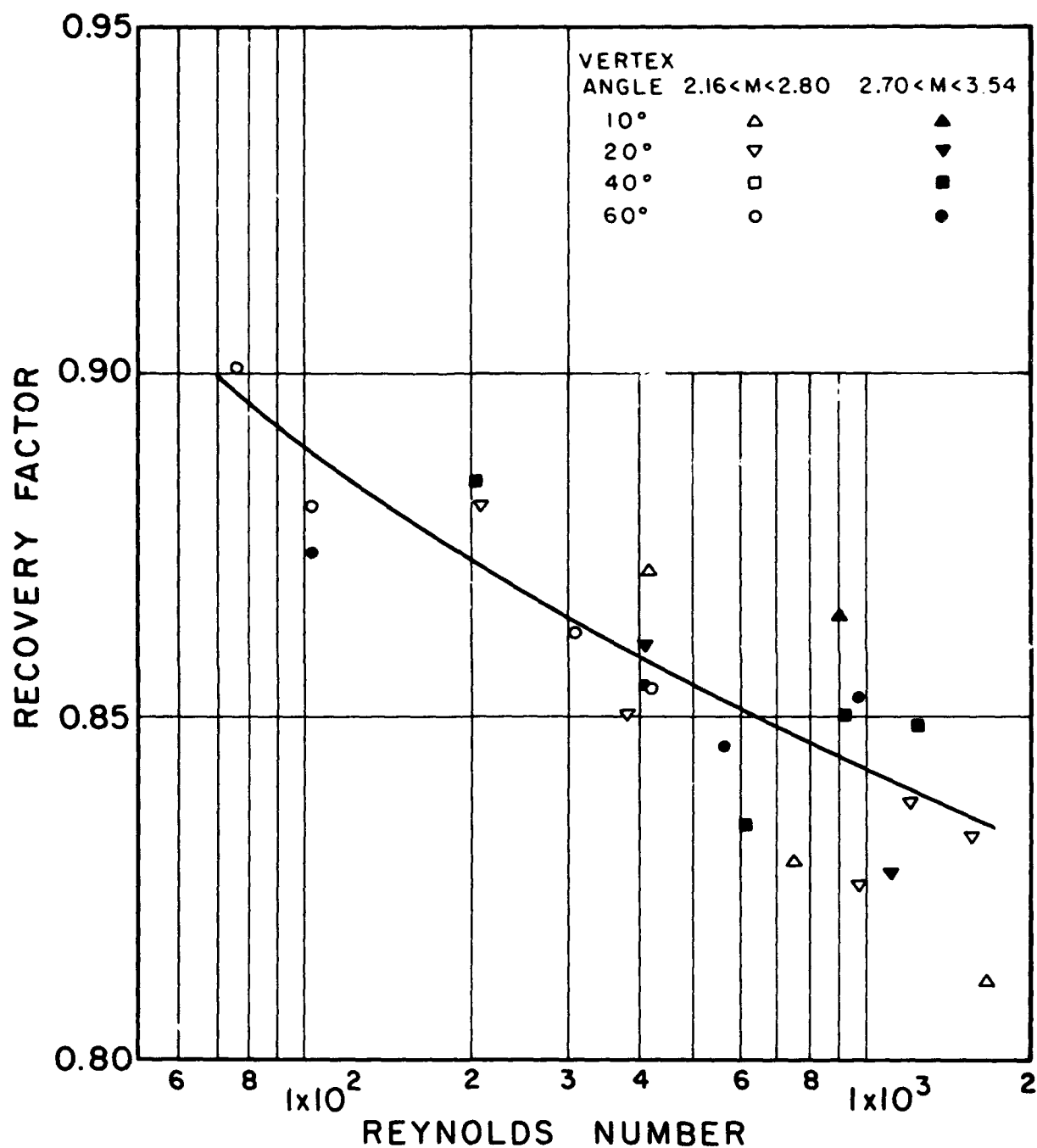
1603.42 Figure 2. Variation of equilibrium temperature for right circular cylinders transverse to the flow. Taken from experimental data (Ref. 29).  $M = 1.3$  to  $4.5$ .



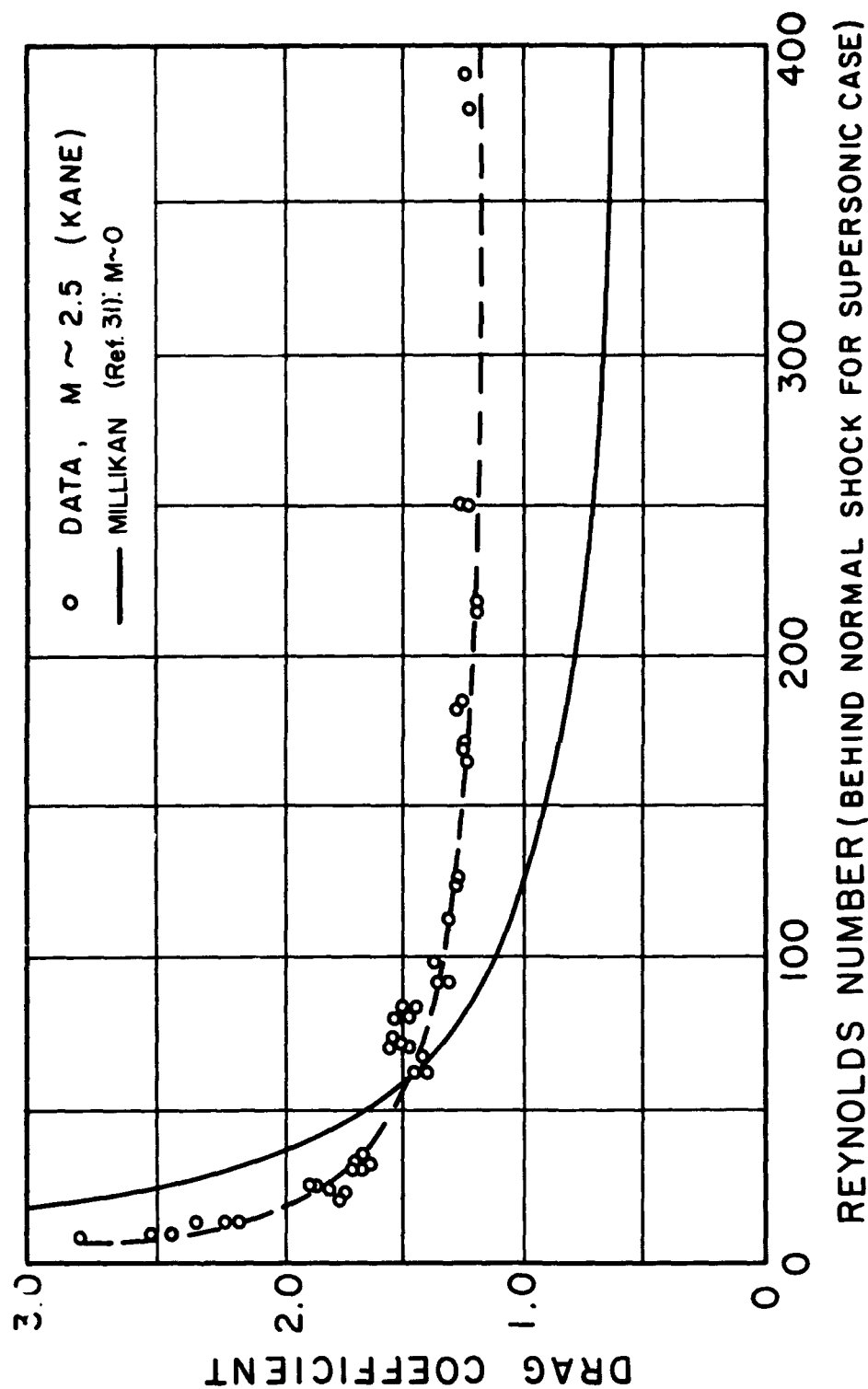
1603.42 Figure 3. Recovery factors for right circular cylinders transverse to the flow. Taken from experimental data (Ref. 28).  $M = 2.0$  to  $3.3$ .



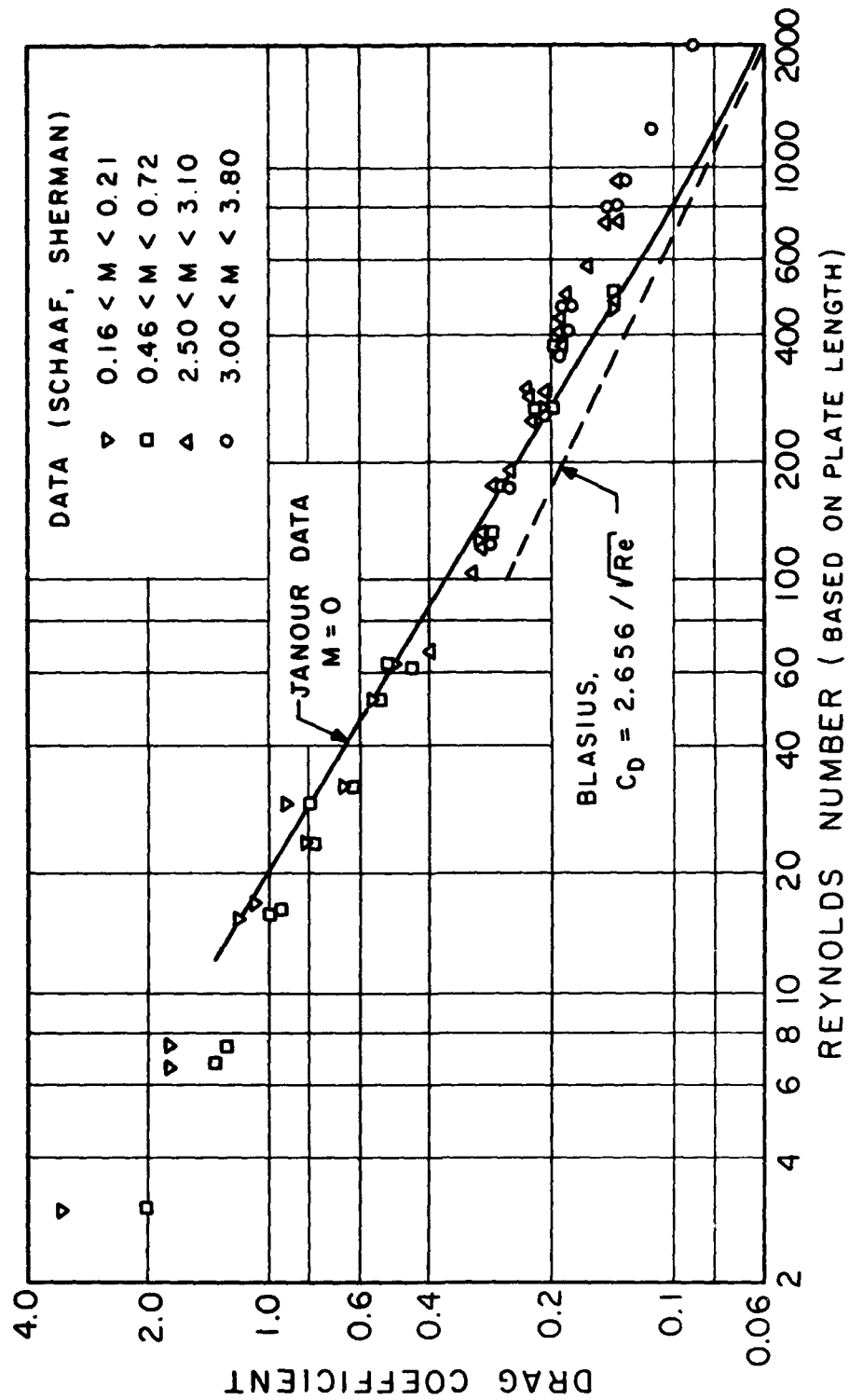
1603.43 Figure 1. Heat transfer coefficients for cones in supersonic flow.



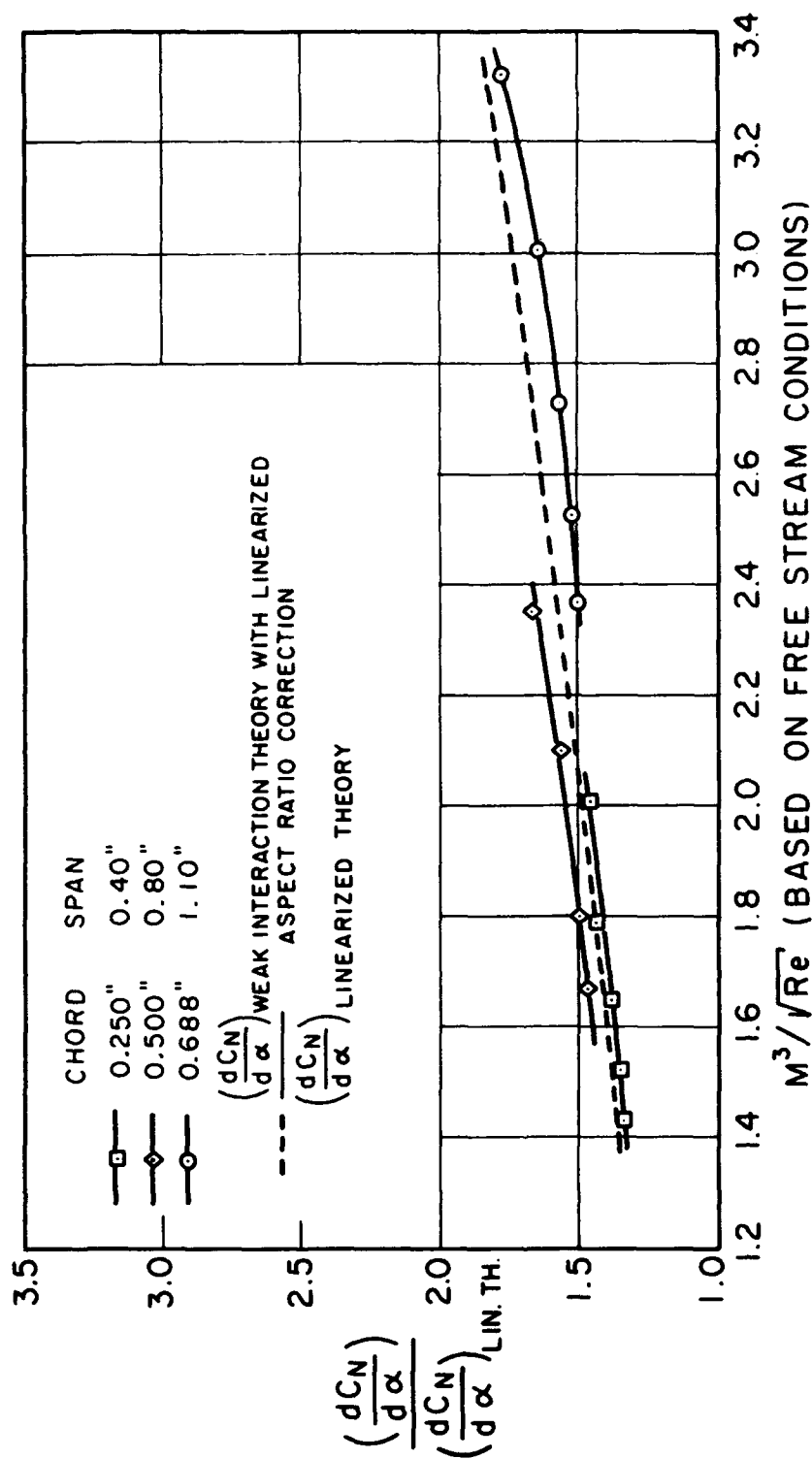
1603.43 Figure 2. Thermal recovery factors for cones in supersonic flow.

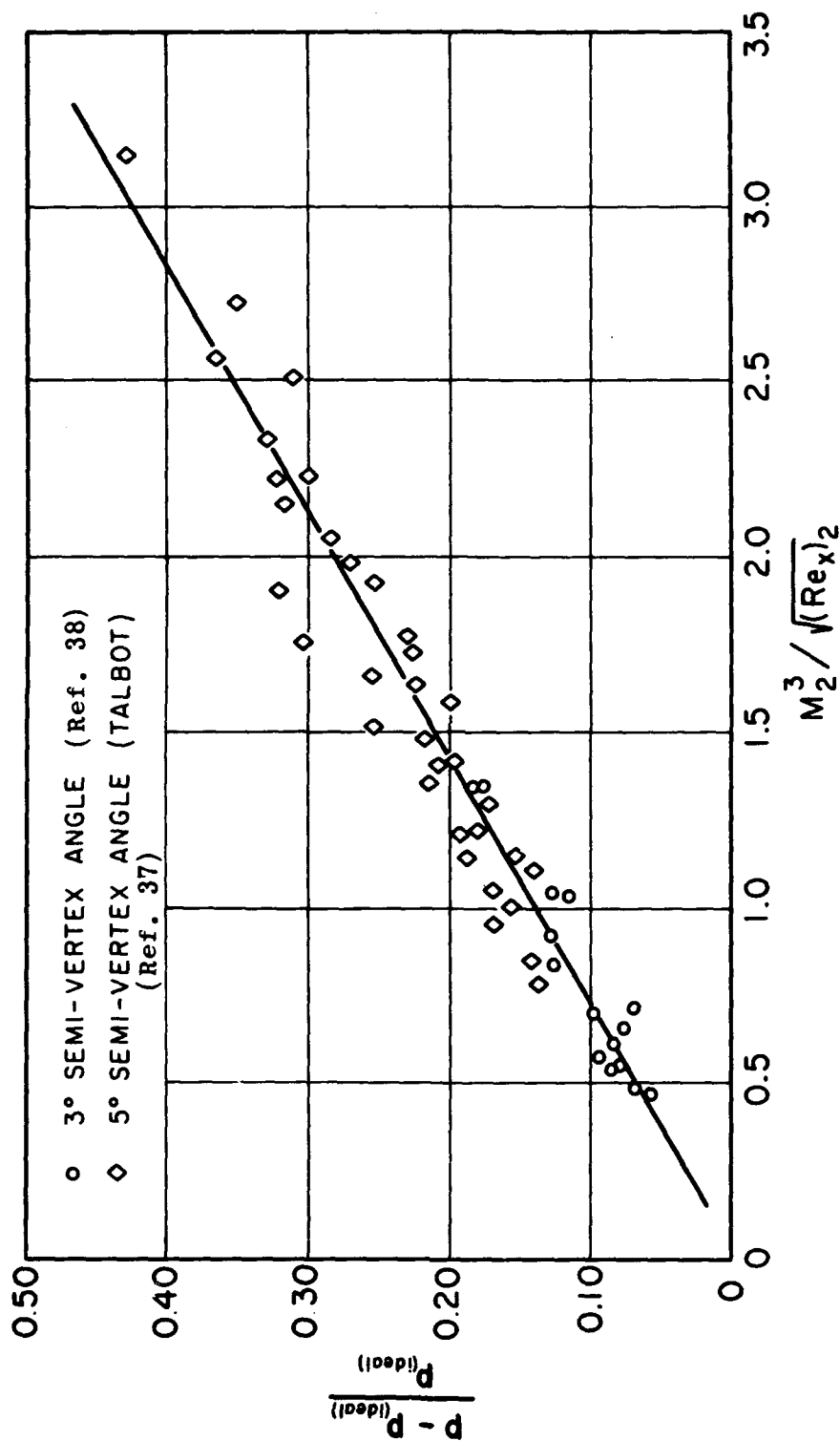


1603.51 Figure 1. Drag coefficient for a sphere.



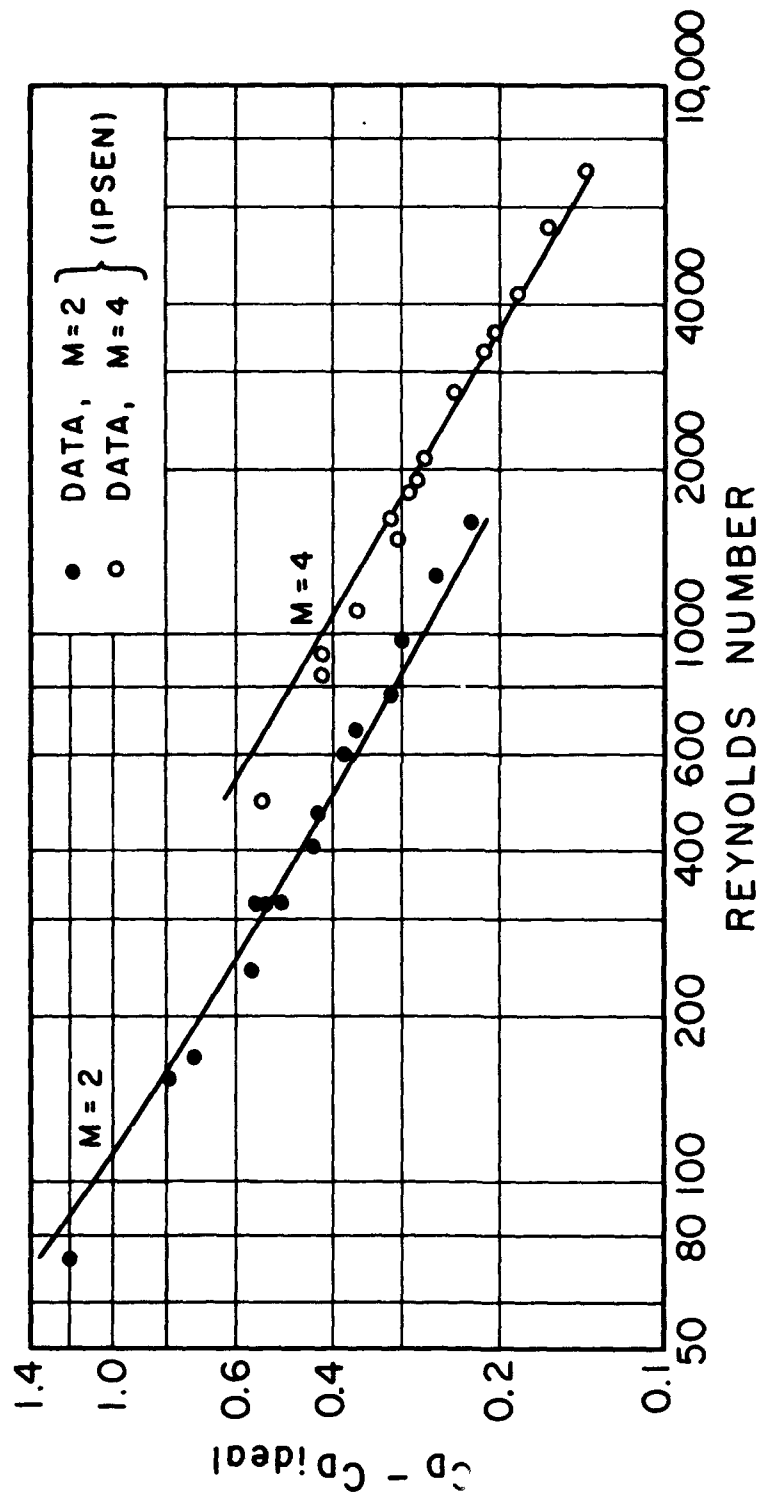
1603.52 Figure 1. Skin friction drag coefficient for a flat plate.

1603.52 Figure 2. Normal force coefficient-curve-slope for flat plates at  $M \sim 4$ .

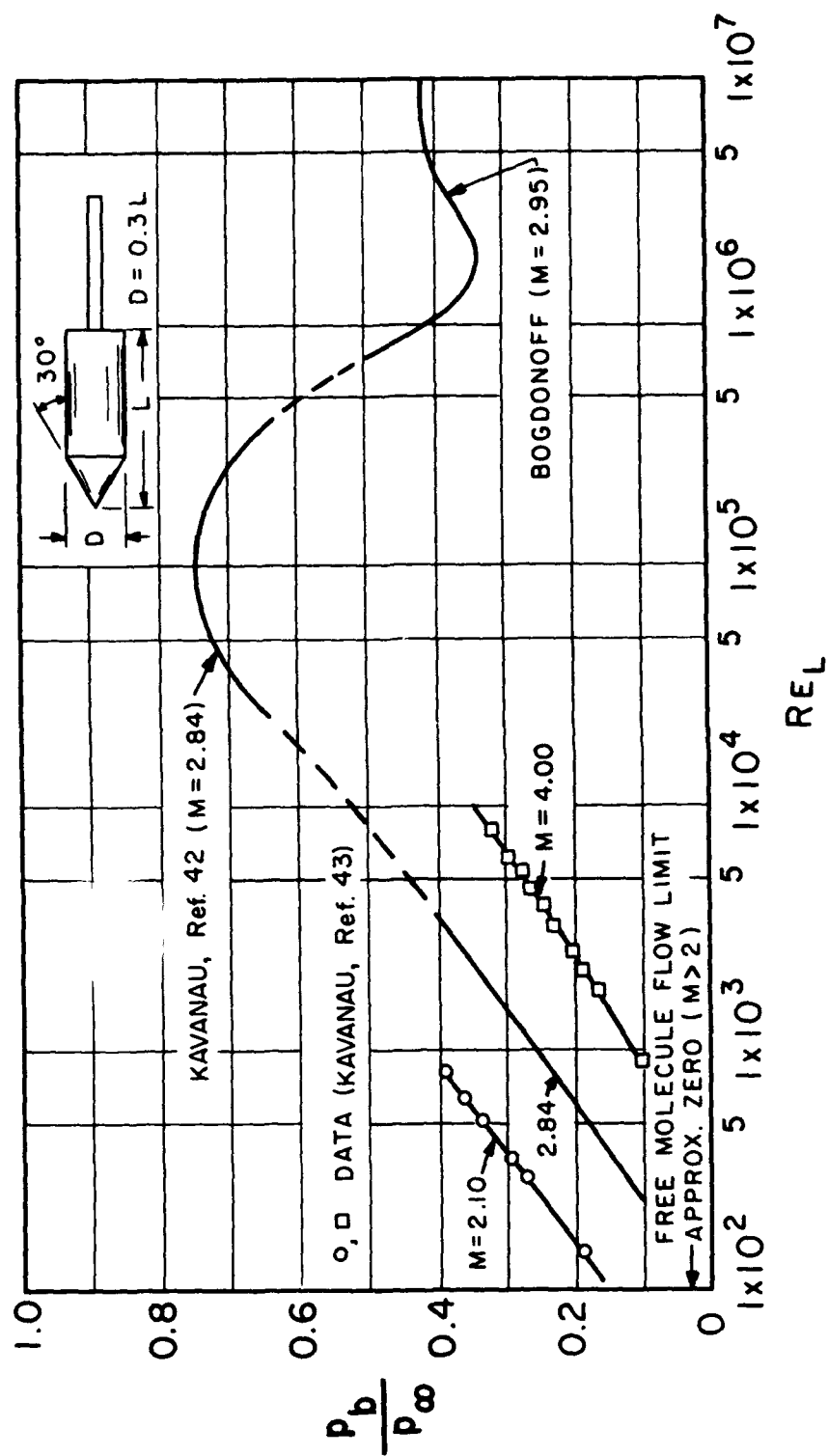


1603.53 Figure 1. Surface pressures on a cone at  $M \sim 4$ . (Note: The characteristic length,  $x$ , is measured from the vertex along the cone surface, and  $M_2$  and  $(Re_x)_2$  are evaluated using ideal flow properties behind a conical shock wave.)

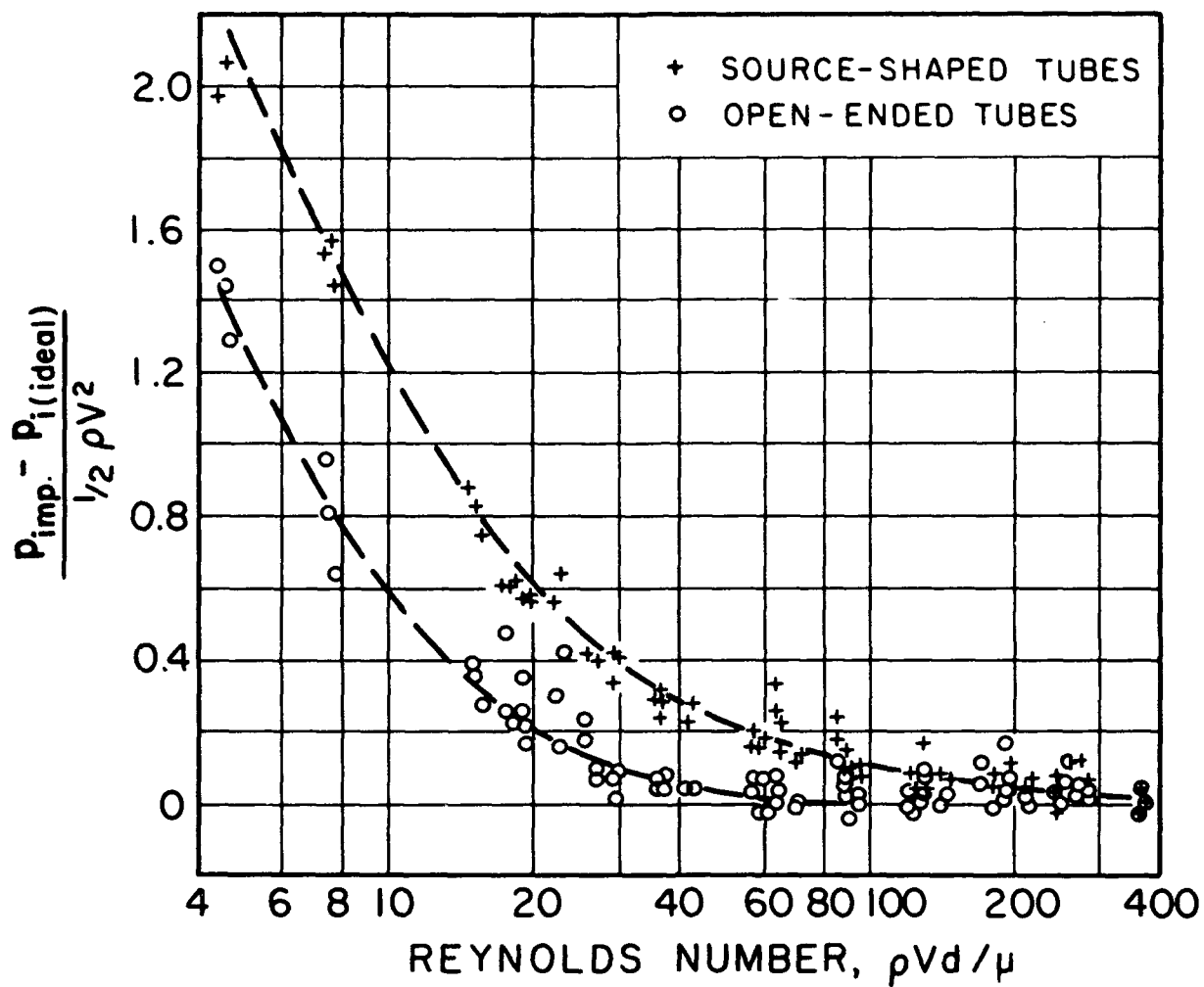




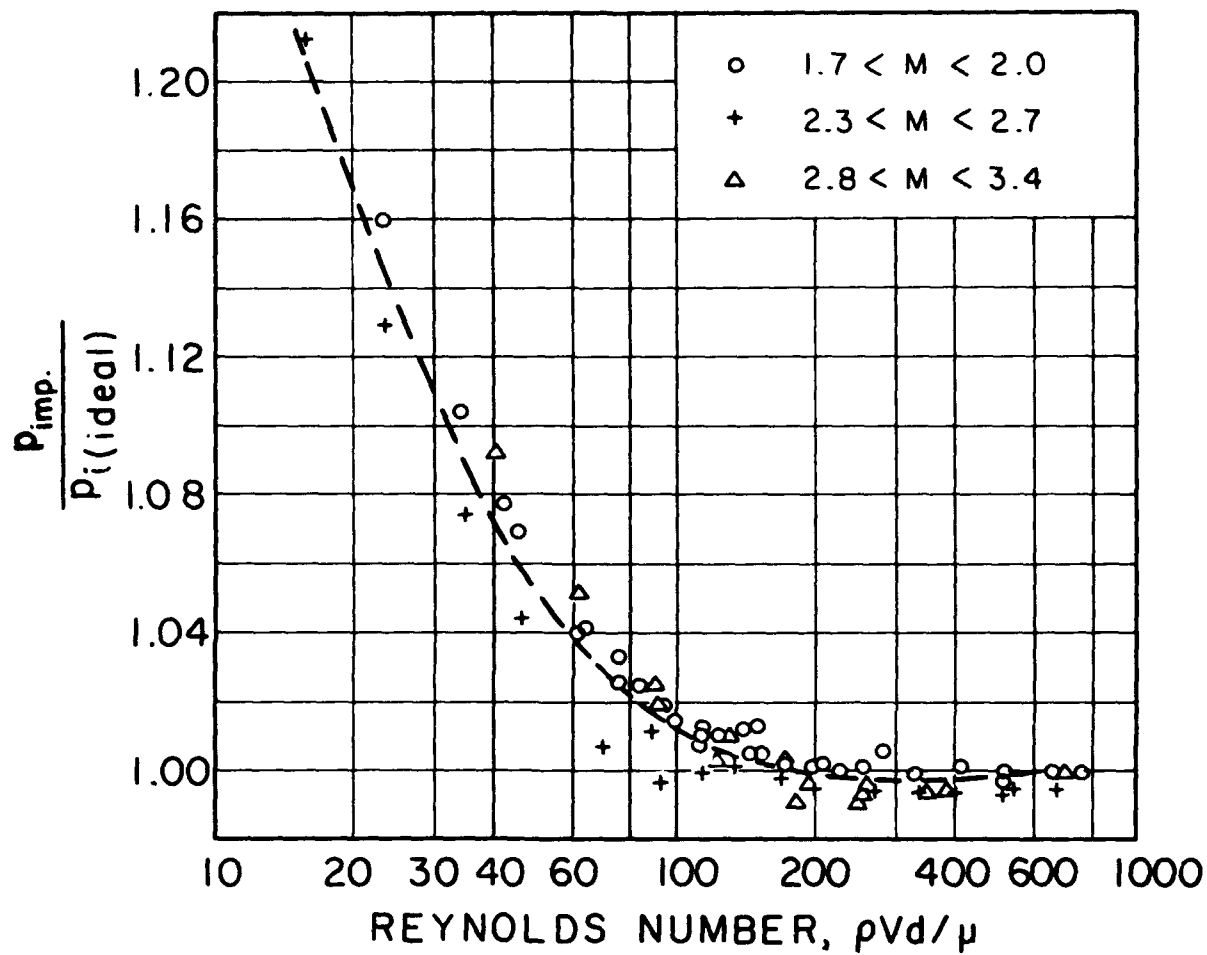
1603.53 Figure 2. Drag coefficients for cones with 15° semi-vertex angle.



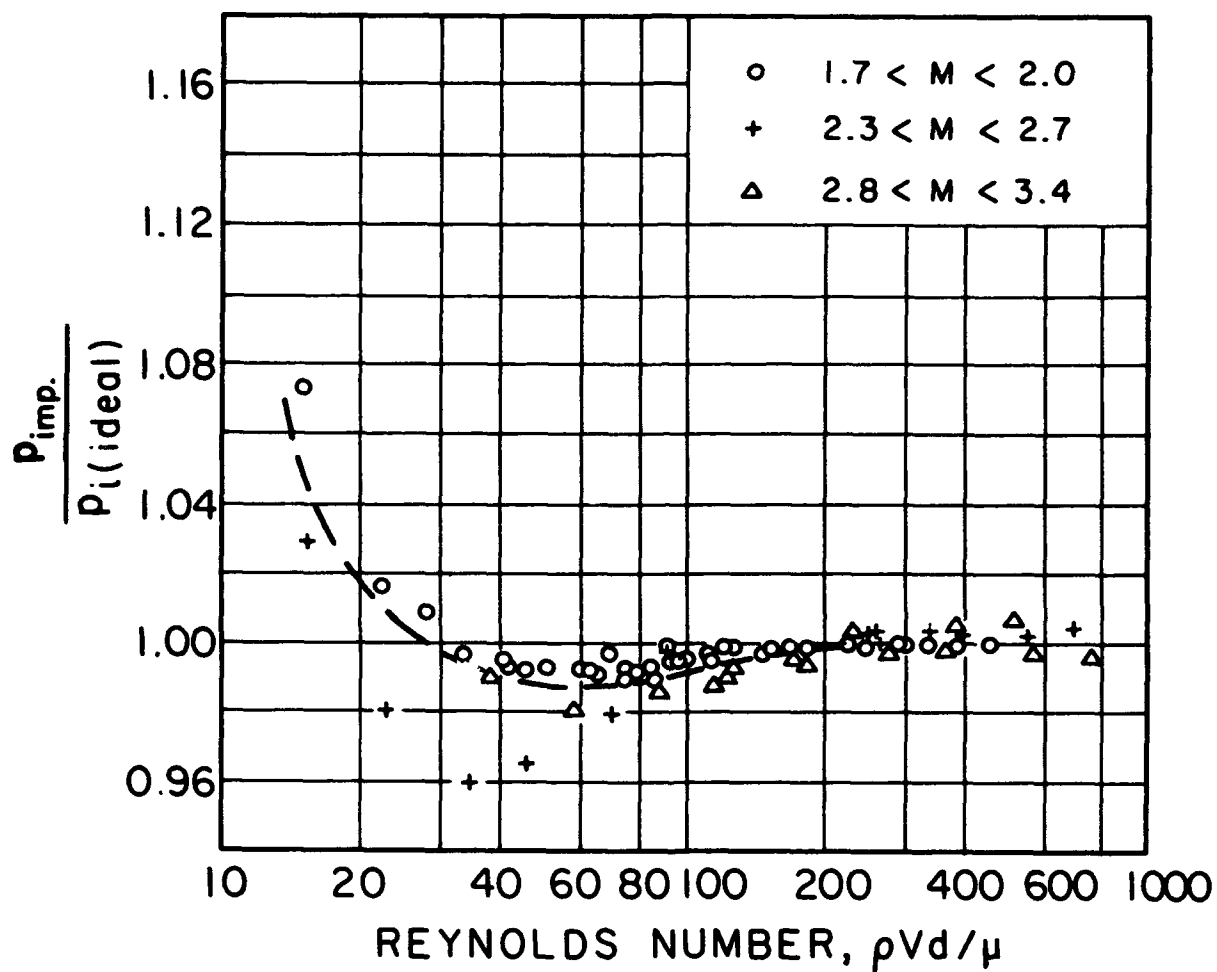
1603.54 Figure 1. Base pressure coefficient for a cone-cylinder configuration.



1603.55 Figure 1. Increment of measured pressure coefficient over ideal value in subsonic flow ( $0.10 < M < 0.67$ ).



1603.55 Figure 2. Correction factors for impact pressure measurements for source-shaped tubes in supersonic flow.



1603.55 Figure 3. Correction factors for impact pressure measurements for open-ended tubes in supersonic flow.

## SECTION 16 MECHANICS OF RAREFIED GASES

## References

1. Kennard, E. H. Kinetic Theory of Gases. New York: McGraw-Hill Book Co., Inc., 1938.
2. Tsien, H. S. "Superaerodynamics, Mechanics of Rarefied Gases," J. Aeronaut. Sci., Vol. 13 (December 1946), pp. 653-664.
3. Sanger, E. "Gas Kinetik Sehr Grosser Flughohen," Schweizer Archiv Fur Angewandte Wissenschaft und Technik, Vol. 16 (1950), pp. 43-63. (Translated Title: Gas Kinetics of Very High Flight Speeds.)
4. Heineman, M. "Theory of Drag in Highly Rarefied Gases," Comm. on Pure and Appl. Math., Vol. 1 (1948), p. 259.
5. Keller, J. "On the Solution of the Boltzmann Equation for Rarefied Gases," Comm. on Pure and Appl. Math., Vol. 1 (1948), p. 275.
6. Wang Chang, C. S. Transport Phenomena in Very Dilute Gases, II, (NORD-7924). Report UMH-3-F. Ann Arbor, Mich.: Engineering Research Institute, University of Michigan, 1950.
7. Wiedmann, M. L. "Thermal Accommodation Coefficient," Trans. ASME, Vol. 68 (1946), pp. 57-64.
8. Millikan, R. A. "Coefficients of Slip in Gases and the Law of Reflection of Molecules from the Surfaces of Solids and Liquids," Phys. Rev., Vol. 21 (1923), pp. 217-238.
9. Stalder, J. R., Goodwin, G., and Creager, M. O. A Comparison of Theory and Experiment for High Speed Free Molecule Flow. NACA TN 2244, 1950.
10. Wong, H. "Design and Development of a Free-Molecule Heat Transfer Probe." Master's Thesis, University of California, June 1956. (Also published as Report HE-150-143. Berkeley, Calif.: Institute of Engineering Research, University of California, October 1956.)
11. Stalder, J. R. and Jukoff, D. Heat Transfer to Bodies Traveling at High Speed in the Upper Atmosphere. NACA Report 944, 1949.
12. Oppenheim, A. K. "Generalized Theory of Convective Heat Transfer in a Free-Molecule Flow," J. Aeronaut. Sci., Vol. 20 (January 1953), pp. 49-58.
13. Heineman, M. "Theory of Drag in Highly Rarefied Gases," Comm. on Pure and Appl. Math., Vol. 1 (September 1948), pp. 259-273.
14. Ashley, H. "Applications of the Theory of Free Molecule Flow to Aeronautics," J. Aeronaut. Sci., Vol. 16 (February 1949), pp. 95-104.

15. Stalder, J. R. and Zurick, V. J. Theoretical Aerodynamic Characteristics of Bodies in a Free-Molecule-Flow Field. NACA TN 2423, 1951.
16. Grimminger, G., Williams, E. P., and Young, G. B. W. "Lift on Inclined Bodies of Revolution in Hypersonic Flow," J. Aeronaut. Sci., Vol. 17 (November 1950), pp. 675-690.
17. Burnett, D. "The Distribution of Molecular Velocities and the Mean Motion in a Non-Uniform Gas," Proc. London Math. Soc., Vol. 40 (December 1935), pp. 382-400.
18. Chapman, S. and Cowling, T. G. The Mathematical Theory of Non-Uniform Gases. Cambridge: The Cambridge University Press, 1939.
19. Grad, Harold. "On the Kinetic Theory of Rarefied Gases," Comm. on Pure and Appl. Math., Vol. 2 (December 1949), pp. 331-407.
20. Koga, T. "A Proposal for Fundamental Equations of Dynamics of Gases under High Stress (A Proposal for Statistical Mechanical Treatment of Systems Not in Thermal Equilibrium Associated with Transport Phenomena)," J. Chem. Phys., Vol. 22 (October 1954), pp. 1633-1646.
21. Greenspan, M. "Combined Translational and Relaxational Dispersion of Sound in Gases," J. Acoustical Soc. of America, Vol. 26 (January 1954), p. 70.
22. Sherman, F. S. A Low Density Wind Tunnel Study of Shock Wave Structure and Relaxation Phenomena in Gases. NACA TN 3298, July 1955.
23. Ikenberry, E. and Truesdell, C. "On the Pressures and Flux of Energy in a Gas According to Maxwell's Kinetic Theory, I," Jour. Rational Mech. and Analysis, Vol. 5 (January 1956), p. 41.
24. Kramers, H. A. "On the Behaviour of a Gas Near a Wall," Nuovo cimento, Vol. 6 (Suppl. No. 2, 1949), pp. 297-304.
25. Drake, R. M. and Backer, G. H. "Heat Transfer from Spheres in Supersonic Flow to a Rarefied Gas," Trans. ASME, Vol. 74 (October 1952).
26. Kavanau, L. L. "Heat Transfer from Spheres to a Rarefied Gas in Subsonic Flow," Trans. ASME, Vol. 77 (July 1955), pp. 617-623.
27. Kovasznay, L. S. G. and Tormarck, S. I. A. Heat Loss to Hot-Wires in Supersonic Flow. Bumblebee Report 127. Baltimore: Department of Aeronautics, The Johns Hopkins University, April 1950.
28. Stalder, J. R., Goodwin, G., and Creager, M. O. Heat Transfer to Bodies in a High-Speed Rarefied-Gas Stream. NACA TN 2438, 1951.
29. Laufer, I. and McClellan, R. "Measurement of Heat Transfer from Hot Wires in Supersonic Flows," J. Fluid Mech., Vol. 1 (September 1956), pp. 276-289.
- 29a. Eberly, D. K. Forced Convection Heat Transfer from Spheres to a Rarefied Gas. Report HE-150-140. Berkeley, Calif: Institute of Engineering Research, University of California, July 1956.

30. Drake, R. M. and Maslach, G. J. Heat Transfer from Right Circular Cones to a Rarefied Gas in Supersonic Flow. Report HE-150-91. Berkeley, Calif.: Institute of Engineering Research, University of California, 1952.
31. Millikan, R. A. "The General Law of Fall of a Small Spherical Body through a Gas, and its Bearing upon the Nature of Molecular Reflection from Surfaces," Phys. Rev., Vol. 22 (1923), pp. 1-23.
32. Kane, E. D. "Sphere Drag Data at Supersonic Speeds and Reynolds Numbers," J. Aeronaut. Sci., Vol. 18 (April 1951), pp. 259-270.
33. Janour, Z. Resistance of a Plate in Parallel Flow at Low Reynolds Numbers. NACA TM 1316, November 1951.
34. Schaaf, S. A. and Sherman, F. S. "Skin Friction in Slip Flow," J. Aeronaut. Sci., Vol. 21 (February 1954), p. 85.
35. Kuo, Y. H. "On the Flow of an Incompressible Viscous Fluid past a Flat Plate at Moderate Reynolds Numbers," J. Math. and Phys., Vol. 32 (1953), pp. 83-101.
36. Tellep, D. M. and Talbot, L. "Normal Forces on Flat Plates in Low Density Supersonic Flow," J. Aeronaut. Sci., Vol. 23 (December 1956), pp. 1099-1108.
37. Talbot, L. Viscosity Corrections to Cone Probes in Rarefied Supersonic Flow at a Nominal Mach Number of 4. NACA TN 3219, November 1954.
38. Talbot, L., Koga, T., and Sherman, P. M. Hypersonic Viscous Flow Over Slender Cones. NACA TN 4327, September 1958.
39. Ipsen, D. C. "Experiments on Cone Drag in a Rarefied Air Flow," Jet Propulsion, Vol. 26 (December 1956), pp. 1076-1077.
40. Probstein, R. F. and Elliott, D. "The Transverse Curvature Effect in Compressible Axially-Symmetric Laminar Boundary Layer Flow," J. Aeronaut. Sci., Vol. 23 (March 1956), pp. 202-224.
41. Bogdonoff, S. M. "A Preliminary Study of Reynolds Number Effects on Base Pressure at  $M = 2.95$ ," J. Aeronaut. Sci., Vol. 19 (March 1952), pp. 201-206.
42. Kavanau, L. L. "Results of Some Base Pressure Experiments at Intermediate Reynolds Numbers with  $M = 2.84$ ," J. Aeronaut. Sci., Vol. 21 (April 1954), p. 257.
43. Kavanau, L. L. "Base Pressure Studies in Rarefied Supersonic Flows," J. Aeronaut. Sci., Vol. 23 (March 1956), pp. 193-207.
44. Homann, F. "Der Einfluss grosser Zahigkeit bei der Stromung um den Zylinder und um die Kugel," ZAMM, Vol. 16 (June 1936), pp. 153-164. (Also available as: The Effect of High Viscosity on the Flow around a Cylinder and around a Sphere. NACA TM 1334, June 1952.)



45. Kane, E. D. and Maslach, G. J. Impact-Pressure Interpretation in a Rarefied Gas at Supersonic Speeds. NACA TN 2210, October 1950.
46. Sherman, F. J. New Experiments on Impact-Pressure Interpretation in Supersonic and Subsonic Rarefied Air Streams. NACA TN 2995, September 1953.
47. National Bureau of Standards. Tables of the Error Function and Its Derivative. National Bureau of Standards Applied Mathematics Series 41. Washington: U. S. Government Printing Office, 1954.
48. Pierce, B. O. A Short Table of Integrals, 4th edition, revised by R. M. Foster. New York: Ginn and Co., 1956.
49. British Association for the Advancement of Science. Mathematical Tables. Vol. I, 2nd edition. Cambridge: Cambridge University Press, 1946.

#### General Bibliography

50. Hirschfelder, J. O., Curtiss, C. F., and Bird, R. B. Molecular Theory of Liquids. Chap. VII. New York: John Wiley and Sons, Inc., 1956.
51. Maxwell, J. C. The Scientific Papers of James Clerk Maxwell. "On the Dynamic Theory of Gases," Vol. 2, Chap. XXVIII, pp. 26-78; "On Stresses in Rarefied Gases Arising from Inequalities of Temperature," Vol. 2, Chap. XCIII, pp. 681-712. Cambridge: The Cambridge University Press, 1890.
52. Patterson, G. N. Molecular Flow of Gases. New York: John Wiley and Sons, Inc., 1956.
53. Sanger, E. The Gas Kinetics of Very High Flight Speeds. NACA TM 1270, May 1950.
54. Schaaf, S. A. and Chambre, P. L. "Flow of Rarefied Gases." High Speed Aerodynamics and Jet Propulsion, Volume III, Section H (edited by H. W. Emmons). Princeton: Princeton University Press, 1958.

## SECTION 16 MECHANICS OF RAREFIED GASES

## Index

	<u>Subsection</u> <u>Number</u>
A	
Aerodynamic Forces	
Free Molecular Flow . . . . .	1602.4
Cone . . . . .	1602.44
Cylinder . . . . .	1602.43
Example, Composite Body . . . . .	1602.45
Flat Plate . . . . .	1602.41
Sphere . . . . .	1602.42
Slip Flow . . . . .	1603.5
Base Pressures . . . . .	1603.54
Cone . . . . .	1603.53
Flat Plate . . . . .	1603.52
Impact Probe Measurements . . . . .	1603.55
Sphere . . . . .	1603.51
B	
Base Pressures (Slip Flow) . . . . .	1603.54
Burnett Equations . . . . .	1603.2
C	
Cone	
Free Molecular Flow	
Aerodynamic Forces . . . . .	1602.44
Heat Transfer . . . . .	1602.34
Slip Flow	
Aerodynamic Forces . . . . .	1603.53
Heat Transfer . . . . .	1603.43
Cylinder	
Free Molecular Flow	
Aerodynamic Forces . . . . .	1602.43
Heat Transfer . . . . .	1602.32
Slip Flow	
Heat Transfer . . . . .	1603.42
D	
Differential Equations, Appropriate for Slip Flow . . . . .	1603.2
Diffuse Reflection . . . . .	1601.3
Direction Cosines . . . . .	1602.44
Drag, Coefficient of . . . . .	1602.2
E	
Energy Flux, Basic Relations . . . . .	1602.1
Energy, Translational and Internal . . . . .	1602.1
Example, Composite Body (Aerodynamic Forces) . . . . .	1602.45

Subsection Number

## F

## Figures (see Contents Page 2)

## Flow

Free Molecular . . . . .	1602
Hypersonic, Results. . . . .	1603.3
Newtonian . . . . .	1602.2
Regimes	
Qualitative Description of . . . . .	1601.1
Significant Characterizing Parameters . . . . .	1601.2
Slip . . . . .	1603
Appropriate Differential Equations . . . . .	1603.2

## Flat Plate

Free Molecular Flow	
Aerodynamic Forces . . . . .	1602.41
Heat Transfer . . . . .	1602.31
Slip Flow	
Aerodynamic Forces . . . . .	1603.52

## H

## Heat Transfer Characteristics

Free Molecular Flow. . . . .	1602.3
Composite Body . . . . .	1602.35
Cone. . . . .	1602.34
Cylinder. . . . .	1602.32
Flat Plate . . . . .	1602.31
Sphere . . . . .	1602.33
Slip Flow . . . . .	1603.4
Cone. . . . .	1603.43
Cylinder. . . . .	1603.42
Sphere . . . . .	1603.41

## I

Impact Probe Measurements . . . . .	1603.55
Internal Energy . . . . .	1602.1

## L

Lift, Coefficient of . . . . .	1602.2
--------------------------------	--------

## M

Momentum Flux, Basic Relations. . . . .	1602.2
---	--------

## N

Navier-Stokes Equations . . . . .	1603.2
-----------------------------------	--------

	<u>Subsection</u>	<u>Number</u>
P		
Pressure Distribution . . . . .	1602.2	
Parameters		
Significant, for Characterizing Flow Regimes .	1601.2	
Surface Interaction. . . . .	1601.3	
R		
Real Gas Effects . . . . .	1601.11	
Recovery Factor . . . . .	1602.1	
References (see Reference Page 1)		
Reflection, Diffuse and Specular . . . . .	1601.3	
S		
Skin Friction Distribution. . . . .	1602.2	
Slip Flow . . . . .	1603	
Sphere		
Free Molecular Flow		
Aerodynamic Forces . . . . .	1602.42	
Heat Transfer . . . . .	1602.33	
Slip Flow		
Aerodynamic Forces . . . . .	1603.51	
Heat Transfer . . . . .	1603.41	
Stanton Number . . . . .	1602.1	
T		
Temperature Jump, Body Surfaces . . . . .	1603.1	
Thirteen Moment Equations . . . . .	1603.2	
Transition Flow . . . . .	1601.1	
Translational Energy . . . . .	1602.1	
V		
Velocity Slip, Body Surfaces . . . . .	1603.1	
Viscous Interaction Effects . . . . .	1603.3	